Tissue Engineering

Tissue Engineering Manuscript Central: http://mc.manuscriptcentral.com/ten

3D Engineered Nerve: Towards A New Era of Patient-Specific Nerve Repair Solutions

Journal:	*Tissue Engineering*
Manuscript ID	TEB-2020-0355.R1
Manuscript Type:	Review Article - Part B
Date Submitted by the Author:	n/a
Complete List of Authors:	Selim, Omar; University College London, Division of Surgery and Interventional Sciences Lakhani, Saad; University College London, Division of Surgery and Interventional Sciences Midha, Swati; University College London, Division of Surgery and Interventional Sciences Mosahebi, Ash; Royal Free Hospital, Department of Plastic Surgery Kalaskar, Deepak; University College London, UCL Division of Surgery and Interventional Sciences ; University College London, Institute of Orthopaedics and Musculoskeletal Science
Keyword:	3-D Printing < Enabling Technologies in Tissue Engineering (DO NOT select this phrase; it is a header ONLY), Bioprinting < Enabling Technologies in Tissue Engineering (DO NOT select this phrase; it is a header ONLY), Peripheral Nerve < Applications in Tissue Engineering (DO NOT select this phrase; it is a header ONLY), Biomimetics < Enabling Technologies in Tissue Engineering (DO NOT select this phrase; it is a header ONLY)
Manuscript Keywords (Search Terms):	peripheral nerve tissue engineering, nerve biofabrication, nerve gap, nerve CAD model
Abstract:	Reconstruction of peripheral nerve injuries (PNIs) with substance loss remains challenging because of limited treatment solutions and unsatisfactory patient outcomes. Currently, nerve autografting is the first-line management choice for bridging critical-sized nerve defects. The procedure, however, is often complicated by donor site morbidity and paucity of nerve tissue, raising a quest for better alternatives. The application of other treatment surrogates, such as nerve guides remains questionable, and inefficient in irreducible nerve gaps. More importantly, these strategies lack customization for personalized patient therapy, which is a significant drawback of these nerve repair options. This negatively impacts the fascicle-to-fascicle regeneration process, critical to restoring the physiological axonal pathway of the disrupted nerve. Recently, the use of additive manufacturing (AM) technologies has offered major advancements to the bioengineering solutions for PNI therapy. These techniques aim to reinstate the native nerve fascicle pathway using biomimetic approaches, thereby augmenting end-organ innervation. AM-based approaches, such as 3D bioprinting, are capable of biofabricating 3D engineered nerve graft scaffolds in a patient-specific manner with high precision. Moreover, representative in vitro models of

peripheral nerve scaffolds could also be developed, thus eliminating the need for preclinical animal testing. However, the technology is still nascent and faces major translational hurdles. In this review, we spotlighted the clinical burden of PNIs and most up-to-date treatment to address nerve gaps. Next, a summarized illustration of the nerve ultrastructure that guides research solutions is discussed. This is followed by a contrast of the existing bioengineering strategies used to repair peripheral nerve discontinuities. In addition, we elaborated on the most recent advances in 3D printing (3DP) and biofabrication applications in peripheral nerve modeling and engineering. Finally, the major challenges that limit the evolution of the field along with their possible solutions are also critically analyzed.

Title: 3D Engineered Nerve: Towards A New Era of Patient-Specific Nerve Repair Solutions[1]

Author names and Affiliations:

1. Omar A. Selim, MBBCh[1] omar.selim.19@ucl.ac.uk
2. Saad Lakhani, MBChB [1] saad.lakhani.19@ucl.ac.uk
3. Swati Midha, PhD[1,2] s.midha@ucl.ac.uk
4. Deepak M. Kalaskar, PhD[1,3] d.kalaskar@ucl.ac.uk
5. Afshin Mosahebi, MBBS, FRCS, PhD[4] a.mosahebi@ucl.ac.uk

[1]Division of Surgery and Interventional Sciences
Royal Free Hospital, University College London (UCL)
Pond St., London NW3 2QG
United Kingdom

[2]Special Centre for Nanoscience, Jawaharlal Nehru University, New Delhi-110067, India

[3]Institute of Orthopaedics and Musculoskeletal Science,
Royal National Orthopaedic Hospital, UCL
Brockley Hill, Stanmore HA7 4AP
United Kingdom

[4]Department of Plastic Surgery
Royal Free Hospital, University College London (UCL)
Pond St., London NW3 2QG
United Kingdom

Corresponding Author: Deepak M. Kalaskar d.kalaskar@ucl.ac.uk

Author contributions:
Omar A. Selim: Conceptualization, Visualization, Methodology, Investigation, Formal analysis, Software, Writing-original draft preparation, Writing-review and editing, **Saad Lakhani:** Writing-review and editing, **Swati Midha:** Writing-Review and editing, Supervision **Deepak M. Kalaskar**: Writing-Review and Editing, Supervision, Project administration **Afshin Mosahebi**: Writing-review and editing, Supervision.

Keywords: **peripheral nerve, nerve graft,** nerve gap, peripheral nerve tissue engineering, nerve biofabrication, 3D printing, nerve CAD model

---

[1] **Abbreviations:** 3DP- 3D printing, AM-additive manufacturing, PNIs-Peripheral Nerve Injuries, **BDNF:** brain-derived neurotrophic factor, **BM-MSCs:** bone marrow-mesenchymal stem cells, **BNB:** blood-nerve barrier, **CAD:** computer-aided design, **CAP:** compound action potential, **CT:** computed tomography, **DPSCs**: dental pulp stem cells, **DLP:** digital light processing, **ECM:** extracellular matrix, **EFLCs:** endoneurial fibroblast-like cells , **EHD:** electrohydrodynamic, **FDM:** fused deposition modeling, **GC-MS:** gelatin methacrylate/chitosan- microspheres, **GDNF:** glial cell line-derive neurotrophic factor, **GelMA:** gelatin methacrylate, **HFSCs**: hair follicle stem cells, **IGF-1:** insulin like growth factor, **iPSCs:** induced pluripotent stem cells, **LAB:** laser-assisted bioprinting, **LFDM:** Low Frozen Deposition Manufacturing (LFDM), **mPa:** milli Pascals, **MPa:** Mega Pascals, **MRI**: magnetic resonance imaging, **NCV:** nerve conduction velocity, **NGCs:** nerve guidance conduits, **NGF-β:** nerve growth factor, **NSCs:** neural stem cells, **NT-3**: neurotrophin-3, **PC12:** pheochromocytoma-derived neuronal cell line, **PAA:** poly acrylic acid, **PCL:** polycaprolactone, **PLA**: poly (lactic acid), **PLCL:** poly (l-lactide-co-ε-caprolactone), **PLGA:** poly (lactic-co-glycolic acid), **PEG:** polyethylene glycol, **PET:** positron emission tomography, **PMR:** preferential motor reinnervation, **PNTE:** peripheral nerve tissue engineering, **PPy:** polypyrrole, **rGO:** reduced graphene oxide, **RP:** rapid prototyping, **RSC96:** rat Schwann cell line, **SC:** Schwann cells, **SLA:** stereolithography, **TEM:** transmission electron microscopy, **VEGF:** vascular endothelial growth factor, **μSL:** microstereolithography.

Abstract:

Reconstruction of peripheral nerve injuries (PNIs) with substance loss remains challenging because of limited treatment solutions and unsatisfactory patient outcomes. Currently, nerve autografting is the first-line management choice for bridging critical-sized nerve defects. The procedure, however, is often complicated by donor site morbidity and paucity of nerve tissue, raising a quest for better alternatives. The application of other treatment surrogates, such as nerve guides remains questionable, and inefficient in irreducible nerve gaps. More importantly, these strategies lack customization for personalized patient therapy, which is a significant drawback of these nerve repair options. This negatively impacts the fascicle-to-fascicle regeneration process, critical to restoring the physiological axonal pathway of the disrupted nerve. Recently, the use of additive manufacturing (AM) technologies has offered major advancements to the bioengineering solutions for PNI therapy. These techniques aim to reinstate the native nerve fascicle pathway using biomimetic approaches, thereby augmenting end-organ innervation. AM-based approaches, such as 3D bioprinting, are capable of biofabricating 3D engineered nerve graft **scaffolds** in a patient-specific manner with high precision. Moreover, representative *in vitro* models of peripheral **nerve scaffolds** could also be developed, thus eliminating the need for preclinical animal testing. However, the technology is still nascent and faces major translational hurdles. In this review, we spotlighted the clinical burden of PNIs and most up-to-date treatment to address nerve gaps. Next, a summarized illustration of the nerve ultrastructure that guides research solutions is discussed**. This is** followed by a contrast of the existing bioengineering strategies used to repair peripheral nerve discontinuities. In addition, we elaborated on the most recent advances in 3D printing (3DP) and biofabrication applications in peripheral nerve modeling and engineering. Finally, the major challenges **that limit the evolution** of the field along with their possible solutions are also critically analyzed.

Impact Statement:

Complex nerve injuries including critical-sized gaps (>3 cm loss of substance), gaps involving nerve bifurcations and those associated with ischemic environments are difficult to manage. A biomimetic, personalized peripheral nerve tissue surrogate can overcome these challanges to address these challanges. The peripheral nerve repair market currently represents a multi-billion-dollar industry that is projected to expand. Given the clinical and economical dilemmas posed by this medical condition, it is crucial to devise novel and effective nerve substitutes. In this review article, we discuss progress in 3D printing technologies including biofabrication and nerve CAD modeling, towards achieving a patient-specific and biomimetic nerve repair solution.

1. Introduction

The surgical management of peripheral nerve injuries (PNIs) remains a major clinical challenge with suboptimal clinical outcomes.[1,2] PNIs cause devastating functional disabilities in patients, leading to impaired quality of life. Annually, more than one million people suffer from PNIs worldwide, with approximately 200,000 patients in the US and 300,000 in Europe requiring surgical repair.[3,4] Moreover, an increasing incidence of PNIs is reflected by the forecasted growth in the peripheral nerve repair market, which is expected to exceed $10 billion by 2022.[5] Traumatic nerve injuries secondary to road traffic accidents, fractures, lacerations, and traction injuries represent the most common entity of PNIs encountered in reconstructive practice. According to the largest published clinical series, the prevalence of PNIs in polytrauma victims is approximately 1-3%. [6,7,8] Other important and under-reported causes of PNI and nerve discontinuity include iatrogenic nerve injuries, most often complicating operative orthopaedic interventions,[9,10] and oncologic resection of nerve sheath tumors such as schwannomas and neurofibromas, which could potentially be complicated by a nerve gap that require reconstruction.[11,12]

1.1 Peripheral nerve repair and current therapeutic options:

Depending upon the severity of the nerve injury, guided by the Seddon-Sunderland classification system, the functional recovery and treatment strategy can be initially established (table 1).[13,14,15] In grade IV and V, surgical intervention is inevitable and the choice of technique is, essentially, contingent on the presence of scarring, nerve substance loss, and size of any nerve gap.[16] Currently, primary repair in the form of tensionless end-to-end neurorrhaphy is the gold standard for nerve reconstruction, where gap size is less than 2 cm.[17,18] It is critical that any nerve repair should not be performed under tension, which could otherwise compromise microvascular blood flow and impair nerve regeneration.[19] Unfortunately, in several instances, initial injury can cause significant substance loss resulting in long gaps (> 2 cm), or, due to the loss of biotensegrity, transected nerves may undergo retraction that makes tension-free repair surgically infeasible.[20]

1.1.1 The nerve autograft

In the presence of irreducible nerve defects, an interposition human autograft, usually the sural nerve, represents the optimal approach to restore nerve continuity.[21] Autografts have the advantages of providing the inherent nerve extra-cellular matrix (ECM) and cellular components including Schwann cells (SCs), thus offering the most physiologic solution to nerve replacement. However, this procedure often results in donor-site morbidity secondary to neuroma formation that presents as tingling, numbness, and pain in the dermatome supplied by the sacrificed nerve.[22] In addition, low success rates can occur due to unpreventable size and fascicular mismatch and scarring in the graft bed. Other limitations of this procedure also include the sparse amount of donor tissue available and creation of additional surgical sites for nerve harvesting.[23]

Furthermore, it is critical to emphasize the importance of vascularization in maintaining the longevity of the transplanted autograft and increasing the rate of axonal regrowth.[24] Theoretically, the presence of adequate perfusion to the graft tissue provides an optimal nutritional milieu permissive for nerve regeneration via the following mechanisms: (1) supporting the viability of SC population, (2) reducing fibroblastic invasion and endoneurial scarring, (3) stimulating axon remyelination, and (4) accelerating the process of Wallerian degeneration and elimination of myelin debris.[25,26,27]

Traditionally, the classic nerve autograft has no vascular supply, and upon implantation, the graft initially survives by plasmatic imbibition during the first week.[28] Later, nerve graft revascularization from the recipient bed capillaries and neighboring reconstructed nerve stumps occurs in the subsequent weeks postoperatively.[29,30] This physiological initial delay in the angiogenesis induction of graft tissue makes it liable to local ischemia that could impair nerve regeneration particularly across wide gaps. To achieve prompt and continuous revascularization of the transplanted neural tissue, a vascularized nerve graft (VNG) represents a clinically promising alternative.[31]

First described by Taylor and Ham in 1976, the free VNG has a dominant arterial pedicle that can be anastomosed to vessels of the recipient bed using microsurgical techniques.[25,32] Experimental and clinical evidence have demonstrated the superiority of VNGs over conventional nerve autografts in supporting nerve regeneration and achieving better outcomes in scarred, ischemic beds and long gaps (>6 cm).[24,33,34] Moreover, VNGs are commonly indicated in proximal nerve lesions e.g. brachial plexus injuries to mitigate denervation atrophy of hand muscles.[31,35,36]

1.1.2 Nerve conduits or tubulization:

Alternatively, nerve conduits can also be used in the repair of PNIs to obviate the complications of autografting. Nowadays, the Food and Drug Administration (FDA) has approved several polymeric nerve conduits, wraps, and decellularized allograft tissues to bridge nerve discontinuities (table 2). However, they are mainly indicated for small gaps (< 3 cm) and fail to outperform the clinical standard.[22] Nerve guidance conduits (NGCs), also referred to as tubulization, are synthetic or biological hollow tubes that aim to appose the proximal and distal transected nerve stumps in an enclosed chamber. Through the creation of this secluded milieu, NGCs are hypothetically anticipated to support nerve regeneration by, first, reducing the loss of neurotropic cues and neurotrophic growth factors to the surroundings, thereby establishing a conductive microenvironment for axonal regrowth and guidance. Secondly, conduits act as a barrier against myofibroblast invasion and fibrosis formation, which can undermine axonal regeneration.[37] Thirdly, they are expected to promote proper migration of sprouting axons to the distal nerve stump and prevent collateral sprouting/axonal misdirection that can lead to neuroma formation.[38]

Despite the wide variety of synthetic conduits available commercially, clinical studies that have compared the outcomes of conduits to nerve autografts are few, unreliable (no double-blinded randomized controlled trials) and show unpredictable performance in gaps above 4 mm.[39,40,41] Furthermore, NGCs fail remarkably to promote nerve functional recovery over gaps exceeding 3 cm due to the lack of SCs, ECM skeletal framework and adhesion molecules that provide trophic and mechanical support to migrating axons over this critical distance (figure 1). These factors have limited the use of conduits to the repair of short gaps (< 3cm) occurring in small diameter non-critical sensory nerves.[22] In addition, biological conduits such as vessels, most commonly veins, and muscle grafts have also been used for peripheral nerve repair.[42,43] The therapeutic basis of venous conduits in nerve regeneration is believed to be mediated by the venous endothelial lining, which secretes nerve growth factor and contains laminin-rich basal lamina that facilitates SC migration and proliferation.[44,45] Likewise, skeletal muscle grafts provide longitudinally arranged basal lamina that can help directing the growth cone of regenerating axons.[42]

1.1.3 The nerve allograft

Another nerve surrogate becoming widely adopted in nerve repair is the acellular allograft, commercially available off-the-shelf under the trade name Avance® (Axogen Inc., Florida, USA).[46] Nerve allotransplantation has been used in cases where autograft tissue might be inadequate to bridge nerve discontinuities.[47] However, unprocessed nerve allotransplants expose the patient to risks of systemic

immunosuppression-related complications. Therefore, decellularized allogeneic nerve tissue was developed to preclude the need for post-transplant immunosuppressive therapy. Decellularization attenuates the allograft antigenicity by eliminating intrinsic cellular elements (SCs, endothelial cells, and fibroblasts), which mediate the rejection mechanism *via* harboring the major histocompatibility complex. Concomitantly, the inherent nerve architecture together with ECM proteins and basal lamina tubes can be preserved to provide mechanical guidance for the regenerating nerve fibers and scaffolding for native SCs for migration. Decellularized cadaveric peripheral nerve tissues using chemical processing (detergents)[48], cold preservation[49], freezing and freeze-thawing[50], and irradiation[51] have been used. But, acellular allografts lack SCs and have an internal microarchitecture that does not match that of the recipient nerve, hence failing to restore optimal neural regeneration.

Irrespective of the type of repair, the prognosis of long gap PNIs is **unsatisfactory**. This is, essentially, the result of erroneous target innervation secondary to the inadvertent axonal misrouting that happens as nerve fibers traverse the critical interphase between the proximal and distal nerve stumps.[52,53] **The field of peripheral nerve surgery lacks an anatomically analogous nerve replacement that clinically matches or surpasses the autograft**. This is partly due to complex regulatory barriers and, most importantly, the failure of conventional tissue engineering strategies to reproduce the anatomical intricacy of the peripheral nerve architecture in terms of the cellular network, native tissue ECM composition, mechanical properties, and the fascicular topography.

1.2 Scope of 3D additive manufacturing (AM) technology:

To address these shortcomings, AM technologies have been leveraged to create complex three-dimensional (3D) tissue constructs in a layer-by-layer fashion from predefined computer-aided design (CAD) models. Recently, 3D printing (3DP) and bioprinting have emerged as powerful advanced fabrication tools due to their ability to develop personalized replacement therapies and implants with high precision.[54,55,56] Furthermore, 3D bioprinting could potentially offer control over the spatial organization of cellular components and biological guidance cues, which would allow researchers to devise a biomimetic fascicular pathway to enhance nerve regeneration. Since the recovery of nerve function is contingent on the correct matching of motor and sensory fibers to their respective motor endplates and sensory receptors, in addition to precisely matching the fascicles in both nerve segments, these technologies should, ultimately, allow the development of patient-specific nerve alternatives that achieve this desired fascicle-to-fascicle regeneration.[23] However, prior to proceeding with the recent developments in the field, a summarized outline of the peripheral nerve ultrastructure is described to understand the target tissue.

2. Gross and histological features of the peripheral nerve:

The peripheral nervous system (PNS) is anatomically composed of the **cranial nerves III to XII** and spinal nerves that emanate directly from the brain (including the brainstem) and spinal cord, respectively.[57] Peripheral nerves travel throughout the body relaying neural signals and commands from the central nervous system (CNS). Individual nerve bundles consist of motor, sensory, and/or autonomic fibers, which have distinctive conduction velocities, functions, and diameters.[58,59,60]

2.1 Connective tissue (CT) layers:

Cross-sectionally, a peripheral nerve is composed of connective tissue with three distinctive layers: the epineurium, perineurium, and endoneurium (figure 2). Dissecting the polymeric and cellular compositions of these layers influences the choice of biomaterials and cells for fabricating nerve guides or tissue engineered nerve alternatives (table 3). The epineurium forms the outermost collagenous layer investing

multiple fascicles and the intrinsic neural vasculature. Each single fascicle is wrapped by concentric layers of cellular ensheathment called the perineurium, which consists of flat perineurial cells separated by collagen fibers.[65] The innermost layer is the endoneurium, which wraps and protects the SC-axon complexes. This layer contains highly anastomosing networks of fine microcapillaries that provide oxygenation and nutrition to the intra-endoneurial structures.[66]

The endoneurial microvessels are formed of endothelial cells that share their basement membrane lining with pericytes. In addition to the intercellular tight junctions between the perineurial cells, the endoneurial microvasculature collectively forms a dynamic anatomical and physiological diffusion barrier known as the blood-nerve barrier (BNB) or the blood-nerve interface (BNI).[66] The BNI maintains the homoeostasis of the endoneurial microenvironment by stringently regulating the entry of electrolytes, water, and other small molecules into this isolated milieu. This restrictive permeability of the BNB prevents drastic changes in ion concentration and endoneurial fluid pressure due to variations in the blood pressure and volume, which could impair efficient action potential transduction.[67,68] Therefore, when engineering artificial biomimetic neural tissues, it is important to ensure that these highly controlled microenvironments are meticulously replicated and maintained.

2.2 Cellular components:

Peripheral nerves are composed of multiple cell types with distinctive functions. SCs are the primary neuroglial cells of the PNS that provide metabolic and trophic support to axons. In mature, adult peripheral nerves, two major SC phenotypes are identified: myelinating and non-myelinating (Remak) SCs (table 4). Myelinating SCs are most abundant in the PNS and produce lipid-rich myelin, which provides electrical insulation for axons that permit fast, saltatory conduction of action potentials across the long distance spanned by peripheral nerves.[76] Interestingly, SCs may also exhibit motor and sensory phenotypes that are associated with modality-specific axonal regeneration.

SCs that are coupled to the sensory nerve fibers express high levels of nerve growth factor (NGF-β), insulin like growth factor (IGF-1), and erythropoietin (Epo). On the contrary, SCs associated with motor axons produce glial cell line-derive neurotrophic factor (GDNF) and pleiotrophin.[77] Thus, it is apparent that SCs may undergo phenotypic modulation to best support the axonal systems with which they are associated.[76]

In addition, other cell types within the peripheral nerves include perineurial cells, endoneurial fibroblast-like cells (EFLCs), mast cells, pericytes, macrophages, and vascular endothelial cells. Perineurial cells, that render elasticity to the perineurium, are specialized myoepithelial fibroblasts. These cells physically contribute to the formation of the perineurial barrier that separates the epineurial and endoneurial interstitial fluid compartments.[78] In the endoneurium, EFLCs are spindle-shaped cells that represent approximately 2-9% of endoneurial cells. EFLCs typically possess irregular basal lamina and extended, angular cytoplasmic processes, which make them distinct from other endoneurial cells. The role of EFLCs has long been debated, however, they might be involved in myelin phagocytosis, immune surveillance, and mediating the inflammatory response following nerve injury.[79] Other endoneurial cells include pericytes, which are specialized smooth muscle cells that control the response of the endoneurial microvasculature to abrupt changes in blood volume and pressure.

The interplay between the various heterogeneous cell populations existing in peripheral nervous tissue is critical for recreating the microenvironment supportive of axonal regeneration following injury.[80,81] For instance, resident and circulating macrophages have shown to play instrumental role in peripheral neural repair.[82] In case of an injury, macrophages are typically the first cells to get recruited and remove the degenerated myelin and fragmented cell and axonal segments.[83] Vascular endothelial growth factor-A (VEGF-A), released by the macrophages, leads to the formation of polarized microvasculature within the regenerative cords of the proximal and distal nerve segments.[84] These vessels were shown to be crucial in

guiding SC migration. Although it may seem counterintuitive, nerve fibroblasts might also promote nerve regeneration *via* favoring the mature SC phenotype and promoting basal lamina deposition.[85] One study explored the effect of nerve regeneration in a 5 mm sciatic nerve gap by transplanting a co-culture of mice nerve fibroblasts and SCs in rodent model.[86] Results revealed that a 1:2 ratio of fibroblasts and SCs enhanced the process of nerve regeneration significantly, resulting in superior functional recovery compared to SCs only. Therefore, these findings underscore the importance of multi-cellular engineered living systems when considering cell-based therapies including biofabricated neural tissues for peripheral nerve regeneration

3. Differential regenerative ability of motor and sensory axons:

As illustrated previously, accurate and specific target (skin and muscle) reinnervation is central to meaningful functional recovery following nerve transection. The misrouting of motor and sensory nerve fibers during nerve repair could explain the poor recovery seen in patients following mixed nerve injury, for instance.[87] Therefore, elucidating the molecular cues during the course of regenerating axons could facilitate engineering of modality-specific trajectories and cell-selective biomaterials.[88] Eventually, the misdirection of nerve collaterals and inappropriate reinnervation could be prevented.

Basic science research has demonstrated that specific cell adhesion molecules and neurotrophic factors are implicated in the selective regeneration of motor and sensory axons after nerve injury, although exact mechanisms remain unclear.[89] In addition, differential gene expression patterns have been observed in motor and sensory SC phenotypes to support selective axonal reinnervation.[90,91] Accordingly, strategies that overexpress proregenerative genes and trophic signals can be employed to modulate or enhance neural functions such as myelination and axonal growth cone motility.[92,93]

3.1 Cell adhesion molecules (CAMs):

Accumulating evidence indicates the involvement of various CAMs in axonal growth cone pathfinding, cell survival and migration during neural repair.[94,95,96] Essentially, CAMs belonging to the immunoglobulin (IgG) superfamily, commonly known as IgCAMs, are highly expressed in the PNS and impact neuron cellular function post injury.[97] IgCAMs are transmembrane glycoproteins composed of extracellular and intracellular domains. The latter is attached to cytoskeletal elements such as actin and microtubules and mediate intracellular signaling pathways. By impacting the polymerization and disassembly of the cytoskeletal molecules, IgCAMs can influence axonal outgrowth and neuronal cell motility. Most notable IgCAMs implicated in peripheral nerve regeneration include neural cell-adhesion molecules (NCAMs), L1-CAM (L1 cell-adhesion molecule), and the close homolog of L1 (CHL1).[97]

NCAMs have been shown to contribute to preferential motor reinnervation (PMR). PMR refers to the intrinsic ability of regenerating motor axons to selectively reinnervate muscle targets.[98] Mixed nerves usually give off branches carrying purely somatosensory or motor supply. Thus, it is critical that following nerve transection, axons of the proximal stump do not intermingle along their regeneration course and selectively resupply their normal peripheral targets through recognition of appropriate growth substrates.[99] In this regard, Franz et al. demonstrated that the expression of polysialic acid (PSA) moiety of NCAM, a negatively charged glycan, by axons was essential for selective muscle reinnervation.[100] The proposed mechanism by which PSA promotes PMR is believed

to be due to direct attenuation of cell-cell adhesive interactions. This effect is thought to enhance the response of sprouting motor axons to specific, instructive guidance ligands expressed in motor pathways.

Moreover, a recent study established the role of CHL1 molecule in the guidance of regenerating motor fibers, thereby promoting PMR.[101] The authors hypothesized that PMR facilitated by CHL1 is mediated via semaphorin 3A and neuropilin 1/2 signalling. In contrast, the L1 adhesion molecule was found to be critical in sensory axon regeneration. In L1-deficient mice, SCs become malformed and fail to ensheath sensory axons and axon survival is impaired.[102,103] These findings emphasize the importance of exploiting cell adhesion signalling towards establishing novel pathways that enable modality-specific axonal regeneration across nerve gaps.

3.2 Trophic signals:

Similarly, SCs from motor and sensory axons overexpress and secrete distinct types of neurotrophic growth factors (NTFs) following axotomy.[104] This differential response might also contribute to the selective regenerative capacity of axons towards their relevant pathways. Several *in vitro* and animal studies have demonstrated that NGF and neurotrophin-3 (NT-3) have preferential sensory profile.[105.106,107] In DRG organotypic cultures, NT-3 was found to exert oriented, organized and linearly direct axonal growth of DRG neurites, unlike NGF. Furthermore, both growth factors can act synergistically, when combined together, to promote the guidance of DRG sensory axons over longer distances.[108] Cao and colleagues demonstrated that combined concentration of NGF/NT-3 of 80 ng/mm/mL each result in 12.5 mm guided distance of axon elongation compared to 7.5 mm when NGF is used alone.[108] Both neurotrophins where shown to mediate their effect on axonal elongation via activation of tyrosine kinase (Trk) receptors and STAT3 (signal transducer and activator of transcription 3) signaling.[109]

Other members of neurotrophins such as brain-derived neurotrophic factor (BDNF) and glial cell line-derived neurotrophic factor (GDNF) were reported to be neuroprotective to motor neurons and play role in PMR.[110,111] A study by Santos et al. demonstrated a dose-dependent effect of BDNF on the regeneration of motor axons both *in vitro* and *in vivo*.[110] The authors showed that a high dose of BDNF (50 ng/mL) significantly stimulated the outgrowth of motor neurites from organotypic spinal cord slices significantly compared to low concentrations (5 and 10 ng/mL). In comparison, the same high BDNF dose did not result in sensory axonal elongation from DRG cultures. Similarly, *in vivo* administration of BDNF in a rat nerve gap model resulted in significantly increased number of regenerated motor neurons in all treated groups compared to control. However, only low concentration (1 ug/mL) of BDNF resulted in higher number of regenerated sensory neurons, which confirm the selective motor regenerative property of BDNF through dose manipulation.

Despite these findings, molecular mechanisms underlying axonal cone guidance remain complex and requires further investigation. Eventually, detailed knowledge of the guidance cues and signaling pathways would allow researchers to immobilize well-defined gradients of trophic signals on various scaffolds to stimulate the effective migration of sprouting nerve fibers to their distal targets. Moreover, the spatiotemporal delivery of trophic signals to a confined nerve gap is challenging, which creates an unmet demand for advanced drug delivery systems that release neurotrophic factors at appropriate timing and dosage.[112]

3.3 Gene expression profile:

The pattern of gene expression also differs between motor and sensory SC phenotypes. Using gene chip analysis, Jesuraj et al. demonstrated upregulation of neurofilament light polypeptide (NEFL) and protein kinase C iota (PRKCi) genes in the motor pathways of rat femoral nerves.[113] Both NEFL and PRCKI gene products regulate SC-axon intercellular signalling, and motor neuron myelination and growth. In comparison, myelin basic protein (MBP) and neuroligin-1 (Nlgn1) genes were found to be upregulated in the sensory branches. Both MBP and neuroligin-1 genes are hypothesized to play role in neural myelination and synaptic transmission across the sensory nervous system. [113]

4. State-of-the-art bioengineering strategies for peripheral nerve repair

Based on the anatomical complexity, reproducing the native peripheral neural tissue architecture is difficult. Historically, the focus of research for bridging nerve gaps relied upon protecting the endogenous reparative mechanism by using conduits, as described earlier. Now, research trends towards developing biomimetic alternatives to the nerve autograft. Furthermore, as healthcare delivery is shifting towards personalized therapy, it will be of paramount importance to tailor nerve repair solutions that would take into account the patient's specific nerve anatomy as well as unique disease condition. Herein, we review the three key bioengineering schemes currently being investigated in this field. In an increasing order of complexity, a biomaterials-based, a conventional tissue engineering-based, and additive manufacturing-based approaches exist for replacing nervous tissue (figure 3). Although an overlap may exist between these different paradigms, it is crucial to elucidate the distinctions between them, as each strategy will eventually have different regulatory paths and translational challenges.

4.1 Biomaterials-based approach:

Recent progress in materials science and polymer synthesis technologies has made huge leaps in the design of artificial nerve guidance devices. A biomaterials-based approach involves, essentially, devising innovative nerve conduits using advanced biomaterials with neuroregenerative capacity.[3] In addition, this approach focuses on optimizing the conduit's interior architecture to facilitate the formation of robust fibrin cables, which can enhance axonal migration. Generally, an ideal biomaterial candidate for the fabrication of peripheral nerve conduits should exhibit the following criteria[114]: 1) biocompatibility, should not elicit an immunological or allergic reaction once implanted in the host, 2) biodegradability with non-toxic degradation byproducts, to eliminate the need for a secondary surgery, 3) neuroinductivity, should be able to induce neuronal and glial cell differentiation 3) neuroconductivity, should be capable of transmitting neural impulses from proximal to distal nerve segments, 4) porosity, to allow for vascular infiltration and tissue remodelling, 5) semi-permeability, should permit gaseous exchange and nutrient transport for supporting cell survival, 5) flexibility, more relevant for repairs across joint sites, 6) suturability and mechanical robustness, should withstand shear stress and compressive pressure from surrounding tissue.[115] In this regard, several natural, synthetic, and hybrid biomaterials have been exploited for the design of novel nerve conduits, each possessing their own advantages and limitations (table 5).

Several fabrication processes have been applied for manufacturing NGCs including injection molding[133], solvent casting (with or without particulate leaching)[134], phase separation[135], freeze-drying[136] and electrospinning.[137] Among these, injection molding and electrospinning are the most commonly utilized techniques for developing NGCs.[138] However, electrospinning results in highly disordered and random fibers, whereas solvent casting uses toxic organic solvents during the fabrication process, which could produce scaffolds with traces of these harmful chemicals. Nevertheless, they are all limited by the lack of reproducibility, inability to control the porosity, pore size, and interconnectivity of the scaffolds.[139]

Furthermore, the fabrication of complex patterns such as multi-lumen conduits using these techniques is technically challenging.

Single-lumen hollow NGCs fail dramatically to induce neural regeneration across critical-sized nerve defects (~30 mm in rabbits and humans, ~15 mm in rat). Thus, research is directed towards modifying their interior architecture and incorporating intrinsic structural frameworks, pivotal for effective axonal regrowth across these critical gaps. In pre-clinical testing, most of these modifications have increased the size of gap that can be repaired in rat sciatic nerve models from 10 to 15-20 mm.[114] Few clinical case reports have demonstrated potential efficacy of poly (glycolic) acid (PGA) filaments, collagen sponges, and other intrinsic structural frameworks in achieving motor and sensory recovery in long gap nerve defects.[140,141] For more comprehensive reviews on the latest progress in conduit design, please refer to articles by Wang and Cai, 2010, Daly et al., 2012, and Vijayavenkataraman, 2020.[3,142,143]

4.2 Conventional tissue engineering (TE)-based approach:

The sole use of biomaterials, however, represents a passive approach for restoring nerve integrity. Being completely reliant on the healing capacity of the patient's body and, eventually, the severed nerve regenerative potential, nerve repair using conduits only, could be insufficient for inducing functional neural recovery.[144] This becomes important in the presence of critical gaps that exhibit extremely limited nerve regeneration as a result of poor ECM formation, diminution in the neurotrophic support, and limited SC migration and proliferation. Accordingly, topographical or molecular modifications of nerve conduits haven been coupled with the presence of an active biological neuroregenerative component such as cells or biological cues to augment the physiological neural repair process. Conventional peripheral nerve tissue engineering strategies applies the classic TE triad that combines (1) scaffolds, (2) cells, and (3) growth factors to develop more robust regenerative templates with desirable mechanical properties mimicking the native nerve.[145,146,147] To this end, cell supplementation of polymeric NGC or decellularized allografts has been pursued as a viable strategy to augment the regenerative cellular response to PNIs.[148]

Being the primary supporting cells in the PNS that orchestrate endogenous reparative mechanisms following PNIs, SC transplantation in combination with nerve scaffolds has been widely investigated, particularly across critical nerve gaps.[149] In comparison to hollow conduits, scaffolds loaded with SCs, *in vivo,* demonstrated superior nerve repair and functional recovery.[3] SCs mediate neural repair through deposition of their own basal lamina, promoting re-myelination of regenerating axons, and more importantly, help in creating cell-secreted chemotropic gradients that are critical for directing the growth cone of nerve fibers, a phenomenon known as growth cone chemotaxis. However, the invasive extraction methods of SCs necessitating the sacrifice of a healthy nerve and prolonged culture period are major drawbacks of SC transplantation.[150] This has motivated researches to consider alternative cell types and sources. Cell-based therapies utilize the potential of autologous stem cells, adipose-derived and bone-derived mesenchymal stem cells (MSCs), for peripheral nerve repair because of their abundance, plasticity, relatively facile isolation and culture techniques.[151,152,153] Although they have different embryological origin, MSCs trigger the process of peripheral nerve regeneration *via* paracrine mechanisms through the release of neurotrophic growth factors such as NGF, GDNF, and BDNF.[154] Besides, the immunomodulatory properties of MSCs could potentially reduce infiltration of collagen and scar tissue formation in the conduit.[155] Other slightly lesser explored sources of stem cell investigated for peripheral nerve tissue engineering are induced pluripotent stem cells (iPSCs), dental pulp stem cells (DPSCs), hair follicle stem cells (HFSCs) and neural stem cells (NSCs).[156,157]

Cells have been introduced into nerve conduits using different techniques including, suspension cultures encapsulated within intraluminal hydrogels[158], seeding prefabricated scaffolds or intraluminal guidance structures in culture and intraluminal injection.[151,159,160] However, these conventional methods have significant limitations. First, simple encapsulation of cells in a hydrogel or top seeding on scaffolds is time-

consuming and often leads to heterogeneous distribution of cells within the 3D structure. This leads to lack of precise control over the cell density arising from non-uniform cell attachment. In addition, weak cell-matrix compliance can potentially result in cell detachment when implanted *in vivo*. Cell leakage and migration out of the conduits are also possible complications of luminal cell injections and seeding.[161] These shortcomings have resulted in the inability of these scaffolds to effectively generate and harness the complete potential of cell-secreted neurotrophic gradients.

Additionally, neurotrophic growth factors including NGF[162], GDNF[163], BDNF[164], neurotrophin-3 (NT-3)[165], and VEGF[166] have also been employed in peripheral nerve regeneration as they play vital role in promoting SC proliferation and migration, guiding neurite outgrowth, and inducing neuroprotection.[37,167] Besides, the presence of spatiotemporal and concentration gradients of chemokines and growth factors are crucial for tissue development, especially for directionally oriented tissues such as peripheral nerves.[168] By creating scaffolds with true biochemical, directional gradients of one or multiple growth factors, the process of driving the migration of SCs into the regenerating nerve bridge and axon elongation could be facilitated. Traditionally, the delivery of neurotrophic growth factors from nerve conduit wall has been achieved by either tethering or physically adsorbing the proteins to the wall material. Several attempts have been made to optimize release kinetics and prolong localized availability of bioactive molecules. These include protein entrapment in hydrogel matrix loaded into the conduit lumen or encapsulation in microspheres embedded in the conduit wall.[169] Nevertheless, problems related to initial burst release, loss of bioactivity, and poor bioavailability remains unresolved. More importantly, theses growth factor presentation strategies do not sufficiently reproduce the complexity of the ECM microenvironment, pivotal for inducing satisfactory nerve regeneration over critical gaps. Accordingly, advanced fabrication strategies such as 3D bioprinting are needed to effectively engineer these spatially controlled niches and gradients.

4.3 Additive manufacturing (AM)-based approach:

With major shortfalls associated with classical biomaterial and TE fabrication methods, there is an immense demand for designing scaffolds that can be fabricated with superior resolution, flexibility, speed, and scalability for regenerating complicated nerve gaps. Recently, sophisticated, cost-effective industrial systems such as rapid prototyping (RP) including additive manufacturing (AM) have been utilized in the healthcare arena. AM-based strategies are centered on the automated and timely production of 3D structures with predefined geometries using computer-aided modeling. Structural assembly is then achieved *via* sequential and precise placement of materials in a layer-by-layer fashion to yield geometrically complex shapes, which could not be produced by other techniques such as subtractive manufacturing.[170] AM-based processes are also widely exploited in pharmaceutical delivery, preoperative surgical planning, and surgical education.

AM is currently being explored to develop personalized nerve substitutes, *in vitro* models for peripheral nerve research, and advanced tissue engineered peripheral nerve solutions. A typical additive manufacturing or 3D printing workflow can be broken down into three steps: (1) image acquisition and segmentation, (2) mesh model creation, and (3) 3D printing. The first step involves capturing images of the organ of interest using tomographic medical imaging such as computed tomography (CT), magnetic resonance imaging (MRI), or positron emission tomography (PET) studies. It is critical to highlight that 'diagnostic' imaging modalities are certainly not the best study for optimal 3D print generation particularly in tissues where minute morphological details are vital. For instance, magnetic resonance neurography (MRN), albeit being an advanced neuroimaging technique, is not optimal for depicting detailed fascicular anatomy including the endoneurial tubes. Nevertheless, Hu and coworkers used MRN as a proof of concept to reconstruct a patient's sciatic nerve and generate NGC conduit model for indirect 3D printing.[171] Generally, scan parameters that allow the accurate visualization of the desired anatomic tissue will be similar to those used to generate the 3D printed structure. Following image acquisition, the organ of interest needs to be segmented. Image segmentation involves isolating the target structure from the rest of the

scanned anatomy and delineating boundaries between various tissues in images to generate patient-specific, highly accurate models of the desired organ. Segmentation can be done using commercially available resources such as Osirix MD, 3D Slicer, or Materialise Mimics Imprint.

In the second step, post-processing of the segmentation into a 3D printable mesh is performed and an .STL (Standard Tessellation Language) file is created from the segmented anatomy using CAD tools. This step involves further manipulation to eliminate flaws and correct errors and discontinuities in the segmented model that arise during the processes of image segmentation or exporting. Following mesh refinement, the final step involves exporting the refined 3D model to the printer using different file formats. The most commonly used file formats for AM are STL, VRML (Virtual Reality Modeling Language), and the .OBJ formats.[172] Several techniques can be utilized for non-biological 3D printing or bioprinting of the designed structure, each with their own advantages and limitations. In this section, we will elaborate more on these processes and their most recent applications to develop personalized nerve conduits and bioprinted constructs for peripheral nerve regeneration.

4.3.1 3DP of nerve guidance conduits

Non-biological 3D printing has been used in clinic to generate anatomical models and bespoke implants for preclinical education and therapeutic applications, respectively.[173,174,175] Generally, this subtype of AM is predominantly focused on hard tissue regeneration such as bones and teeth owing to the inherent rigidity of the majority of used biomaterials.[176] Nevertheless, this technology has found further applications in the research field of peripheral nerve surgery through the development of customized 3D-printed nerve guides. This could potentially enable repairing injuries involving complex injuries involving nerve bifurcations that are surgically irreparable using currently available nerve conduits (figure 4). From a technical perspective, 3DP offers also more versatility over controlling the internal structure of the fabricated scaffold including the ability to modulate porosity, pore size, and mechanical properties, unlike conventional approaches.

To date, several advanced multi-functional NGCs have been additively manufactured using various 3DP approaches and polymers. Technically, 3DP methods can be classified into stereolithography apparatus (SLA), digital light processing (DLP), fused deposition modeling (FDM), and inkjet 3D printing. Each printing modality is associated with unique merits and drawbacks, and more importantly, uses different types of printable biomaterials. A summary of the biomaterials most recently used for fabricating NGCs using 3D printing techniques and salient design features and *in vitro* and *in vivo* findings can be found in table 6. Herein, we will delineate and contrast the different techniques that have been utilized in the 3DP of nerve guides.

<u>SLA 3DP</u>

SLA is regarded as the earliest and most mature RP technique available nowadays[193,194]. NGCs developed using SLA exhibited excellent mechanical performance and advanced structural features such as intraluminal topographical guidance cues concurrently (**table 6**). SLA is essentially a liquid-based technology that converts liquid polymer resins to complex and multi-functional solid architectures in a cost-effective and scalable fashion. The method is based on photopolymerization reactions that proceed under visible or ultraviolet (UV) light in the presence of a photosensitive system of unsaturated prepolymers and photoinitiators (PIs)[195]. Light irradiation controlled by CAD releases initiating species (e.g. radicals or cations) from the PIs, which then attack the electron-poor carbon-carbon (C=C) double bonds of monomers or oligomers to form covalent bonds between monomeric units leading to liquid-solid phase transition of the resin. Traditionally, an SLA system consists of three components: (1) a bath (vat) of photocrosslinkable resin, (2) a mobile platform residing inside the vat, and (3) a UV laser source to cure the resin in layers as

the platform descends deeper into the vat. The solidification of the resin continues on a slice-by-slice basis until the entire solid 3D object is generated.

An interesting feature of SLA is the ability to control the pattern formation of each individual layer by moving the laser beam, which permits the facile printing of large volume models with intricate designs. Compared to other 3DP methods, SLA produces constructs with high resolution, up to 20 μm, and smooth surface finishes[196]. However, one major disadvantage that could restrict the utility of this technique is the paucity of candidate printable materials; currently only photopolymers such as acrylates, methacrylates, and epoxy resins are compatible with SLA-based platforms[197]. Additionally, neural scaffolds produced using SLA might not represent a good cytocompatible option for post-printing cell seeding or supplementation. Albeit most polymers employed in SLA for medical applications are biocompatible such as polyethylene glycol (PEG), fabricated scaffolds might contain residual free radicals that are carcinogenic, toxic byproducts of the photocrosslinking reaction, and unreacted monomers. Unless robust quality control systems are implemented to achieve acceptable safety standards, these factors might potentially undermine the viability of cells transplanted onto these scaffolds and would require long-term monitoring to exclude possible mutagenic effects.

DLP 3DP

Another vat polymerization technique similar to SLA that uses laser beam is DLP 3DP[198]. Unlike SLA, which is a bottom-up printing approach, DLP is a top-down process. DLP uses a digital projector to project an image, composed of squared voxels, of the two-dimensional cross section of the desired structure into a photocurable liquid resin[194]. The printing process in DLP uses a digital mirror device (DMD), which is an array of micro-mirrors, to control the curing laser beam (figure 5 IV**[a]**). By using a DMD, a complete layer of the resin can be cured at once making DLP relatively faster than SLA[198]. Despite the high resolution achievable by DLP-based printers, only small-sized objects can be printed, as a limited projection size is mandatory to achieve this high precision. In addition, DLP systems are very expensive and produce a characteristic "boxy" surface finish due to its squared voxel. Although the technique uses photosensitive polymers, nerve conduits produced using DLP were flexible and had high compressive moduli (figure 5 IV[d-e]). In addition, they have shown to support very high cell survival rates in vitro and promoted human SCs proliferation[191].

Fused-deposition modeling (FDM): or extrusion 3DP

FDM or extrusion 3DP offers a more affordable option for customized 3D scaffold fabrication compared to light-based 3DP approaches. FDM is based on the hot melt extrusion (HEM) technology. This technique uses a polymer filament of thermoplastic material such as poly (lactic-co-glycolic acid) (PLGA), poly (lactic acid) (PLA), or polycaprolactone (PCL) to build objects in a layer-by-layer fashion. Essentially, the polymer is fed into a heated metal cylinder, liquefied, and then extruded into the printing bed *via* a nozzle of predetermined size along with a computer-controlled path.[199,200,201] Whilst the neural regenerative potential of FDM-manufactured nerve guides remains unexplored, FDM was employed to create a nerve graft model using PLA with a simulated nerve defect in a recent study. The authors investigated the feasibility of printing a customized nerve graft using 3D reconstruction data from micro-MRI scans of human tibial nerve samples. Interestingly, the 3D printed model demonstrated appreciable similarity to the original nerve fascicles, and matched with the proximal and distal segments of the nerve defect (figure 10 II[a-e]). FDM 3DP offers a great advantage in the field due to the ability to create personalized NGCs from currently available FDA-approved thermoplastics such as PGA and poly-l-lactide-co-ε-caprolactone (PLCL) (table 2). In the future, this could immensely facilitate the translational process of patient-specific nerve conduits prepared from these polymers.

However, FDM 3DP has some serious constraints. The application of heat in FDM to melt the polymer can have undesirable effects on resultant material properties, and strictly limits this technique to printing synthetic thermoplastic materials only. The high operating temperature of this system limits their application for biological supplementation with cells and biomolecules during printing. These materials possess Young's moduli different than living tissues and lack biologically active motifs, which make them unfavorable for soft tissue engineering[202]. Alternatively, a lower temperature-cooling platform called Low Frozen Deposition Manufacturing (LFDM) was developed to overcome these shortfalls[198]. In LFDM, the extruded ink immediately freezes as it comes into contact with the low temperature plate, thus the structure does not collapse during printing. LFDM was used by Cui and coworkers to fabricate an integrated double-layered conduit of outer polyurethane and inner collagen filament layer[190]. The resulting porous conduits supported SC adhesion and proliferation *in vitro* compared to PU only conduits. Nonetheless, there will be a need for more innovative approaches to augment the bioactivity of future FDM fabricated nerve guides such as using intraluminal hydrogel coatings or biofunctionalization with ECM molecules.

Inkjet 3DP

Inkjet 3DP is a non-contact printing method that involves ejecting controlled volumes of ink droplets through a printhead orifice to predefined locations on a collecting plate. Inkjet printing can be broadly categorized into: continuous-inkjet 3DP and drop-on-demand inkjet 3DP.[203] The latter will be reviewed within the context of 3D bioprinting. The printing principle of inkjet techniques is fundamentally centered on binder jetting technology. This process involves the dispensing of precisely controlled droplets of a liquid binder solution onto a powder bed of the desirable material (e.g. polymers, ceramics, etc.). The release binder induces fusion of powder particles to create an agglomerated 3D object. T Inkjet-based 3DP has the combined advantage of achieving cost-effective and high resolution (~20-50 μm) printing in both the x and y-axes. The printing process can also be expedited through using multi-nozzle systems.[204] However, inkjet platforms are capable only of printing low viscosity solutions (< 10 mPa/s) and result in low cell densities if employed for biofabrication.

A recently emerging subtype of inkjet 3DP that was investigated in NGCs fabrication is electrohydrodynamic (EHD) jetting (figure 5 II). In principle, EHD printing uses an electric field, resulting from the electrical potential difference between the printhead and substrate, to pull a stream of ink droplets through the nozzle rather than pushing out as seen in the conventional inkjet systems. Advantages of EHD jetting include the ability to manufacture high resolution, complex scaffolds in addition to allowing for precise control of the pore size, porosity, and fiber diameter and alignment using computer-controlled software. Vijayavenkataraman et al. constructed a library of PCL-based nerve conduits with tunable degradation rates using EHD-jet 3DP[97]. PCL scaffolds of five different pore sizes (125–550 μm) and porosities (65%–88%) were fabricated. It was reported that ultimate tensile strength of NGCs with pore sizes of 125 μm and 215 μm mimicked those of the native peripheral nerve (6.5 to 11.7 MPa) (Dumont and Born, 2005). Furthermore, the EHD 3D printed scaffolds supported neuronal tissue differentiation upon incorporation of electrically conductive polymers such as reduced graphene oxide (rGO) and polypyrrole (PPy) in related studies.[182,183]

4.3.2 3D bioprinting of peripheral nerve tissue

Although non-biological 3DP could support anatomically complex geometries for injured nerves, they are limited in functional restoration. Thus, this paves the way for personalized grafts with cellular and biological components *via* 3D bioprinting. 3D bioprinting, also referred to as biofabrication, is another

rapidly progressing domain of AM that has been recently exploited in advanced peripheral nerve tissue engineering. This automated paradigm offers user-driven spatial positioning of the encapsulated bioactive substrates with the ability to create complex structures towards developing biologically inspired functional tissue constructs. For peripheral nerve repair, biofabrication offers the ability to develop patient-specific engineered nerves containing exogenously fabricated bands of Büngner, that recapitulate the physiological nerve regeneration process. Following nerve injury, regenerative tracks, referred to as the bands of Büngner, comprising of longitudinally arrayed columns of SCs and fibrin cables are formed.[205] These pathways are critical for selectively guiding regrowing axons to the target sites of innervation. Conventional strategies focus on inducing the formation of these regenerative corridors through the addition of topographical and biological cues to synthetic conduits, without actively constructing this complex microenvironment.[205] It is speculated that biofabrication technologies could allow more versatility and precision concerning the placement of neurotrophic factors and cells within the 3D space, thus enabling the development of patient-specific biomimetic fascicle pathways.

In addition to potential therapeutic applications, bioprinted nerve grafts and nerve organoids composed of patient-derived cells could serve as *in vitro* 3D tissue models for neuropathic disorders e.g. demyelination and neurodegenerative conditions, drug screening, and toxicology studies. Conventional *in vitro* assays for studying peripheral nerve disorders and regeneration are relatively simple and based solely on two dimensional monolayer neuronal cultures or nerve explants.[206] However, they fail to echo the complex 3D characteristics of living tissues, providing unreliable data of neuronal function. To circumvent this, Khoshakhlagh et al. fabricated a physiologically relevant 3D model of myelinated peripheral nerve using micro-photolithography.[207] This *in vitro* model consisted of a photocurable dual hydrogel system comprising a cell-restrictive component and a cell-permissive component. The cell-restrictive part was formed of polyethylene glycol (PEG) diacrylate and served as a hydrogel micro-mold, whereas, the cell-permissive hydrogel component consisted of either methacrylated dextran or heparin that supported rat neuronal cell culture (figure 6A[I]). This 3D configuration promoted both linearly directed neurite outgrowth from rat dorsal root ganglia (DRG) explants and myelin deposition by rat SCs. The final hydrogel construct mimicked the myelinated axonal tracts of the native PNS tissue. In addition, myelin formation was identifiable on both histology and the characteristic spiral, compact structure of myelin sheath was demonstrated on transmission electron microscopy (TEM) imaging (figure 6A[II]).

Moreover, Sharma and co-workers took a step further and developed the first human biomimetic myelinated peripheral nerve organ-on-a-chip model, using a similar photolithographic approach. In their study, the authors developed an innovative 3D peripheral nerve model utilizing spheroidal co-cultures of human primary SCs and human iPSCs-derived motor neuronal cells (figure 6B[I]).[208] Interestingly, this novel co-culture of SCs and human motor neurons not only deemed viable (~4 weeks) but also supported extensive neurite outgrowth (~5 mm *in vitro*) and effective myelination of the motor neurons by human SCs (figure 6B[II]). Besides, such microengineered nerve models permitted the measurement of clinically significant electrophysiological metrics such as nerve conduction velocity (NCV) and compound action potential (CAP), which objectively evaluate neuropathological conditions. Additionally, the cardinal histomorphometric parameters of peripheral nerves, normally obtained from *in vivo* studies, such as axonal diameter, myelin thickness, and g-ratio (ratio of inner axonal diameter to the diameter of the whole nerve fiber including myelin sheath) were analyzable from TEM of these 3D functional nerve models. These 3D systems should potentially offer more representative models, thereby reducing burden on animal testing, resolving the associated ethical dilemmas[209].

Currently, peripheral nerve tissue bioprinting is in its infancy, focusing towards standardization of bioinks for printing, spatio-temporal cell alignment in the bioprinted constructs, *in vitro* neurite outgrowth assays, and *in vivo* biocompatibility. This section aims to summarize the principles of scaffold-based and scaffold-free bioprinting techniques and recent advances in the field to develop biomimetic peripheral nerve tissues.

4.3.2.1 Scaffold-based peripheral nerve tissue biofabrication

4.3.2.1.1 Bioinks:

Bioinks are the cornerstone of scaffold-based approaches for the biofabrication of living tissues with pre-programmed geometries. Although a consensus on bioink definition is currently lacking, the term usually encompasses materials that enable the 3D printing of cells and biologics including signalling molecules and growth factors. Bioinks generally include cell-encapsulating hydrogel precursor solutions and extracellular-matrix (ECM)-based materials.[210,211] Hydrogels possess various favorable features that make them the material of choice for bioprinting cell-laden constructs including peripheral nervous tissue.[212] Along with their biocompatibility, hydrogel-based bioinks are highly hydrated, tunable networks that can be formulated from a diversity of natural and synthetic multi-functional biopolymers.[213] The high-water content makes hydrogels inherently porous and permeable. These features permit the prompt diffusion of oxygen and nutrients throughout the scaffold, which is necessary for maintaining survival of the encapsulated cells. The porosity of hydrogels also facilitates cell migration and remodelling of the surroundings. Finally, advances in gelation mechanisms enables cell-friendly crosslinking of hydrogels into solid stable structures while minimizing the physiological stress on printed cells. Thus, these specifications allow hydrogels to closely mimic the native microenvironment of cells. A downside of hydrogel bioinks, however, is their inherent fragility. They often fail to maintain their designed shape. Notwithstanding, different reinforcing strategies have been researched to buttress these mechanically unstable printable materials while retaining their favourable biological properties. These include the use of hydrogel composites as printable materials, supramolecular bioinks, double network bioinks, and co-printing thermoplastic reinforcement.[212]

The printing fidelity of bioinks can also be enhanced by either in-process or post-process crosslinking approaches.[213] Examples of in-process cross-linking polymers are alginate and fibrin. To induce cross-linking of the hydrogel precursor during the printing process, a coaxial printhead can be used to simultaneously extrude both the bioink and cross-linker, thereby enabling instantaneous stabilization of the printed structure. On the contrary, post-process crosslinking methods provide structural fidelity once the entire structure is fully deposited onto the printing bed. Although the method could pose cytotoxicity, curing the printed tissue using UV or light is typically used to achieve post-bioprinting crosslinking. Recently, the deposition of hydrogel bioinks within a temporary sacrificial support material has also proven a viable technique to fabricate intricate-shaped structures, at scale, to date not feasible to generate with conventional 3DP methods[214,215]. Further details on bioink designs and crosslinking schemes are beyond the scope of this review.

Bioinks ideal for the 3D printing of neural tissue must render adequate biocompatibility to allow the encapsulation of neural cells and neurotrophic growth factors, and offer prolonged viability and differentiation. Bioinks must possess functional motifs that support cell adhesion, spreading, differentiation, and can induce basal lamina deposition by SCs. In addition, bioinks must produce scaffolds mechanically analogous to native nerve tissue (~6.5 MPa) by having controlled degradation in synchronization with axonal regeneration. Another important consideration for nozzle-dependent biofabrication (Microextrusion and inkjet-based techniques) is that optimal bioinks should display viscoelasticity as well as shear-thinning (or thixotropic) properties i.e. the viscosity correspondingly decreases under increased shear stress.[216] The shear-thinning property of extrudable bioinks aids in alleviating the printing-induced stress caused to the cells, and enhances the printing fidelity. In addition, to produce multi-layered 3D structures with high resolution, extrusion-based biofabrication also utilizes self-healable bioinks. A self-healing hydrogel ink is capable of restoring its functionalities, morphological and mechanical integrity after cessation of the extrusion shear stress[217]. Self-healing mechanisms are

essentially based on dynamic or reversible covalent bonding and non-covalent physical interactions (hydrogen bonding, hydrophobic interactions, electrostatic interactions). Post-printing, the self-healable bioink should also harden, in a cytocompatible fashion, to conserve the structural stability.[218, 219]

Identifying the optimal cell-laden bioink formulation is the keystone step toward realistic, successful nerve bioprinting. Despite the variety of constituent materials present, an overwhelming challenge facing the field is the significantly limited amount of bioinks suitable for neural biofabrication meeting the criteria above[220]. Polymeric bioinks derived from natural sources, such as gelatin, hyaluronic acid, alginate, and fibrinogen are generally used in biofabrication owing to their ubiquity, low cost, biodegradability, and bioactivity. However, the sole use of natural bioinks could not be adequate for fabricating self-standing structures and it is exceedingly troublesome to obtain regulatory permission for biological therapies.[221] Besides, natural polymers are associated with quality control issues and batch-to-batch inconsistencies. Thus, the addition of synthetic polymers should be considered. Biomaterials such as PEG, Pluronic, and polyvinyl alcohol (PVA) offer the benefits of bestowing mechanical strength, tunability, pH and temperature responsiveness. In addition, synthetic bioinks lack manufacturing heterogeneities typical of their natural counterparts such as collagen, chitosan, and silk. Despite that, synthetic bioinks are inert to cellular activities such as adhesion and proliferation. Therefore, it is often mandatory to functionalize synthetic bioinks with cell-cell-adhesive motifs, such as RGD (Arg-Gly-Asp) tri-peptide and IKVAV (Ile-Lys-Val-Ala-Val) fragments, or with incorporated growth factors for improving the cell-matrix compliance, necessary for facilitating cell attachment and survival.

Most of the present bioinks designed for PNTE, typically in the form of SC-laden constructs, are simply formulated by blending cells of interest with hydrogels. This approach is, however, an oversimplification of the hierarchal alignment of native neural tissues, which is characterized by a multiscale modular design.[222] Essentially, these modules describe the spatial organization of cells and ECM as repeated units of 3D building blocks. Modularity allows uncoupling of the cellular and tissue micro- and macroenvironments, which is pivotal for achieving the multifunctionality that is a prerequisite for proper tissue performance. [223] In its simplest form, modularity aims to develop 3D biomimetic scaffolds that recapitulate the smallest living functional units i.e. cells coated by connective tissue matrix. A commonly exploited technique to implement modular bioinks is *via* encapsulation of cells in microgels, which are micrometer-sized hydrogels.

Recently, Chen et al. hypothesized a multiscale modular bioink for PNTE using hydrogel microspheres (figure 7I). In their design, they combined PC12 (a pheochromocytoma-derived neuronal cell line) laden microgels and rat SCs (RSC96 cells) laden gelatin methacrylate (GelMA) hydrogel to assemble the 3D composite scaffolds using extrusion bioprinting.[224] The hydrogel microspheres were fabricated from chitosan and GelMA (GC-MS) using a microfluidic chip. Results demonstrated that GC-MS provided a suitable surface microenvironment for PC12 cell adhesion and growth. GC-MS were also shown to stimulate neurite outgrowth and elongation of PC12 cells when loaded with NGF. Interestingly, bioprinting of the modular composite scaffold revealed uncoupling of the cellular microenvironments on confocal microscopy in which RSCs were homogenously distributed throughout the bioink and PC12 cells were found adherent and proliferating on the microspheres (figure 7III[g-h]). This 3D environment mimicked the anatomical organization of SCs wrapping the neuronal axons observed in mammalian nerves.

4.3.2.1.2 <u>3D Bioprinting techniques</u>

According to the technique characteristic, the common categories of biofabrication include microextrusion, inkjet, and laser-assisted methods.[225,226]

Microextrusion bioprinting:

Microextrusion-based bioprinters currently represent the most commonly utilized platform for biomanufacturing SC-laden constructs (table 7). This technique utilizes pneumatic or mechanical (piston-driven or screw-driven) extruding pumps to continuously dispense filaments of cell-laden viscous bioinks onto a pre-defined location on receiving substrates such as a culture dish, growth medium, or support gel.[233] The instrumentation simplicity, low cost, and ability to eject bioinks with high cell densities are some apparent advantages of extrusion bioprinting that accounted for its extensive popularity.[234] Moreover, the resolution of the final bioprinted structures can be easily modified by manipulating printing parameters such as extrusion pressure, nozzle diameter, printing speed, path interval, etc.[235] In order to identify the appropriate extrusion conditions, rheological studies of bioinks are usually conducted to compute ink's viscosity and complex modulus.

Bioinks printable using extrusion-based techniques tend to have high viscosities (up to $6x10^7$ mPa/s), as they better maintain their structures.[218] However, the high viscosity prerequisite could lead to nozzle tip obstruction and comes at the expense of compromising cell survival due to the resultant shear and extensional stresses involved.[236] Nonetheless, Ning and coworkers used extrusion-based printing to fabricate cell-dense, rat SC-laden tissue constructs, using a RGD-modified alginate, fibrinogen, and hyaluronic acid bioink.[229] Cell-laden scaffolds printed at 6 mm/s by a steel needle with 200 μm internal diameter were associated with approximately 90% SC survival rates on day 10 post printing. Furthermore, the study demonstrated the feasibility of bioprinting speed in altering rat SC alignment within the scaffolds to replicate their native linearly arrayed end-to-end orientation in peripheral nerves, necessary for achieving nerve regeneration (figure 8I).

Inkjet bioprinting:

Inkjet or drop-on-demand bioprinting involves ejecting controlled volumes of hydrogel ink to predefined locations on a receiving substrate. Ink droplets can be created by either thermal or piezoelectric approaches.[237] In thermal-based inkjet systems, heat is used to nucleate an air bubble in the print head or nozzle that provides pressure pulses to eject ink droplets of varying sizes of ink drops. Typically, the volume of the drop ranges between 10-150 picoliter (pL) and is dependent upon several factors including, applied temperature gradient, viscosity of the ink, and frequency of current pulse. On the contrary, piezoelectric-based systems rely on the generation of acoustic waves using polycrystalline ceramic actuators. The acoustic wave creates transient pressure that disrupts the bioink at regular intervals. Inkjet bioprinting is capable of producing high-resolution scaffolds (50 μm) with rapid printing speeds, affordable setups and acceptable cell viabilities (up to 90%). However, the technique is limited to low viscosity materials and does not achieve high densities.[238]

Laser-assisted bioprinting:

Laser-assisted bioprinting (LAB) is a printing technique, which is typically nozzle-free. The technique is broadly divided into laser induced forward transfer (LIFT) and laser guided direct writing (LGDW). LIFT is the most prevalent form of LAB. Essentially, the technique uses a pulsed laser beam, focused on an absorbing layer called the donor film, which is composed of a layer of cell-encapsulating bioink. The incident laser pulse increases the pressure of the bioink by generating sufficient energy that propels hydrogel droplets from the donor film onto a support stage.[239] The fallen bioink is then immediately cross-linked. Unlike other biofabrication technologies, LAB has unique advantages. First, the technique is a non-contact printing, thereby eliminating potential sources of contamination. In addition, highly viscous

materials, up to 300 mPa/s, can be employed and the technique results in satisfactory cell viabilities (up to 85%).[238] Moreover, LAB is also capable of producing cell-level resolution (10 μm) using rapid printing speeds.[240] Despite these benefits, LAB is associated with high system costs, and laser energy could result in increased cell fatalities.[218] For these reasons, LAB has not been investigated extensively for biofabrication applications and, to date, this technique has not been explored in printing peripheral nervous tissue.

4.3.2.2 Scaffold-free (Cellular) bioprinting:

To address the challenges related to unpredictable biodegradation and cytotoxicity of biomaterial-based 3D printing, cellular or scaffold-free biofabrication is a viable alternative.[241] The rationale for this "bottom-up" method is based on the premise that replacement tissues and organs can be printed solely using autologous cells. Taking inspiration from the embryonic organogenesis process guiding self-assembly of resident cells, scaffold-free bioprinting strategies depend upon the juxtacrine signalling of cells for ECM secretion to generate patient-derived 3D tissue constructs for clinical applications. The approach is cell-friendly and typically generates macroscale tissues with high cell densities and long-term viability by printing spheroidal aggregates. Compared to their classical scaffold-dependent counterpart, cells are not exposed to xenogenic materials or harsh processing parameters including shear stresses, UV or chemical cross-linkers that compromise their resultant viability.[242] Furthermore, cellular bioprinting fosters intercellular interactions, of both homotypic and heterotypic nature, to guide the process of cell maturation and tissue morphogenesis.

Spheroids are typically formed by culturing cell lines under non-adhesive conditions, where they cluster to generate cellular aggregates.[243,244] Although they could arguably be classified as bioinks, spheroids constitute the basic building blocks of bioprinted tissues in a biomaterial-independent approach. The dynamic 3D spheroids comprise of multicellular organizations facilitating the complex interplay between cell-cell and cell-ECM interactions, resembling native tissue architecture, which is impossible to achieve using 2D monolayer cultures. Moreover, spheroidal stem cell cultures express pluripotency markers such as Oct-4 and Nanog, and secrete higher levels of proangiogenic factors and signalling cytokines that promote cellular processes and viability compared to monolayer cultures.[245] Different approaches have been utilized to generate such 3D tissue spheroids *in vitro;* using hanging drop[246], spinner culture[247], rotating wall vessel[248] , microfluidic culture[249], pellet culture[250], and liquid overlay techniques[251] Recently, fabrication of biomimetic nerve bio conduits using 3D printing of spheroids has become increasingly popular.

Spheroidal aggregates are frequently assembled using the famous "Kenzan" technique (figure 9 II), using an automated printing strategy, which has so far been applied to bioassembly of blood vessels[252], trachea[253] , cardiac patches[254], and nerve conduits[255] (figure 9II[5]). The approach relies upon cellular organization on stainless steel microneedles at micron-level precision that provides a temporary bolster to allow maturation and fusion of spheroids, instead of the hydrogel systems.[243] Pre-formed spheroids are robotically aligned on micro-needles by pre-defined CAD models using a commercial platform, Regenova® (Cyfuse, Tokyo, Japan). Needle arrays can be available in square (9x9 and 26x26 needles) and circular formats. Following placement of the 3D spheroids in the micro-needles, they are incubated in a perfusion bioreactor system for allowing cell maturation to form macroscale tissues. Once the cellular tubes "conduits" are mechanically stable, they are then detached and become available for implantation. In Table 8 below, we have highlighted some recent research within the domain of nerve bio conduit fabrication by employing Kenzan technique. In spite of the several advantages associated with the Regenova® system, the tubular nerve conduits generated so far were simple, lacking some of the key features of the fascicle tracts. Nevertheless, pilot studies on neural regeneration conducted *in vivo* using these nerve bio conduits have provided meaningful results. However, their application in critical sized gaps (e.g. > 15 mm in rats) needs to be further explored for evaluating their clinical potential in long gap nerve regeneration in humans.

Another extrusion-based bioprinting technique for developing functional nerve grafts utilizing the principles of spheroidal assembly is NovoGen MMX Bioprinter™ (Organovo, Delaware, USA).[260] The bioprinted is equipped with dual dispensers; the first one is used for printing the cellular material using pre-defined user settings and the other concurrently prints an inert sacrificial hydrogel such as agarose or alginate to act as a temporary support (figure 9I[A-E]). Similar to the Kenzan technique, tissue spheroids are then allowed to fuse together to attain structural integrity before the fugitive gel can be removed later. As a proof of concept, Owens et al. fabricated a multi-luminal nerve graft composed of an outer ring of bone marrow mesenchymal stem cells (BM-MSCs) that circumscribed an inner core of alternating multicellular cylinders (90% of BMSCs and 10% SCs) and agarose rods.[259] The whole structure was supported by agarose rods on the exterior, which were removed afterwards following self-assembly of the spheroids to form three internal channels mimicking the nerve fascicles (figure 9I[G)]. Interestingly, the fully cellular nerve graft was able to perform on par with the nerve autograft when evaluated in an in vivo model of nerve gap.

Despite the merits of spheroid-based bioprinting, the approach has several limitations. Essentially, 3D cell culture techniques are expensive, labor-intensive, time-consuming, and require extensive experimental experience. This could potentially be associated with enormous manufacturing overheads when considering scaling-up this technology for clinical translation. Although the procedure generates superdense cellular aggregates, spheroid 3D printing poses technical challenges, as they are prone to premature aggregation that could easily clog the nozzle tip. Furthermore, the biomechanical performance of spheroids is less predictable compared to using pre-determined materials such as hydrogels. Poor and inconsistent ECM production could yield unstable structures not feasible for clinical implantation.[242] It is also critical to maintain the size of cell aggregates for scaffold-free bioprinting. Spheroids with diameters exceeding 400-500 μm are vulnerable to hypoxia of the central core, due to mass transport limitations, leading to ischemic cell necrosis.[261]

For these reasons, proponents of scaffold-based bioprinting argue that this method offers greater versatility in terms of bioink composition and enables the fabrication of more complex structures mimicking native ECM. In addition, hydrogel-based bioinks can be printed using various techniques and cross-linked *via* multiple physical and chemical interactions, thereby the mechanical properties of the bioprinted construct can be tuned to match that of the desired tissue. Additionally, the incorporation of polymers with pendant chemical groups bestows multi-functionality to the scaffold, which could allow the conjugation of neurotrophic factors and establishing gradients of guidance cues that might help directing the growth cone of regenerating axons.

5. Challenges of AM processes in peripheral nerve engineering and potential solutions:

As the research field of nerve repair is currently trending towards personalized nerve guides and tissue constructs, it is of paramount importance to identify the major potential roadblocks facing this technology and coin effective solutions that could be instrumental in overcoming these obstacles.

5.1 Patient-specific nerve CAD modeling:

Non-invasive conventional imaging such as the CT scan and MRI have been indispensable in the 3D printing of complex anatomical models and fabrication of customized cell-laden scaffolds for repairing body tissue including cartilage or bone defects.[262,263] Unfortunately, these modalities along with contemporary clinical neuroimaging systems including MRN are far from optimal in delineating intraneural structures and fascicular orientation with high resolution. This makes generating patient-specific 3D nerve CAD models for biofabrication extremely challenging. Compared to the aforementioned tissues, the peripheral nerve anatomy is relatively intricate due to, primarily, the heterogeneity in fascicular topography

throughout the nerve pathway, and, secondly, the presence of bifurcations and undulations along the anatomical course of the nerve.[264,265] Therefore, there is a need for more advanced imaging platforms and protocols that could allow the complexity of the fascicular anatomy to be appreciated. This is critical for reconstructing personalized biomimetic nerve pathways that are anticipated to significantly enhance neural regeneration over longer gaps.

Ideally, an optimal nerve scanner should be capable of mapping the individual fascicle bundles up to the endoneurial tubes and accurately delimiting the normally occurring fascicular splitting and merging.[266] Moreover, in the context of PNIs, a reliable imaging protocol should involve the *in situ* scanning of the proximal and distal severed nerve stumps followed by extrapolating the lost segment to match the original nerve structure. Alternatively, a digital library of peripheral nerve scans could be constructed from cadaveric donors or individuals with various demographic backgrounds that would assist in the 3D modeling of a nerve graft homologous to the nerve of interest. Another more realistic and technically feasible option to pursue could also involve scanning the contralateral unaffected nerve of the same patient to aid in 3D modelling of the lost nerve segment in the affected limb.[267] In this regard, emerging imaging methods have been applied to reverse engineer the native fascicular pathway such as microfocus computed tomography (micro-CT) and micro magnetic resonance imaging (micro-MRI). These tools might represent promising solutions that could capture the internal morphological details of the peripheral nerve with high fidelity.

Micro-CT is a powerful sub-micron scanning modality that can generate very high-resolution 3D images, with voxel sizes in the micrometer range, which could be useful in designing more anatomically precise nerve CAD models for biofabrication.[268] In addition, nanotomography, the most recent innovation in μCT-based platforms yet to be applied in 3D printing, could open new frontiers for 3D nanoprinting and expand resolution limits.[269] Although μCT has now well-established applications in analyzing the microstructure of mineralized tissues and morphologic characterization of engineered scaffolds, it is not widely utilized in the evaluation of soft tissues including peripheral nerves due to their inherently low X-ray attenuation coefficients.[270,271,272] Nevertheless, iodine staining and freeze-drying have been used as viable solutions to enhance the contrast of peripheral nerves and allow for the 3D reconstruction of the intraneural fascicular topography.[272,273] As a proof of concept, Zhu and co-workers successfully scanned lyophilized decellularized human nerve allografts using μCT and produced high-resolution images of the nerve microstructure with visualization of the distinctive connective tissue layers including the endoneurial tubes.[274] Moreover, the authors demonstrated the feasibility of 3D printing a nerve model with visibly delineated fascicles using 2D scans of the freeze-dried nerve sample. Despite the advantages of μCT, the higher resolution of tissues is currently achievable using *ex-vivo* imaging systems.[275]

Another soft tissue-sensitive imaging is the microMRI that has been investigated by Yao and co-workers to 3D reconstruct nerve fascicles of the lower extremity nerves with high resolution (50 μm).[276] Using the database generated from the 3D reconstruction of nerve scans, 3D models clearly delineating the individual nerve fascicles of the tibial, common peroneal, and sciatic nerves could be designed with high accuracy (figure 11 I-III). In contrast with μCT, microMRI lacks exhaustive sample preparation and samples can be recycled for use in later experiments, which makes it a more convenient non-destructive tool. Despite the enormous leap created by these innovative imaging technologies in the study of fascicular microstructure, both techniques are limited by their inability to perform in situ scanning of peripheral nerves. This *ex vivo* imaging nature makes the practicality of these scanning methods from the clinical perspective questionable. Another drawback of high-resolution microscale imaging is the laborious segmentation and time-consuming 3D reconstruction of multiple scans, which could limit the length of the nerve scanned.

5.2 Peripheral nerve biofabrication hurdles

The biofabrication of a fully functional nerve graft is at a primordial stage, and several milestones need to be achieved for clinical intervention. Constraints in the manufacturing technology, bioink material properties, and post-processing maturation of the viable, printed tissue, are among some of the most critical factors limiting the biofabrication of centimetre-scale constructs.[236] The layer-by-layer stacking technique of AM biofabrication methods is generally associated with relatively extended processing times.[277] Due to this, cells are left outside optimal culture conditions for prolonged durations, thereby inducing cellular stress and jeopardizing the viability of the encapsulated biologics. Moreover, the time of fabrication could also extend, if single-cell resolution and inherently low throughput technologies such as μSL or two-photon polymerization (2PP), are opted for bioprinting human-scale nerve grafts.[278] Thus, it might be difficult to ensure the viability of bioprinted cells with the application of these processes. Eventually, the production of clinically relevant graft constructs would likely involve advanced bioprinting platforms that merge different modalities to leverage their advantages and simplify parts of the biofabrication protocol.

Another formidable challenge, especially in extrusion-based methods, is the fidelity of the 3D bioprinted constructs. The 3D neural scaffolds and nerve bio-conduits fabricated to date are rather simple in design and far away from the desirable level of architectural complexity of nerve biomimicry. High-resolution scaffolds are prerequisite to satisfy the overall aim of biofabrication in achieving nerve biomimicry. In addition, they would facilitate elucidating the influence of micro-topography on cellular behaviour and functions such as survival, differentiation, and migration.[279,280] Compared to the printing of hard polymers, hydrogel-based bioinks mainly employed in biofabrication have limited the spatial resolution of the printed living tissue because they are prone to structural collapse and spreading post-printing. Apart from the narrow choice of materials, other factors that could also influence the resolution of the 3D bioprinted structure including bioink physicochemical properties and composition, technical features of the bioprinter system e.g. nozzle size, printing speed, etc., and cross-linking mechanisms. Thus, it is imperative to mention that manipulating one of these printing parameters to achieve a higher resolution could compromise another critical feature, which makes the process of optimization a challenging task. For instance, using a larger gauge needle might yield structures with high-resolution, in turn compromising the cell viability.[281] Recently, volumetric bioprinting (VBP) has emerged that permits rapid fabrication, typically within a time frame of seconds, of clinically relevant 3D structures with preserved cell viabilities. Briefly, VBP uses cytocompatible visible laser light to cast multiple differential 2D projections onto a photocurable cell-laden resin to generate complex patient-specific biomimetic architectures with high resolution.[277] This technological advancement could open new frontiers in nerve biofabrication.

Another fundamental obstacle for the scaling-up of bioprinted tissues is mass transfer limitations. Vascularization of a bioprinted nerve graft is crucial for functionality of cells and axons as it ensures the timely delivery of nutrients and oxygen and removal of metabolic waste products, thereby maintaining the longevity of the product. Current technology fails to maintain adequate mass transport conditions that are protective against hypoxic necrosis of cells in the inner core of the engineered tissues, and is unable to replicate the hierarchical intraneural vascular plexus spanning arteries and veins down to capillaries. Thus, a logical future target to aim for in the scaffold-based bioprinting of peripheral nerves would involve simultaneously integrating interconnected vasculature. **However, this task might be tricky considering the differential medial requirements of the nerves and the vasculature. Further experiments need to be conducted to assess co-culturing conditions of these tissues simultaneously.[282]**

Several approaches have been investigated to bioprint tissues embedding synthetic vasculature including the use of microfluidics and indirect bioprinting of fugitive bioinks, which can be thermally de-crosslinked leaving behind perfusable microchannels that can be infused later with vascular endothelial cells.[283,284] **Using these techniques, several groups have printed hollow vascular structures, diameters ranging from micro- to milli-metre scale, with inner wall incorporated with endothelial cells.[283,284] However, generating vasculature in smaller scale to produce anatomically relevant dimensions demands fine**

tuning several aspects of the printing process, including resolution, nozzle diameter, and mechanical properties of the material and bioink to build free-standing hollow structures, among others.[282] Another caveat here is that the design of a bioprinted intrinsic vascular network should ensure its connection to a larger feeding vessel that can be anastomosed to the recipient vasculature; thus graft perfusion can be resumed once the engineered nerve is implanted in the patient.[236]

Furthermore, most of the research attempts in biofabrication involve the use of a single material bioink to print cell-laden structures. This, however, does not accurately emulate the complex structural heterogeneity and composition of living tissues including peripheral nerves. In the future, advances in multi-material and multi-cell bioprinting could help address the complexity of nerve engineering where a single representative biofabrication session would typically involve the use of sacrificial bioinks for vascularization, multiple tissue bioinks, and scaffolding polymers to generate heterocellular structures integrating intricate perfusable vascular networks with peripheral cellular networks.[286,287]

5.3 Regulatory, ethical, and cost concerns of personalized nerve repair solutions

Country-specific regulatory bodies have different rulings on additively manufactured medical products.[288,289,290] Even though the FDA has set guidelines for the bulk manufacturing (mass production) of medical devices or drugs using 3D printing, clear regulatory frameworks or specific legislative guidance pertaining to the additive manufacturing of personalized therapeutics largely remains unaddressed. Robust and lucid regulatory measures to ensure CGMP (Current Good Manufacturing Practice) standards are integral to maintaining quality control and avoiding faulty products that could impair the healing process in patients. AM processes are also associated with unclear legalities that need to be addressed. The fabrication of custom-made devices or biological tissues will require individual patient data at one stage, which might require the patient's data to be included in the care plan.[288] Besides, intellectual property disputes and privacy concerns may arise since the ownership of medical scans, CAD model design, and final printed products are not yet known. Without identifying proprietary rights, it might become problematic to determine individual's responsibility for any serious harm that occurs in the patient and legally challenge the culprit.[291]

Although biofabrication is a subtype of AM, more sophisticated regulatory considerations are associated with 3D bioprinting compared to non-biological printing. Biofabrication intersects with the fields of cell therapy and stem cell research therefore the inherent risks and translational hurdles of those disciplines will pass over to 3D bioprinting. Additionally, several factors will require evaluation, including the effect of the manufacturing process on cell viability and function and post-printing integrity of the biological product. Moreover, devising appropriate testing and techniques to ensure the maintenance of aseptic printed parts will be necessary. The consistency of the printing process will also need careful assessment. Parameters like the cell distribution, construct dimensions, and mechanical and physico-chemical properties could potentially help evaluating the reliability of the biofabrication technique.[292] Eventually, researchers will need to integrate non-destructive in-line quality-control systems in AM processes to ensure that the aforementioned quality attributes of the biomanufactured clinical products are well defined, characterized, and conform to regulatory standards.[293] Taking these factors into account, a longer translational time frame is anticipated, before a bioprinted nerve graft is fabricated in contrast with 3D printed nerve guides. Ultimately, as research on nerve graft biofabrication and 3D printing continues to surge, policy makers in regulatory bodies, such as FDA, need to articulate more effective validation tools and tailored legislation in a commensurate pace.

Moreover, as therapies become more individualized, the reliability of clinical outcomes might be undermined due to difficulties in standardization of the study design. In addition, the personalized nature of biofabrication raises ethical dilemmas on the clinical testing of these patient-specific products in otherwise normal human subjects. It is certainly unethical and of questionable clinical value to prove the

safety and efficacy of 3D bioprinted organs constructed from the cells of a specific patient with unique pathology in disease-free individuals. At the end, the aim of AM is to tailor treatment to individuals and not to develop a universal technology that can be tested on other groups.[294] Thus, there is a need to develop new models to test the effectiveness and safety of personalized regenerative medicine therapies; otherwise, the patient will serve as his/her test subject, which is ethically controversial.

In the future, it might be also crucial to evaluate the process of the 3D fabrication of nerve grafts from an economical standpoint. Nerve conduits currently available in the market are expensive, with some exceeding the $1000 unit price and their functional outcomes still remain controversial.[295] Given the long chain of production of any custom-made bioprinted nerve graft, the technology will definitely be associated with exorbitant manufacture costs and high-priced solutions, which could limit the accessibility of financially disadvantaged patients to these novel treatments leading to what has been referred to as the "social stratification of bioprinting".[209] Therefore, conducting a cost-benefit analysis will be imperative in the future in such scenarios to weigh the benefits of such technologically and economically demanding innovation against the cost. A bioprinted nerve graft that could fully mitigate the debilitating functional deficits in those diagnosed with intractable PNIs, restore the patient's productivity, and offer equal access to treatment would prove itself as a worthwhile investment.

6. Conclusion:

Repair of nerve injuries remains a surgical challenge. Despite the advances in microsurgical techniques and nerve substitutes, failure rates are high with suboptimal nerve regeneration outcomes. There is an unmet demand for a fully functional 3D engineered nerve graft that can recapitulate the native nerve microstructure, and allow for patient-specific fascicle-to-fascicle regeneration. Apparently, optimizing the design of commercially available nerve surrogates or supplementing them with patient cells appears a pragmatic solution to enhance nerve regeneration over long gaps in the shorter timeframe. However, they do not offer personalized therapies, and might not achieve the expected functional recovery as a result of the ineluctable fascicular mismatch. Automated fabrication methods such as 3D printing are speculated to create a paradigm shift in the field of peripheral nerve surgery. Essentially, they offer spatial control over the deposition of materials and biologics, and thus could allow the creation of a biomimetic fascicle pathway relevant to the patient's anatomy. Although replicating the intraneural microstructure might not be a conceivable goal with the present technology, several milestones must be accomplished to prevent this research field from stagnation and accelerate the reaping of attainable gains. These include, but are not limited to, utilizing high-resolution imaging and developing 3D scanning protocols for patient-specific nerve modeling, incorporating interconnected vascular networks within bioprinted scaffolds, developing more versatile multi-functional bioinks for nerve biofabrication, and validating regulatory paths for the translation of additively manufactured nerve grafts.

Acknowledgement: no funding source to disclose.

References:

1. Yang, M., Rawson, J.L., Zhang, E.W., Arnold, P.B., Lineaweaver, W., and Zhang, F. Comparisons of outcomes from repair of median nerve and ulnar nerve defect with nerve graft and tubulization: a meta-analysis. J Reconstr Microsurg. **27**, 451, 2011.
2. Ruijs, A.C.J., Jaquet, J.-B., Kalmijn, S., Giele, H., and Hovius, S.E.R. Median and Ulnar Nerve Injuries: A Meta-Analysis of Predictors of Motor and Sensory Recovery after Modern Microsurgical Nerve Repair: Plastic and Reconstructive Surgery. **116**, 484, 2005.
3. Daly, W., Yao, L., Zeugolis, D., Windebank, A., and Pandit, A. A biomaterials approach to peripheral nerve regeneration: bridging the peripheral nerve gap and enhancing functional recovery. J R Soc Interface. **9**, 202, 2012.
4. Zhu, W., Tringale, K.R., Woller, S.A., You, S., Johnson, S., Shen, H., et al. Rapid continuous 3D printing of customizable peripheral nerve guidance conduits. Materials Today. **21**, 951, 2018.
5. Nerve Repair and Regeneration Market by Products (Nerve Conduits, Nerve Wraps, Vagus Nerve Stimulation, Sacral Nerve Stimulation, Spinal Cord Stimulation, TENS, TMS), Application (Neurorrhaphy, Nerve Grafting, Stem Cell Therapy) - Global Forecast to 2025.
6. Saadat, S., Eslami, V., and Rahimi-movaghar, V. The incidence of peripheral nerve injury in trauma patients in Iran. Ulus Travma Acil Cerrahi Derg. **17**, 539, 2011.
7. Huckhagel, T., Nüchtern, J., Regelsberger, J., and Lefering, R. Nerve injury in severe trauma with upper extremity involvement: evaluation of 49,382 patients from the TraumaRegister DGU® between 2002 and 2015. Scand J Trauma Resusc Emerg Med. **26**, 76, 2018.
8. Noble, J., Munro, C.A., Prasad, V.S.S.V., and Midha, R. Analysis of Upper and Lower Extremity Peripheral Nerve Injuries in a Population of Patients with Multiple Injuries: The Journal of Trauma: Injury, Infection, and Critical Care. **45**, 116, 1998.
9. Anesti, K., and Caine, P. Peripheral nerve injuries. Plast Aesthet Res. **2**, 309, 2015.

10. Kretschmer, T., Antoniadis, G., Braun, V., Rath, S.A., and Richter, H.-P. Evaluation of iatrogenic lesions in 722 surgically treated cases of peripheral nerve trauma. Journal of Neurosurgery. **94**, 905, 2001.

11. Paredes-Carnero, X., and Álvarez-Jorge, J.A. An Ulnar Neurofibroma: Management with Sural Graft Reconstruction. J Hand Microsurg. **07**, 332, 2016.

12. Ramos, D.S., Bonnard, D., Franco-Vidal, V., Liguoro, D., and Darrouzet, V. Stitchless Fibrin Glue-Aided Facial Nerve Grafting After Cerebellopontine Angle Schwannoma Removal: Technique and Results in 15 Cases. Otology & Neurotology. **36**, 498, 2015.

13. Seddon, H.J. THREE TYPES OF NERVE INJURY. Brain. **66**, 237, 1943.

14. Chhabra, A., Ahlawat, S., Belzberg, A., and Andreseik, G. Peripheral nerve injury grading simplified on MR neurography: As referenced to Seddon and Sunderland classifications. Indian J Radiol Imaging. **24**, 217, 2014.

15. Sunderland, S. A CLASSIFICATION OF PERIPHERAL NERVE INJURIES PRODUCING LOSS OF FUNCTION. Brain. **74**, 491, 1951.

16. Grinsell, D., and Keating, C.P. Peripheral Nerve Reconstruction after Injury: A Review of Clinical and Experimental Therapies. BioMed Research International. **2014**, 1, 2014.

17. Diao, E., and Vannuyen, T. Techniques for primary nerve repair. Hand Clin. **16**, 53, 2000.

18. Haastert-Talini, K., Assmus, H., and Antoniadis, G., eds. Modern Concepts of Peripheral Nerve Repair. Cham: Springer International Publishing, 2017, **pp. 43**.

19. Terzis, J., Faibisoff, B., and Williams, H.B. THE NERVE GAP: SUTURE UNDER TENSION VS. GRAFT. Plastic and Reconstructive Surgery. **56**, 166, 1975.

20. Nassimizadeh, M., Nassimizadeh, A., and Power, D. Managing the nerve gap: New tools in the peripheral nerve repair toolbox. J Musculoskelet Surg Res. **3**, 4, 2019.

21. Poppler, L.H., Davidge, K., Lu, J.C.Y., Armstrong, J., Fox, I.K., and Mackinnon, S.E. Alternatives to Sural Nerve Grafts in the Upper Extremity. Hand (New York, N,Y). **10**, 68, 2015.

22. Ray, W.Z., and Mackinnon, S.E. Management of nerve gaps: Autografts, allografts, nerve transfers, and end-to-side neurorrhaphy. Experimental Neurology. **223**, 77, 2010.

23. Grinsell, D., and Keating, C.P. Peripheral Nerve Reconstruction after Injury: A Review of Clinical and Experimental Therapies. BioMed Research International. **2014**, 1, 2014.

24. Saffari, T., Bedar, M., Hundepool, C., Bishop, A., and Shin, A. The role of vascularization in nerve regeneration of nerve graft. Neural Regen Res. **15**, 1573, 2020.

25. Terzis, J.K., Skoulis, T.G., and Soucacos, P.N. Vascularized nerve grafts. A review. Int Angiol. **14**, 264, 1995.

26. Ozcan, G., Shenaq, S., Mirabi, B., and Spira, M. Nerve Regeneration in a Bony Bed: Vascularized versus Nonvascularized Nerve Grafts. Plastic and Reconstructive Surgery. **91**, 1322, 1993.

27. Koshima, I., and Harii, K. Experimental study of vascularized nerve grafts: Multifactorial analyses of axonal regeneration of nerves transplanted into an acute burn wound. The Journal of Hand Surgery. **10**, 64, 1985.

28. Comtet, J.J. [Vascularized nerve grafts]. Acta Chir Belg. **83**, 293, 1983.

29. Penkert, G., Bini, W., and Samii, M. Revascularization of Nerve Grafts: An Experimental Study. J reconstr Microsurg. **4**, 319, 1988.

30. Lind, R., and Wood, M.B. Comparison of the pattern of early revascularization of conventional versus vascularized nerve grafts in the canine. J Reconstr Microsurg. **2**, 229, 1986.

31. D′Arpa, S., Claes, K.Y., Stillaert, F., Colebunders, B., Monstrey, S., and Blondeel, P. Vascularized nerve “grafts”: just a graft or a worthwhile procedure? Plast Aesthet Res. **2**, 183, 2015.

32. Taylor, G.I., and Ham, F.J. The free vascularized nerve graft. A further experimental and clinical application of microvascular techniques. Plast Reconstr Surg. **57**, 413, 1976.

33. Kimata, Y., Sakuraba, M., Hishinuma, S., Ebihara, S., Hayashi, R., and Asakage, T. Free vascularized nerve grafting for immediate facial nerve reconstruction. Laryngoscope. **115**, 331, 2005.

34. Matsumine, H., Sasaki, R., Takeuchi, Y., Miyata, M., Yamato, M., Okano, T., et al. Vascularized versus nonvascularized island median nerve grafts in the facial nerve regeneration and functional recovery of rats for facial nerve reconstruction study. J Reconstr Microsurg. **30**, 127, 2014.

35. Terzis, J.K., and Kostopoulos, V.K. Vascularized ulnar nerve graft: 151 reconstructions for posttraumatic brachial plexus palsy. Plast Reconstr Surg. **123**, 1276, 2009.

36. Donzelli, R., Capone, C., Sgulò, F.G., Mariniello, G., and Maiuri, F. Vascularized nerve grafts: an experimental study. Neurol Res. **38**, 669, 2016.

37. Carvalho, C.R., Oliveira, J.M., and Reis, R.L. Modern Trends for Peripheral Nerve Repair and Regeneration: Beyond the Hollow Nerve Guidance Conduit. Front Bioeng Biotechnol. **7**, 337, 2019.

38. Battiston, B., Geuna, S., Ferrero, M., and Tos, P. Nerve repair by means of tubulization: Literature review and personal clinical experience comparing biological and synthetic conduits for sensory nerve repair. Microsurgery. **25**, 258, 2005.

39. Bertleff, M.J.O.E., Meek, M.F., and Nicolai, J.-P.A. A Prospective Clinical Evaluation of Biodegradable Neurolac Nerve Guides for Sensory Nerve Repair in the Hand. The Journal of Hand Surgery. **30**, 513, 2005.

40. Gerth, D.J. Clinical outcomes for Conduits and Scaffolds in peripheral nerve repair. WJCC. **3**, 141, 2015.

41. Weber, R.A., Breidenbach, W.C., Brown, R.E., Jabaley, M.E., and Mass, D.P. A Randomized Prospective Study of Polyglycolic Acid Conduits for Digital Nerve Reconstruction in Humans: Plastic and Reconstructive Surgery. **106**, 1036, 2000.

42. Meek, M.F., Varejão, A.S.P., and Geuna, S. Use of Skeletal Muscle Tissue in Peripheral Nerve Repair: Review of the Literature. Tissue Engineering. **10**, 1027, 2004.

43. Barcelos, A.S., Rodrigues, A.C., Silva, M.D.P., and Padovani, C.R. Inside-out vein graft and inside-out artery graft in rat sciatic nerve repair. Microsurgery. **23**, 66, 2003.

44. Levine, M.H., Yates, K.E., and Kaban, L.B. Nerve growth factor is expressed in rat femoral vein. Journal of Oral and Maxillofacial Surgery. **60**, 729, 2002.

45. Ferrari, F., De Castro Rodrigues, A., Malvezzi, C.K., Dal Pai Silva, M., and Padovani, C.R. Inside-out vs. standard vein graft to repair a sensory nerve in rats. Anat Rec. **256**, 227, 1999.

46. Kornfeld, T., Vogt, P.M., and Radtke, C. Nerve grafting for peripheral nerve injuries with extended defect sizes. Wien Med Wochenschr. **169**, 240, 2019.

47. Mackinnon, S.E., Doolabh, V.B., Novak, C.B., and Trulock, E.P. Clinical Outcome following Nerve Allograft Transplantation: Plastic and Reconstructive Surgery. **107**, 1419, 2001

48. Hudson, T.W., Zawko, S., Deister, C., Lundy, S., Hu, C.Y., Lee, K., et al. Optimized Acellular Nerve Graft Is Immunologically Tolerated and Supports Regeneration. Tissue Engineering. **10**, 1641, 2004.

49. Fox, I.K., Jaramillo, A., Hunter, D.A., Rickman, S.R., Mohanakumar, T., and Mackinnon, S.E. Prolonged cold-preservation of nerve allografts. Muscle Nerve. **31**, 59, 2005.

50. Gulati, A.K. Evaluation of acellular and cellular nerve grafts in repair of rat peripheral nerve. Journal of Neurosurgery. **68**, 117, 1988.

51. He, B., Zhu, Q., Chai, Y., Ding, X., Tang, J., Gu, L., et al. Safety and efficacy evaluation of a human acellular nerve graft as a digital nerve scaffold: a prospective, multicentre controlled clinical trial. J Tissue Eng Regen Med. **9**, 286, 2015.

52. Witzel, C., Rohde, C., and Brushart, T.M. Pathway sampling by regenerating peripheral axons. J Comp Neurol. **485**, 183, 2005

53. Höke, A. Mechanisms of Disease: what factors limit the success of peripheral nerve regeneration in humans? Nat Rev Neurol. **2**, 448, 2006.

54. Mota, C., Puppi, D., Chiellini, F., and Chiellini, E. Additive manufacturing techniques for the production of tissue engineering constructs: Additive manufacturing techniques for the production of tissue engineering constructs. J Tissue Eng Regen Med. **9**, 174, 2015.

55. Roopavath, U.K., and Kalaskar, D.M. Introduction to 3D printing in medicine. 3D Printing in Medicine [Internet]. Elsevier, pp. 1–20, 2017.

56. Kalaskar, D.M., ed. 3D printing in medicine. Duxford Cambridge, MA Kidlington: WP, Woodhead Publishing, an imprint of Elsevier, 2017.

57. Catala, M., and Kubis, N. Gross anatomy and development of the peripheral nervous system. Handb Clin Neurol. **115**, 29, 2013.

58. Campero, M., Verdugo, R.J., and Ochoa, J.L. Vasomotor innervation of the skin of the hand: a contribution to the study of human anatomy. J Anat. **182 (Pt 3)**, 361, 1993.

59. Menorca, R.M.G., Fussell, T.S., and Elfar, J.C. Nerve Physiology. Hand Clinics. **29**, 317, 2013.

60. Misra, U., Kalita, J., and Nair, P. Diagnostic approach to peripheral neuropathy. Ann Indian Acad Neurol. **11**, 89, 2008.

61. Sunderland, S. A CLASSIFICATION OF PERIPHERAL NERVE INJURIES PRODUCING LOSS OF FUNCTION. Brain. **74**, 491, 1951.

62. Schwann cell extracellular matrix molecules and their receptors. Histology and Histopathology. 593, 2000.

63. Lundborg, G. Nerve injury and repair: regeneration, reconstruction, and cortical remodeling. Philadelphia: Elsevier Churchill Livingstone, 2004.

64. Richner, M., Ferreira, N., Dudele, A., Jensen, T.S., Vaegter, C.B., and Gonçalves, N.P. Functional and Structural Changes of the Blood-Nerve-Barrier in Diabetic Neuropathy. Front Neurosci. **12**, 1038, 2019.

65. Piña-Oviedo, S., and Ortiz-Hidalgo, C. The Normal and Neoplastic Perineurium: A Review. Advances in Anatomic Pathology. **15**, 147, 2008.

66. Mizisin, A.P., and Weerasuriya, A. Homeostatic regulation of the endoneurial microenvironment during development, aging and in response to trauma, disease and toxic insult. Acta Neuropathol. **121**, 291, 2011.

67. Hamilton, N.B. Pericyte-mediated regulation of capillary diameter: a component of neurovascular coupling in health and disease. Front Neuroenerg [Internet]. **2**, 2010.

68. Reina, M.A., López, A., Villanueva, M.C., De Andrés, J.A., and Machés, F. [The blood-nerve barrier in peripheral nerves]. Rev Esp Anestesiol Reanim. **50**, 80, 2003.

69. Trapp, B.D., Quarles, R.H., and Griffin, J.W. Myelin-associated glycoprotein and myelinating Schwann cell-axon interaction in chronic B,B'-iminodipropionitrile neuropathy. Journal of Cell Biology. **98**, 1272, 1984.

70. Gillespie, C.S., Sherman, D.L., Blair, G.E., and Brophy, P.J. Periaxin, a novel protein of myelinating schwann cells with a possible role in axonal ensheathment. Neuron. **12**, 497, 1994.

71. Cheng, L., and Mudge, A.W. Cultured Schwann Cells Constitutively Express the Myelin Protein P0. Neuron. **16**, 309, 1996.

72. Shi, Y., Zhang, L., and Yang, T. Nuclear Export of L-Periaxin, Mediated by Its Nuclear Export Signal in the PDZ Domain. Palazzo, A.F., ed. PLoS ONE. **9**, e91953, 2014.

73. Griffin, J.W., and Thompson, W.J. Biology and pathology of nonmyelinating Schwann cells. Glia. **56**, 1518, 2008.

74. Harty, B.L., and Monk, K.R. Unwrapping the unappreciated: recent progress in Remak Schwann cell biology. Current Opinion in Neurobiology. **47**, 131, 2017.

75. Jessen, K.R., Mirsky, R., and Lloyd, A.C. Schwann Cells: Development and Role in Nerve Repair. Cold Spring Harb Perspect Biol. **7**, a020487, 2015.

76. Campana, W.M. Schwann cells: Activated peripheral glia and their role in neuropathic pain. Brain, Behavior, and Immunity. **21**, 522, 2007.

77. Höke, A. Schwann Cells Express Motor and Sensory Phenotypes That Regulate Axon Regeneration. Journal of Neuroscience. **26**, 9646, 2006.

78. Pummi, K.P., Heape, A.M., Grénman, R.A., Peltonen, J.T.K., and Peltonen, S.A. Tight Junction Proteins ZO-1, Occludin, and Claudins in Developing and Adult Human Perineurium. J Histochem Cytochem. **52**, 1037, 2004.

79. Richard, L., Topilko, P., Magy, L., Decouvelaere, A.-V., Charnay, P., Funalot, B., et al. Endoneurial Fibroblast-Like Cells. J Neuropathol Exp Neurol. **71**, 938, 2012.

80. Rotshenker, S. Wallerian degeneration: the innate-immune response to traumatic nerve injury. J Neuroinflammation. **8**, 109, 2011.

81. Caillaud, M., Richard, L., Vallat, J.-M., Desmoulière, A., and Billet, F. Peripheral nerve regeneration and intraneural revascularization. Neural Regen Res. **14**, 24, 2019.

82. Zigmond, R.E., and Echevarria, F.D. Macrophage biology in the peripheral nervous system after injury. Progress in Neurobiology. **173**, 102, 2019.

83. Tomlinson, J.E., Žygelytė, E., Grenier, J.K., Edwards, M.G., and Cheetham, J. Temporal changes in macrophage phenotype after peripheral nerve injury. J Neuroinflammation. **15**, 185, 2018.

84. Cattin, A.-L., Burden, J.J., Van Emmenis, L., Mackenzie, F.E., Hoving, J.J.A., Garcia Calavia, N., et al. Macrophage-Induced Blood Vessels Guide Schwann Cell-Mediated Regeneration of Peripheral Nerves. Cell. **162**, 1127, 2015.

85. Obremski, V.J., Johnson, M.I., and Bunge, M.B. Fibroblasts are required for Schwann cell basal lamina deposition and ensheathment of unmyelinated sympathetic neurites in culture. J Neurocytol. **22**, 102, 1993.

86. Wang, Y., Li, D., Wang, G., Chen, L., Chen, J., Liu, Z., et al. The effect of co-transplantation of nerve fibroblasts and Schwann cells on peripheral nerve repair. Int J Biol Sci. **13**, 1507, 2017.

87. de Ruiter, G.C.W., Spinner, R.J., Verhaagen, J., and Malessy, M.J.A. Misdirection and guidance of regenerating axons after experimental nerve injury and repair. J Neurosurg. **120**, 493, 2014.

88. Cui, Y., Yang, Y., and Qiu, D. Design of selective cell migration biomaterials and their applications for tissue regeneration. J Mater Sci. **56**, 4080, 2021.

89. Bolívar, S., Navarro, X., and Udina, E. Schwann Cell Role in Selectivity of Nerve Regeneration. Cells. **9**, 2131, 2020.

90. Hercher, D., Kerbl, M., Schuh, C.M.A.P., Heinzel, J., Gal, L., Stainer, M., et al. Spatiotemporal Differences in Gene Expression Between Motor and Sensory Autografts and Their Effect on Femoral Nerve Regeneration in the Rat. Front Cell Neurosci. **13**, 182, 2019.

91. Jesuraj, N.J., Nguyen, P.K., Wood, M.D., Moore, A.M., Borschel, G.H., Mackinnon, S.E., et al. Differential gene expression in motor and sensory Schwann cells in the rat femoral nerve. J Neurosci Res. **90**, 96, 2012.

92. Tammia, M., Mi, R., Sluch, V.M., Zhu, A., Chung, T., Shinn, D., et al. Egr2 overexpression in Schwann cells increases myelination frequency in vitro. Heliyon. **4**, e00982, 2018.

93. Qin, Q., Baudry, M., Liao, G., Noniyev, A., Galeano, J., and Bi, X. A novel function for p53: regulation of growth cone motility through interaction with Rho kinase. J Neurosci. **29**, 5183, 2009.

94. Roumazeilles, L., Dokalis, N., Kaulich, E., and Lelievre, V. It is all about the support - The role of the extracellular matrix in regenerating axon guidance. Cell Adh Migr. **12**, 87, 2018.

95. Saito, F., Moore, S.A., Barresi, R., Henry, M.D., Messing, A., Ross-Barta, S.E., et al. Unique Role of Dystroglycan in Peripheral Nerve Myelination, Nodal Structure, and Sodium Channel Stabilization. Neuron. **38**, 747, 2003.

96. Lilja, J., and Ivaska, J. Integrin activity in neuronal connectivity. J Cell Sci. **131**, jcs212803, 2018.

97. Irintchev, A., and Schachner, M. The injured and regenerating nervous system: immunoglobulin superfamily members as key players. Neuroscientist. **18**, 452, 2012.

98. Brushart, T.M., Gerber, J., Kessens, P., Chen, Y.G., and Royall, R.M. Contributions of pathway and neuron to preferential motor reinnervation. J Neurosci. **18**, 8674, 1998.

99. Cattin, A.-L., and Lloyd, A.C. The multicellular complexity of peripheral nerve regeneration. Current Opinion in Neurobiology. **39**, 38, 2016.

100. Saini, V., Lutz, D., Kataria, H., Kaur, G., Schachner, M., and Loers, G. The polysialic acid mimetics 5-nonyloxytryptamine and vinorelbine facilitate nervous system repair. Sci Rep. **6**, 26927, 2016.

101. Guseva, D., Jakovcevski, I., Irintchev, A., Leshchyns'ka, I., Sytnyk, V., Ponimaskin, E., et al. Cell Adhesion Molecule Close Homolog of L1 (CHL1) Guides the Regrowth of Regenerating Motor Axons and Regulates Synaptic Coverage of Motor Neurons. Front Mol Neurosci. **11**, 174, 2018.

102. Haney, C.A., Sahenk, Z., Li, C., Lemmon, V.P., Roder, J., and Trapp, B.D. Heterophilic binding of L1 on unmyelinated sensory axons mediates Schwann cell adhesion and is required for axonal survival. J Cell Biol. **146**, 1173, 1999.

103. Dahme, M., Bartsch, U., Martini, R., Anliker, B., Schachner, M., and Mantei, N. Disruption of the mouse L1 gene leads to malformations of the nervous system. Nat Genet. **17**, 346, 1997.

104. Bolívar, S., Navarro, X., and Udina, E. Schwann Cell Role in Selectivity of Nerve Regeneration. Cells. **9**, 2131, 2020.

105. Jones, D.M., Tucker, B.A., Rahimtula, M., and Mearow, K.M. The synergistic effects of NGF and IGF-1 on neurite growth in adult sensory neurons: convergence on the PI 3-kinase signaling pathway. J Neurochem. **86**, 1116, 2003.

106. Turney, S.G., Ahmed, M., Chandrasekar, I., Wysolmerski, R.B., Goeckeler, Z.M., Rioux, R.M., et al. Nerve growth factor stimulates axon outgrowth through negative regulation of growth cone actomyosin restraint of microtubule advance. Mol Biol Cell. **27**, 500, 2016.

107. Fornaro, M., Giovannelli, A., Foggetti, A., Muratori, L., Geuna, S., Novajra, G., et al. Role of neurotrophic factors in enhancing linear axonal growth of ganglionic sensory neurons in vitro. Neural Regen Res. **15**, 1732, 2020.

108. Cao, X., and Shoichet, M.S. Investigating the synergistic effect of combined neurotrophic factor concentration gradients to guide axonal growth. Neuroscience. **122**, 381, 2003.

109. Ng, Y.P., Cheung, Z.H., and Ip, N.Y. STAT3 as a Downstream Mediator of Trk Signaling and Functions. J Biol Chem. **281**, 15636, 2006.

110. Santos, D., Gonzalez-Perez, F., Navarro, X., and del Valle, J. Dose-Dependent Differential Effect of Neurotrophic Factors on In Vitro and In Vivo Regeneration of Motor and Sensory Neurons. Neural Plasticity. **2016**, 1, 2016.

111. Henderson, C., Phillips, H., Pollock, R., Davies, A., Lemeulle, C., Armanini, M., et al. GDNF: a potent survival factor for motoneurons present in peripheral nerve and muscle. Science. **266**, 1062, 1994.

112. Duraikannu, A., Krishnan, A., Chandrasekhar, A., and Zochodne, D.W. Beyond Trophic Factors: Exploiting the Intrinsic Regenerative Properties of Adult Neurons. Front Cell Neurosci. **13**, 128, 2019.

113. Jesuraj, N.J., Nguyen, P.K., Wood, M.D., Moore, A.M., Borschel, G.H., Mackinnon, S.E., et al. Differential gene expression in motor and sensory Schwann cells in the rat femoral nerve. J Neurosci Res. **90**, 96, 2012.

114. de Ruiter, G.C.W., Malessy, M.J.A., Yaszemski, M.J., Windebank, A.J., and Spinner, R.J. Designing ideal conduits for peripheral nerve repair. FOC. **26**, E5, 2009.

115. Hasirci, V., Arslantunali, D., Dursun, T., Yucel, D., and Hasirci, N. Peripheral nerve conduits: technology update. MDER. 405, 2014.

116. Lee, J.-Y., Giusti, G., Friedrich, P.F., Archibald, S.J., Kemnitzer, J.E., Patel, J., et al. The Effect of Collagen Nerve Conduits Filled with Collagen-Glycosaminoglycan Matrix on Peripheral Motor Nerve Regeneration in a Rat Model: The Journal of Bone and Joint Surgery-American Volume. **94**, 2084, 2012.

117. Ghaznavi, A.M., Kokai, L.E., Lovett, M.L., Kaplan, D.L., and Marra, K.G. Silk Fibroin Conduits: A Cellular and Functional Assessment of Peripheral Nerve Repair. Annals of Plastic Surgery. **66**, 273, 2011.

118. Rao, J., Cheng, Y., Liu, Y., Ye, Z., Zhan, B., Quan, D., et al. A multi-walled silk fibroin/silk sericin nerve conduit coated with poly(lactic-co-glycolic acid) sheath for peripheral nerve regeneration. Materials Science and Engineering: C. **73**, 319, 2017.

119. Gisbert Roca, F., Lozano Picazo, P., Pérez-Rigueiro, J., Guinea Tortuero, G.V., Monleón Pradas, M., and Martínez-Ramos, C. Conduits based on the combination of hyaluronic acid and silk fibroin: Characterization, in vitro studies and in vivo biocompatibility. International Journal of Biological Macromolecules. **148**, 378, 2020.

120. Hsu, S.-H., Kuo, W.-C., Chen, Y.-T., Yen, C.-T., Chen, Y.-F., Chen, K.-S., et al. New nerve regeneration strategy combining laminin-coated chitosan conduits and stem cell therapy. Acta Biomaterialia. **9**, 6606, 2013.

121. Boecker, A., Daeschler, S.C., Kneser, U., and Harhaus, L. Relevance and Recent Developments of Chitosan in Peripheral Nerve Surgery. Front Cell Neurosci. **13**, 104, 2019.

122. Jansen, K., van der Werff, J.F.A., van Wachem, P.B., Nicolai, J.-P.A., de Leij, L.F.M.H., and van Luyn, M.J.A. A hyaluronan-based nerve guide: in vitro cytotoxicity, subcutaneous tissue reactions, and degradation in the rat. Biomaterials. **25**, 483, 2004.

123. Li, R., Liu, H., Huang, H., Bi, W., Yan, R., Tan, X., et al. Chitosan conduit combined with hyaluronic acid prevent sciatic nerve scar in a rat model of peripheral nerve crush injury. Mol Med Report [Internet]. 2018 [cited 2020 Nov 7].

124. Gámez, E., Goto, Y., Nagata, K., Iwaki, T., Sasaki, T., and Matsuda, T. Photofabricated Gelatin-Based Nerve Conduits: Nerve Tissue Regeneration Potentials. Cell Transplant. **13**, 549, 2004.

125. Chang, Y.-C., Chen, M.-H., Liao, S.-Y., Wu, H.-C., Kuan, C.-H., Sun, J.-S., et al. Multichanneled Nerve Guidance Conduit with Spatial Gradients of Neurotrophic Factors and Oriented Nanotopography for Repairing the Peripheral Nervous System. ACS Appl Mater Interfaces. **9**, 37623, 2017.

126. Duncan, S.F.M., Kakinoki, R., Rizzo, M., and Kang, W. Extrusion of a NeuroTube: A Case Report. Ochsner J. **15**, 191, 2015.

127. Chiriac, S., Facca, S., Diaconu, M., Gouzou, S., and Liverneaux, P. Experience of using the bioresorbable copolyester poly(DL-lactide-ε-caprolactone) nerve conduit guide Neurolac™ for nerve repair in peripheral nerve defects: Report on a series of 28 lesions. J Hand Surg Eur Vol. **37**, 342, 2012.

128. Labroo, P., Ho, S., Sant, H., Shea, J., Gale, B.K., and Agarwal, J. Controlled Delivery of FK506 to Improve Nerve Regeneration. Shock. **46**, 154, 2016.

129. Wlaszczuk, A., Marcol, W., Kucharska, M., Wawro, D., Palen, P., and Lewin-Kowalik, J. Poly(D,L-Lactide-Co-Glycolide) Tubes With Multifilament Chitosan Yarn or Chitosan Sponge Core in Nerve Regeneration. Journal of Oral and Maxillofacial Surgery. **74**, 2327.e1, 2016.

130. Mosahebi, A., Wiberg, M., and Terenghi, G. Addition of Fibronectin to Alginate Matrix Improves Peripheral Nerve Regeneration in Tissue-Engineered Conduits. Tissue Engineering. **9**, 209, 2003.

131. Young, R.C., Terenghi, G., and Wiberg, M. Poly-3-hydroxybutyrate (PHB): a resorbable conduit for long-gap repair in peripheral nerves. British Journal of Plastic Surgery. **55**, 235, 2002.

132. Lundborg, G., Dahlin, L.B., Danielsen, N., Gelberman, R.H., Longo, F.M., Powell, H.C., et al. Nerve regeneration in silicone chambers: Influence of gap length and of distal stump components. Experimental Neurology. **76**, 361, 1982.

133. Sundback, C. Manufacture of porous polymer nerve conduits by a novel low-pressure injection molding process. Biomaterials. **24**, 819, 2003.

134. Shen, X., Ruan, J., Zhou, Z., Zeng, Z., and Xie, L. Evaluation of PLGA/chitosan/HA conduits for nerve tissue reconstruction. J Wuhan Univ Technol-Mat Sci Edit. **24**, 566, 2009.

135. Ao, Q., Wang, A., Cao, W., Zhang, L., Kong, L., He, Q., et al. Manufacture of multimicrotubule chitosan nerve conduits with novel molds and characterizationin vitro. J Biomed Mater Res. **77A**, 11, 2006.

136. Muheremu, A., Chen, L., Wang, X., Wei, Y., Gong, K., and Ao, Q. Chitosan nerve conduits seeded with autologous bone marrow mononuclear cells for 30 mm goat peroneal nerve defect. Sci Rep. **7**, 44002, 2017.

137. Yu, W., Jiang, X., Cai, M., Zhao, W., Ye, D., Zhou, Y., et al. A novel electrospun nerve conduit enhanced by carbon nanotubes for peripheral nerve regeneration. Nanotechnology. **25**, 165102, 2014.

138. Jiang, X., Lim, S.H., Mao, H.-Q., and Chew, S.Y. Current applications and future perspectives of artificial nerve conduits. Experimental Neurology. **223**, 86, 2010.

139. Vijayavenkataraman, S., Zhang, S., Thaharah, S., Sriram, G., Lu, W.F., and Fuh, J.Y.H. Electrohydrodynamic Jet 3D Printed Nerve Guide Conduits (NGCs) for Peripheral Nerve Injury Repair. Polymers. **10**, 753, 2018.

140. Inada, Y., Hosoi, H., Yamashita, A., Morimoto, S., Tatsumi, H., Notazawa, S., et al. REGENERATION OF PERIPHERAL MOTOR NERVE GAPS WITH A POLYGLYCOLIC ACID-COLLAGEN TUBE. Neurosurgery. **61**, E1105, 2007.

141. Fan, W., Gu, J., Hu, W., Deng, A., Ma, Y., Liu, J., et al. Repairing a 35-mm-long median nerve defect with a chitosan/PGA artificial nerve graft in the human: A case study. Microsurgery. **28**, 238, 2008.

142. Wang, S., and Cai, L. Polymers for Fabricating Nerve Conduits. International Journal of Polymer Science. **2010**, 1, 2010.

143. Vijayavenkataraman, S. Nerve guide conduits for peripheral nerve injury repair: A review on design, materials and fabrication methods. Acta Biomaterialia. **106**, 54, 2020.

144. Du, J., Chen, H., Qing, L., Yang, X., and Jia, X. Biomimetic neural scaffolds: a crucial step towards optimal peripheral nerve regeneration. Biomater Sci. **6**, 1299, 2018.

145. Langer, R., and Vacanti, J. Tissue engineering. Science. **260**, 920, 1993.

146. O'Brien, F.J. Biomaterials & scaffolds for tissue engineering. Materials Today. **14**, 88, 2011.

147. Hopley, E.L., Salmasi, S., Kalaskar, D.M., and Seifalian, A.M. Carbon nanotubes leading the way forward in new generation 3D tissue engineering. Biotechnology Advances. **32**, 1000, 2014.

148. Pedrini, F.A., Boriani, F., Bolognesi, F., Fazio, N., Marchetti, C., and Baldini, N. Cell-Enhanced Acellular Nerve Allografts for Peripheral Nerve Reconstruction: A Systematic Review and a Meta-Analysis of the Literature. Neurosurgery. **85**, 575, 2019.

149. Hood, B., Levene, H.B., and Levi, A.D. Transplantation of autologous Schwann cells for the repair of segmental peripheral nerve defects. FOC. **26**, E4, 2009.

150. Wakao, S., Matsuse, D., and Dezawa, M. Mesenchymal Stem Cells as a Source of Schwann Cells: Their Anticipated Use in Peripheral Nerve Regeneration. Cells Tissues Organs. **200**, 31, 2015.

151. di Summa, P.G., Kingham, P.J., Raffoul, W., Wiberg, M., Terenghi, G., and Kalbermatten, D.F. Adipose-derived stem cells enhance peripheral nerve regeneration. Journal of Plastic, Reconstructive & Aesthetic Surgery. **63**, 1544, 2010.

152. Frattini, F., Pereira Lopes, F.R., Almeida, F.M., Rodrigues, R.F., Boldrini, L.C., Tomaz, M.A., et al. Mesenchymal Stem Cells in a Polycaprolactone Conduit Promote Sciatic Nerve Regeneration and Sensory Neuron Survival after Nerve Injury. Tissue Engineering Part A. **18**, 2030, 2012.

153. Zack-Williams, S.D. Current progress in use of adipose derived stem cells in peripheral nerve regeneration. WJSC. **7**, 51, 2015.

154. Lopatina, T., Kalinina, N., Karagyaur, M., Stambolsky, D., Rubina, K., Revischin, A., et al. Adipose-Derived Stem Cells Stimulate Regeneration of Peripheral Nerves: BDNF Secreted by These Cells Promotes Nerve Healing and Axon Growth De Novo. Egles, C., ed. PLoS ONE. **6**, e17899, 2011.

155. Di Summa, P.G., Schiraldi, L., Cherubino, M., Oranges, C.M., Kalbermatten, D.F., Raffoul, W., et al. Adipose Derived Stem Cells Reduce Fibrosis and Promote Nerve Regeneration in Rats. Anat Rec. **301**, 1714, 2018.

156. Bhangra, K.S., Busuttil, F., Phillips, J.B., and Rahim, A.A. Using Stem Cells to Grow Artificial Tissue for Peripheral Nerve Repair. Stem Cells International. **2016**, 1, 2016.

157. Amoh, Y., Li, L., Campillo, R., Kawahara, K., Katsuoka, K., Penman, S., et al. Implanted hair follicle stem cells form Schwann cells that support repair of severed peripheral nerves. Proceedings of the National Academy of Sciences. **102**, 17734, 2005.

158. Kalbermatten, D.F., Kingham, P.J., Mahay, D., Mantovani, C., Pettersson, J., Raffoul, W., et al. Fibrin matrix for suspension of regenerative cells in an artificial nerve conduit. Journal of Plastic, Reconstructive & Aesthetic Surgery. **61**, 669, 2008.

159. Meyer, C., Stenberg, L., Gonzalez-Perez, F., Wrobel, S., Ronchi, G., Udina, E., et al. Chitosan-film enhanced chitosan nerve guides for long-distance regeneration of peripheral nerves. Biomaterials. **76**, 33, 2016.

160. Li, Y., Yu, Z., Men, Y., Chen, X., and Wang, B. Laminin-chitosan-PLGA conduit co-transplanted with Schwann and neural stem cells to repair the injured recurrent laryngeal nerve. Exp Ther Med [Internet]. 2018

161. Sun, A.X., Prest, T.A., Fowler, J.R., Brick, R.M., Gloss, K.M., Li, X., et al. Conduits harnessing spatially controlled cell-secreted neurotrophic factors improve peripheral nerve regeneration. Biomaterials. **203**, 86, 2019.

162. Labroo, P., Shea, J., Edwards, K., Ho, S., Davis, B., Sant, H., et al. Novel drug delivering conduit for peripheral nerve regeneration. J Neural Eng. **14**, 066011, 2017.

163. Fadia, N.B., Bliley, J.M., DiBernardo, G.A., Crammond, D.J., Schilling, B.K., Sivak, W.N., et al. Long-gap peripheral nerve repair through sustained release of a neurotrophic factor in nonhuman primates. Sci Transl Med. **12**, eaav7753, 2020

164. Su, H., Xu, F., Sun, H., Fu, X., and Zhao, Y. Preparation and Evaluation of BDNF Composite Conduits for Regeneration of Sciatic Nerve Defect in Rats. Journal of Pharmaceutical Sciences. **109**, 2189, 2020.

165. Yang, Y., De Laporte, L., Rives, C.B., Jang, J.-H., Lin, W.-C., Shull, K.R., et al. Neurotrophin releasing single and multiple lumen nerve conduits. Journal of Controlled Release. **104**, 433, 2005.

166. Mohammadi, R., Ahsan, S., Masoumi, M., and Amini, K. Vascular endothelial growth factor promotes peripheral nerve regeneration after sciatic nerve transection in rat. Chin J Traumatol. **16**, 323, 2013.

167. Madduri, S., and Gander, B. Schwann cell delivery of neurotrophic factors for peripheral nerve regeneration. Journal of the Peripheral Nervous System. **15**, 93, 2010.

168. Bittner, S.M., Guo, J.L., and Mikos, A.G. Spatiotemporal control of growth factors in three-dimensional printed scaffolds. Bioprinting. **12**, e00032, 2018.

169. Pfister, L.A., Papaloïzos, M., Merkle, H.P., and Gander, B. Nerve conduits and growth factor delivery in peripheral nerve repair. J Peripher Nerv Syst. **12**, 65, 2007.

170. Murphy, S.V., and Atala, A. 3D bioprinting of tissues and organs. Nat Biotechnol. **32**, 773, 2014.

171. Hu, Y., Wu, Y., Gou, Z., Tao, J., Zhang, J., Liu, Q., et al. 3D-engineering of Cellularized Conduits for Peripheral Nerve Regeneration. Sci Rep. **6**, 32184, 2016.

172. Bücking, T.M., Hill, E.R., Robertson, J.L., Maneas, E., Plumb, A.A., and Nikitichev, D.I. From medical imaging data to 3D printed anatomical models. Chen, H.-C.I., ed. PLoS ONE. **12**, e0178540, 2017.

173. Höhne, C., and Schmitter, M. 3D Printed Teeth for the Preclinical Education of Dental Students. Journal of Dental Education. **83**, 1100, 2019.

174. Mangano, C., Bianchi, A., Mangano, F.G., Dana, J., Colombo, M., Solop, I., et al. Custom-made 3D printed subperiosteal titanium implants for the prosthetic restoration of the atrophic posterior mandible of elderly patients: a case series. 3D Print Med. **6**, 1, 2020.

175. Xu, H.-D., Miron, R.J., Zhang, X.-X., and Zhang, Y.-F. Allogenic tooth transplantation using 3D printing: A case report and review of the literature. WJCC. **7**, 2587, 2019.

176. Aimar, A., Palermo, A., and Innocenti, B. The Role of 3D Printing in Medical Applications: A State of the Art. Journal of Healthcare Engineering. **2019**, 1, 2019.

177. Pateman, C.J., Harding, A.J., Glen, A., Taylor, C.S., Christmas, C.R., Robinson, P.P., et al. Nerve guides manufactured from photocurable polymers to aid peripheral nerve repair. Biomaterials. **49**, 77, 2015.

178. Arcaute, K., Mann, B.K., and Wicker, R.B. Fabrication of Off-the-Shelf Multilumen Poly(Ethylene Glycol) Nerve Guidance Conduits Using Stereolithography. Tissue Engineering Part C: Methods. **17**, 27, 2011.

179. Evangelista, M., Perez, M., Salibian, A., Hassan, J., Darcy, S., Paydar, K., et al. Single-Lumen and Multi-Lumen Poly(Ethylene Glycol) Nerve Conduits Fabricated by Stereolithography for Peripheral Nerve Regeneration In Vivo. J reconstr Microsurg. **31**, 327, 2015.

180. Johnson, B.N., Lancaster, K.Z., Zhen, G., He, J., Gupta, M.K., Kong, Y.L., et al. 3D Printed Anatomical Nerve Regeneration Pathways. Adv Funct Mater. **25**, 6205, 2015.

181. Vijayavenkataraman, S., Zhang, S., Thaharah, S., Sriram, G., Lu, W.F., and Fuh, J.Y.H. Electrohydrodynamic Jet 3D Printed Nerve Guide Conduits (NGCs) for Peripheral Nerve Injury Repair. Polymers. **10**, 753, 2018.

182. Vijayavenkataraman, S., Thaharah, S., Zhang, S., Lu, W.F., and Fuh, J.Y.H. 3D-Printed PCL/rGO Conductive Scaffolds for Peripheral Nerve Injury Repair. Artif Organs. **43**, 515, 2019.

183. Vijayavenkataraman, S., Kannan, S., Cao, T., Fuh, J.Y.H., Sriram, G., and Lu, W.F. 3D-Printed PCL/PPy Conductive Scaffolds as Three-Dimensional Porous Nerve Guide Conduits (NGCs) for Peripheral Nerve Injury Repair. Front Bioeng Biotechnol. **7**, 266, 2019.

184. Vijayavenkataraman, S., Thaharah, S., Zhang, S., Lu, W.F., and Fuh, J.Y.H. Electrohydrodynamic jet 3D-printed PCL/PAA conductive scaffolds with tunable biodegradability as nerve guide conduits (NGCs) for peripheral nerve injury repair. Materials & Design. **162**, 171, 2019.

185. Radulescu, D., Dhar, S., Young, C.M., Taylor, D.W., Trost, H.-J., Hayes, D.J., et al. Tissue engineering scaffolds for nerve regeneration manufactured by ink-jet technology. Materials Science and Engineering: C. **27**, 534, 2007.

186. Singh, D., Harding, A.J., Albadawi, E., Boissonade, F.M., Haycock, J.W., and Claeyssens, F. Additive manufactured biodegradable poly(glycerol sebacate methacrylate) nerve guidance conduits. Acta Biomaterialia. **78**, 48, 2018.

187. Jakus, A.E., Secor, E.B., Rutz, A.L., Jordan, S.W., Hersam, M.C., and Shah, R.N. Three-Dimensional Printing of High-Content Graphene Scaffolds for Electronic and Biomedical Applications. ACS Nano. **9**, 4636, 2015.

188. Gong, H., Fei, H., Xu, Q., Gou, M., and Chen, H.H. 3D-engineered GelMA conduit filled with ECM promotes regeneration of peripheral nerve. J Biomed Mater Res. **108**, 805, 2020.

189. Tao, J., Zhang, J., Du, T., Xu, X., Deng, X., Chen, S., et al. Rapid 3D printing of functional nanoparticle-enhanced conduits for effective nerve repair. Acta Biomaterialia. **90**, 49, 2019.

190. Cui, T., Yan, Y., Zhang, R., Liu, L., Xu, W., and Wang, X. Rapid Prototyping of a Double-Layer Polyurethane–Collagen Conduit for Peripheral Nerve Regeneration. Tissue Engineering Part C: Methods. **15**, 1, 2009.

191. Chen, Chen, Ng, Lou, Chen, and Shie. Additive Manufacturing of Nerve Decellularized Extracellular Matrix-Contained Polyurethane Conduits for Peripheral Nerve Regeneration. Polymers. **11**, 1612, 2019.

192. Zhu, W., Tringale, K.R., Woller, S.A., You, S., Johnson, S., Shen, H., et al. Rapid continuous 3D printing of customizable peripheral nerve guidance conduits. Materials Today. **21**, 951, 2018.

193. Schmidleithner, C., and Kalaskar, D.M. Stereolithography. In: Cvetković, D., ed. 3D Printing. InTech, 2018.

194. Quan, H., Zhang, T., Xu, H., Luo, S., Nie, J., and Zhu, X. Photo-curing 3D printing technique and its challenges. Bioactive Materials. **5**, 110, 2020.

195. Zhang, J., and Xiao, P. 3D printing of photopolymers. Polym Chem. **9**, 1530, 2018.

196. George, E., Liacouras, P., Rybicki, F.J., and Mitsouras, D. Measuring and Establishing the Accuracy and Reproducibility of 3D Printed Medical Models. RadioGraphics. **37**, 1424, 2017.

197. Hoang, D., Perrault, D., Stevanovic, M., and Ghiassi, A. Surgical applications of three-dimensional printing: a review of the current literature & how to get started. Ann Transl Med. **4**, 456, 2016.

198. Wu, G.-H., and Hsu, S. Review: Polymeric-Based 3D Printing for Tissue Engineering. J Med Biol Eng. **35**, 285, 2015.

199. Provaggi, E., and Kalaskar, D.M. 3D printing families. 3D Printing in Medicine. Elsevier, pp. 21–42, 2017.

200. Salentijn, G.IJ., Oomen, P.E., Grajewski, M., and Verpoorte, E. Fused Deposition Modeling 3D Printing for (Bio)analytical Device Fabrication: Procedures, Materials, and Applications. Anal Chem. **89**, 7053, 2017.

201. Calignano, F., Galati, M., Iuliano, L., and Minetola, P. Design of Additively Manufactured Structures for Biomedical Applications: A Review of the Additive Manufacturing Processes Applied to the Biomedical Sector. Journal of Healthcare Engineering. **2019**, 1, 2019.

202. Gunatillake, P.A., and Adhikari, R. Biodegradable synthetic polymers for tissue engineering. eCM. **5**, 1, 2003.

203. Derakhshanfar, S., Mbeleck, R., Xu, K., Zhang, X., Zhong, W., and Xing, M. 3D bioprinting for biomedical devices and tissue engineering: A review of recent trends and advances. Bioactive Materials. **3**, 144, 2018.

204. Hwang, H.H., Zhu, W., Victorine, G., Lawrence, N., and Chen, S. 3D-Printing of Functional Biomedical Microdevices via Light- and Extrusion-Based Approaches. Small Methods. **2**, 1700277, 2018.

205. Ribeiro-Resende, V.T., Koenig, B., Nichterwitz, S., Oberhoffner, S., and Schlosshauer, B. Strategies for inducing the formation of bands of Büngner in peripheral nerve regeneration. Biomaterials. **30**, 5251, 2009.

206. Vyas, A., Li, Z., Aspalter, M., Feiner, J., Hoke, A., Zhou, C., et al. An in vitro model of adult mammalian nerve repair. Experimental Neurology. **223**, 112, 2010.

207. Khoshakhlagh, P., Sivakumar, A., Pace, L.A., Sazer, D.W., and Moore, M.J. Methods for fabrication and evaluation of a 3D microengineered model of myelinated peripheral nerve. J Neural Eng. **15**, 064001, 2018

208. Sharma, A.D., McCoy, L., Jacobs, E., Willey, H., Behn, J.Q., Nguyen, H., et al. Engineering a 3D functional human peripheral nerve in vitro using the Nerve-on-a-Chip platform. Sci Rep. **9**, 8921, 2019.

209. Vermeulen, N., Haddow, G., Seymour, T., Faulkner-Jones, A., and Shu, W. 3D bioprint me: a socioethical view of bioprinting human organs and tissues. J Med Ethics. **43**, 618, 2017.

210. Ji, S., and Guvendiren, M. Recent Advances in Bioink Design for 3D Bioprinting of Tissues and Organs. Front Bioeng Biotechnol. **5**, 2017.

211. Choudhury, D., Tun, H.W., Wang, T., and Naing, M.W. Organ-Derived Decellularized Extracellular Matrix: A Game Changer for Bioink Manufacturing? Trends in Biotechnology. **36**, 787, 2018.

212. Chimene, D., Kaunas, R., and Gaharwar, A.K. Hydrogel Bioink Reinforcement for Additive Manufacturing: A Focused Review of Emerging Strategies. Adv Mater. **32**, 1902026, 2020.

213. Lee, J.M., and Yeong, W.Y. Design and Printing Strategies in 3D Bioprinting of Cell-Hydrogels: A Review. Adv Healthcare Mater. **5**, 2856, 2016.

214. Hinton, T.J., Jallerat, Q., Palchesko, R.N., Park, J.H., Grodzicki, M.S., Shue, H.-J., et al. Three-dimensional printing of complex biological structures by freeform reversible embedding of suspended hydrogels. Sci Adv. **1**, e1500758, 2015.

215. Moxon, S.R., Cooke, M.E., Cox, S.C., Snow, M., Jeys, L., Jones, S.W., et al. Suspended Manufacture of Biological Structures. Adv Mater. **29**, 1605594, 2017.

216. Morgan, F.L.C., Moroni, L., and Baker, M.B. Dynamic Bioinks to Advance Bioprinting. Adv Healthcare Mater. **9**, 1901798, 2020.

217. Liu, Y., and Hsu, S. Synthesis and Biomedical Applications of Self-healing Hydrogels. Front Chem. **6**, 449, 2018.

218. Donderwinkel, I., van Hest, J.C.M., and Cameron, N.R. Bio-inks for 3D bioprinting: recent advances and future prospects. Polym Chem. **8**, 4451, 2017.

219. Biswas, A., Maiti, S., Kalaskar, D.M., and Das, A.K. Redox-Active Dynamic Self-Supporting Thixotropic 3D-Printable G-Quadruplex Hydrogels. Chem Asian J. **13**, 3928, 2018.

220. Gillispie, G., Prim, P., Copus, J., Fisher, J., Mikos, A.G., Yoo, J.J., et al. Assessment methodologies for extrusion-based bioink printability. Biofabrication. **12**, 022003, 2020.

221. Bedell, M.L., Navara, A.M., Du, Y., Zhang, S., and Mikos, A.G. Polymeric Systems for Bioprinting. Chem Rev. **120**, 10744, 2020.

222. Liu, J.S., and Gartner, Z.J. Directing the assembly of spatially organized multicomponent tissues from the bottom up. Trends in Cell Biology. **22**, 683, 2012.

223. Kamperman, T., Henke, S., van den Berg, A., Shin, S.R., Tamayol, A., Khademhosseini, A., et al. Single Cell Microgel Based Modular Bioinks for Uncoupled Cellular Micro- and Macroenvironments. Adv Healthcare Mater. **6**, 1600913, 2017.

224. Chen, J., Huang, D., Wang, L., Hou, J., Zhang, H., Li, Y., et al. 3D bioprinted multiscale composite scaffolds based on gelatin methacryloyl (GelMA)/chitosan microspheres as a modular bioink for enhancing 3D neurite outgrowth and elongation. Journal of Colloid and Interface Science. **574**, 162, 2020

225. Murphy, S.V., and Atala, A. 3D bioprinting of tissues and organs. Nat Biotechnol. **32**, 773, 2014

226. Xia, Z., Jin, S., and Ye, K. Tissue and Organ 3D Bioprinting. SLAS TECHNOLOGY: Translating Life Sciences Innovation. **23**, 301, 2018.

227. Naghieh, S., Sarker, M.D., Abelseth, E., and Chen, X. Indirect 3D bioprinting and characterization of alginate scaffolds for potential nerve tissue engineering applications. Journal of the Mechanical Behavior of Biomedical Materials. **93**, 183, 2019.

228. Ning, L., Sun, H., Lelong, T., Guilloteau, R., Zhu, N., Schreyer, D.J., et al. 3D bioprinting of scaffolds with living Schwann cells for potential nerve tissue engineering applications. Biofabrication. **10**, 035014, 2018.

229. Ning, L., Zhu, N., Mohabatpour, F., Sarker, M.D., Schreyer, D.J., and Chen, X. Bioprinting Schwann cell-laden scaffolds from low-viscosity hydrogel compositions. J Mater Chem B. **7**, 4538, 2019.

230. Li, X., Wang, X., Wang, X., Chen, H., Zhang, X., Zhou, L., et al. 3D bioprinted rat Schwann cell-laden structures with shape flexibility and enhanced nerve growth factor expression. 3 Biotech. **8**, 342, 2018.

231. Wu, Z., Li, Q., Xie, S., Shan, X., and Cai, Z. In vitro and in vivo biocompatibility evaluation of a 3D bioprinted gelatin-sodium alginate/rat Schwann-cell scaffold. Materials Science and Engineering: C. **109**, 110530, 2020.

232. Tse, C., Whiteley, R., Yu, T., Stringer, J., MacNeil, S., Haycock, J.W., et al. Inkjet printing Schwann cells and neuronal analogue NG108-15 cells. Biofabrication. **8**, 015017, 2016

233. Gu, Z., Fu, J., Lin, H., and He, Y. Development of 3D bioprinting: From printing methods to biomedical applications. Asian Journal of Pharmaceutical Sciences. **15**, 529, 2020.

234. Jiang, T., Munguia-Lopez, J.G., Flores-Torres, S., Kort-Mascort, J., and Kinsella, J.M. Extrusion bioprinting of soft materials: An emerging technique for biological model fabrication. Applied Physics Reviews. **6**, 011310, 2019.

235. Suntornnond, R., Tan, E., An, J., and Chua, C. A Mathematical Model on the Resolution of Extrusion Bioprinting for the Development of New Bioinks. Materials. **9**, 756, 2016.

236. Ozbolat, I.T., and Yin Yu. Bioprinting Toward Organ Fabrication: Challenges and Future Trends. IEEE Trans Biomed Eng. **60**, 691, 2013.

237. Cui, X., Boland, T., D.D'Lima, D., and K. Lotz, M. Thermal Inkjet Printing in Tissue Engineering and Regenerative Medicine. DDF. **6**, 149, 2012.

238. Derakhshanfar, S., Mbeleck, R., Xu, K., Zhang, X., Zhong, W., and Xing, M. 3D bioprinting for biomedical devices and tissue engineering: A review of recent trends and advances. Bioactive Materials. **3**, 144, 2018.

239. Xia, Z., Jin, S., and Ye, K. Tissue and Organ 3D Bioprinting. SLAS TECHNOLOGY: Translating Life Sciences Innovation. **23**, 301, 2018.

240. Guillotin, B., Souquet, A., Catros, S., Duocastella, M., Pippenger, B., Bellance, S., et al. Laser assisted bioprinting of engineered tissue with high cell density and microscale organization. Biomaterials. **31**, 7250, 2010.

241. Ozbolat, I.T. Scaffold-Based or Scaffold-Free Bioprinting: Competing or Complementing Approaches? Journal of Nanotechnology in Engineering and Medicine. **6**, 024701, 2015.

242. Moldovan, N.I., Hibino, N., and Nakayama, K. Principles of the *Kenzan* Method for Robotic Cell Spheroid-Based Three-Dimensional Bioprinting <sup/>. Tissue Engineering Part B: Reviews. **23**, 237, 2017.

243. Nunes, A.S., Barros, A.S., Costa, E.C., Moreira, A.F., and Correia, I.J. 3D tumor spheroids as in vitro models to mimic in vivo human solid tumors resistance to therapeutic drugs: NUNES ET AL. Biotechnology and Bioengineering. **116**, 206, 2019.

244. Hamilton, G., and Rath, B. Role of circulating tumor cell spheroids in drug resistance. CDR [Internet]. 2019

245. Cheng, N.-C., Wang, S., and Young, T.-H. The influence of spheroid formation of human adipose-derived stem cells on chitosan films on stemness and differentiation capabilities. Biomaterials. **33**, 1748, 2012.

246. Bartosh, T.J., and Ylostalo, J.H. Preparation of Anti-Inflammatory Mesenchymal Stem/Precursor Cells (MSCs) Through Sphere Formation Using Hanging-Drop Culture Technique: Spheroid

Formation Using Hanging Drop Culture Technique. Current Protocols in Stem Cell Biology. **28**, 2B.6.1, 2014.

247. Han, Y., Liu, X.-M., Liu, H., Li, S.-C., Wu, B.-C., Ye, L.-L., et al. Cultivation of Recombinant Chinese hamster ovary cells grown as suspended aggregates in stirred vessels. Journal of Bioscience and Bioengineering. **102**, 430, 2006.

248. Carpenedo, R.L., Sargent, C.Y., and McDevitt, T.C. Rotary Suspension Culture Enhances the Efficiency, Yield, and Homogeneity of Embryoid Body Differentiation. STEM CELLS. **25**, 2224, 2007.

249. Vadivelu, R., Kamble, H., Shiddiky, M., and Nguyen, N.-T. Microfluidic Technology for the Generation of Cell Spheroids and Their Applications. Micromachines. **8**, 94, 2017.

250. Li, J., He, F., and Pei, M. Creation of an in vitro microenvironment to enhance human fetal synovium-derived stem cell chondrogenesis. Cell Tissue Res. **345**, 357, 2011.

251. Costa, E.C., de Melo-Diogo, D., Moreira, A.F., Carvalho, M.P., and Correia, I.J. Spheroids Formation on Non-Adhesive Surfaces by Liquid Overlay Technique: Considerations and Practical Approaches. Biotechnol J. **13**, 1700417, 2018.

252. Itoh, M., Nakayama, K., Noguchi, R., Kamohara, K., Furukawa, K., Uchihashi, K., et al. Scaffold-Free Tubular Tissues Created by a Bio-3D Printer Undergo Remodeling and Endothelialization when Implanted in Rat Aortae. Zhu, D., ed. PLoS ONE. **10**, e0136681, 2015.

253. Taniguchi, D., Matsumoto, K., Tsuchiya, T., Machino, R., Takeoka, Y., Elgalad, A., et al. Scaffold-free trachea regeneration by tissue engineering with bio-3D printing†. Interactive CardioVascular and Thoracic Surgery. **26**, 745, 2018.

254. Arai, K., Murata, D., Verissimo, A.R., Mukae, Y., Itoh, M., Nakamura, A., et al. Fabrication of scaffold-free tubular cardiac constructs using a Bio-3D printer. Matsusaki, M., ed. PLoS ONE. **13**, e0209162, 2018.

255. Yurie, H., Ikeguchi, R., Aoyama, T., Kaizawa, Y., Tajino, J., Ito, A., et al. The efficacy of a scaffold-free Bio 3D conduit developed from human fibroblasts on peripheral nerve regeneration in a rat sciatic nerve model. Nógrádi, A., ed. PLoS ONE. **12**, e0171448, 2017.

256. Takeuchi, H., Ikeguchi, R., Aoyama, T., Oda, H., Yurie, H., Mitsuzawa, S., et al. A scaffold-free Bio 3D nerve conduit for repair of a 10-mm peripheral nerve defect in the rats. Microsurgery. **40**, 207, 2020.

257. Zhang, Q., Nguyen, P.D., Shi, S., Burrell, J.C., Cullen, D.K., and Le, A.D. 3D bio-printed scaffold-free nerve constructs with human gingiva-derived mesenchymal stem cells promote rat facial nerve regeneration. Sci Rep. **8**, 6634, 2018.

258. Mitsuzawa, S., Ikeguchi, R., Aoyama, T., Takeuchi, H., Yurie, H., Oda, H., et al. The Efficacy of a Scaffold-free Bio 3D Conduit Developed from Autologous Dermal Fibroblasts on Peripheral Nerve Regeneration in a Canine Ulnar Nerve Injury Model: A Preclinical Proof-of-Concept Study. Cell Transplant. **28**, 1231, 2019.

259. Owens, C.M., Marga, F., Forgacs, G., and Heesch, C.M. Biofabrication and testing of a fully cellular nerve graft. Biofabrication. **5**, 045007, 2013.

260. Marga, F., Jakab, K., Khatiwala, C., Shepherd, B., Dorfman, S., Hubbard, B., et al. Toward engineering functional organ modules by additive manufacturing. Biofabrication. **4**, 022001, 2012.

261. Mehta, G., Hsiao, A.Y., Ingram, M., Luker, G.D., and Takayama, S. Opportunities and challenges for use of tumor spheroids as models to test drug delivery and efficacy. Journal of Controlled Release. **164**, 192, 2012.

262. Shao, H., Sun, M., Zhang, F., Liu, A., He, Y., Fu, J., et al. Custom Repair of Mandibular Bone Defects with 3D Printed Bioceramic Scaffolds. J Dent Res. **97**, 68, 2018.

263. Li, L., Yu, F., Shi, J., Shen, S., Teng, H., Yang, J., et al. In situ repair of bone and cartilage defects using 3D scanning and 3D printing. Sci Rep. **7**, 9416, 2017.

264. Badia, J., Pascual-Font, A., Vivó, M., Udina, E., and Navarro, X. Topographical distribution of motor fascicles in the sciatic-tibial nerve of the rat. Muscle Nerve. **42**, 192, 2010.

265. Haninec, P. Undulating course of nerve fibres and bands of Fontana in peripheral nerves of the rat. Anat Embryol. **174**, 407, 1986.

266. Stewart, J.D. Peripheral nerve fascicles: Anatomy and clinical relevance. Muscle Nerve. **28**, 525, 2003.

267. Dixon, A.R., Jariwala, S.H., Bilis, Z., Loverde, J.R., Pasquina, P.F., and Alvarez, L.M. Bridging the gap in peripheral nerve repair with 3D printed and bioprinted conduits. Biomaterials. **186**, 44, 2018.

268. Shelmerdine, S.C., Simcock, I.C., Hutchinson, J.C., Aughwane, R., Melbourne, A., Nikitichev, D.I., et al. 3D printing from microfocus computed tomography (micro-CT) in human specimens: education and future implications. BJR. 20180306, 2018.

269. Kampschulte, M., Langheinirch, A., Sender, J., Litzlbauer, H., Althöhn, U., Schwab, J., et al. Nano-Computed Tomography: Technique and Applications. Fortschr Röntgenstr. **188**, 146, 2016.

270. Bertoldi, S., Farè, S., and Tanzi, M.C. Assessment of scaffold porosity: the new route of micro-CT. JABB. **9**, 165, 2011.

271. Wu, G.-H., and Hsu, S. Review: Polymeric-Based 3D Printing for Tissue Engineering. J Med Biol Eng. **35**, 285, 2015.

272. Heimel, P., Swiadek, N.V., Slezak, P., Kerbl, M., Schneider, C., Nürnberger, S., et al. Iodine-Enhanced Micro-CT Imaging of Soft Tissue on the Example of Peripheral Nerve Regeneration. Contrast Media & Molecular Imaging. **2019**, 1, 2019.

273. Thompson, N., Ravagli, E., Mastitskaya, S., Iacoviello, F., Aristovich, K., Perkins, J., et al. MicroCT optimisation for imaging fascicular anatomy in peripheral nerves. Journal of Neuroscience Methods. **338**, 108652, 2020.

274. Zhu, S., Zhu, Q., Liu, X., Yang, W., Jian, Y., Zhou, X., et al. Three-dimensional Reconstruction of the Microstructure of Human Acellular Nerve Allograft. Sci Rep. **6**, 30694, 2016.

275. Sharir, A., Ramniceanu, G., and Brumfeld, V. High Resolution 3D Imaging of Ex-Vivo Biological Samples by Micro CT. JoVE. 2688, 2011.

276. Yao, Z., Yan, L.-W., Qiu, S., He, F.-L., Gu, F.-B., Liu, X.-L., et al. Customized Scaffold Design Based on Natural Peripheral Nerve Fascicle Characteristics for Biofabrication in Tissue Regeneration. BioMed Research International. **2019**, 1, 2019.

277. Bernal, P.N., Delrot, P., Loterie, D., Li, Y., Malda, J., Moser, C., et al. Volumetric Bioprinting of Complex Living-Tissue Constructs within Seconds. Adv Mater. **31**, 1904209, 2019.

278. Zhang, B., Gao, L., Ma, L., Luo, Y., Yang, H., and Cui, Z. 3D Bioprinting: A Novel Avenue for Manufacturing Tissues and Organs. Engineering. **5**, 777, 2019.

279. Claeyssens, F., Hasan, E.A., Gaidukeviciute, A., Achilleos, D.S., Ranella, A., Reinhardt, C., et al. Three-Dimensional Biodegradable Structures Fabricated by Two-Photon Polymerization. Langmuir. **25**, 3219, 2009.

280. Malkoc, V. Challenges and the future of 3D bioprinting. Journal of Biomedical Imaging and Bioengineering. **2**, 1, 2018.

281. Chang, R., Nam, J., and Sun, W. Effects of Dispensing Pressure and Nozzle Diameter on Cell Survival from Solid Freeform Fabrication–Based Direct Cell Writing. Tissue Engineering Part A. **14**, 41, 2008.

282. Qiu, B., Bessler, N., Figler, K., Buchholz, M., Rios, A.C., Malda, J., et al. Bioprinting Neural Systems to Model Central Nervous System Diseases. Adv Funct Mater. **30**, 1910250, 2020.

283. Kolesky, D.B., Truby, R.L., Gladman, A.S., Busbee, T.A., Homan, K.A., and Lewis, J.A. 3D Bioprinting of Vascularized, Heterogeneous Cell-Laden Tissue Constructs. Adv Mater. **26**, 3124, 2014.

284. Schöneberg, J., De Lorenzi, F., Theek, B., Blaeser, A., Rommel, D., Kuehne, A.J.C., et al. Engineering biofunctional in vitro vessel models using a multilayer bioprinting technique. Sci Rep. **8**, 10430, 2018.

285. Ling, Y., Rubin, J., Deng, Y., Huang, C., Demirci, U., Karp, J.M., et al. A cell-laden microfluidic hydrogel. Lab Chip. **7**, 756, 2007

286. Rocca, M., Fragasso, A., Liu, W., Heinrich, M.A., and Zhang, Y.S. Embedded Multimaterial Extrusion Bioprinting. SLAS TECHNOLOGY: Translating Life Sciences Innovation. **23**, 154, 2018.

287. Sodupe-Ortega, E., Sanz-Garcia, A., Pernia-Espinoza, A., and Escobedo-Lucea, C. Accurate Calibration in Multi-Material 3D Bioprinting for Tissue Engineering. Materials. **11**, 1402, 2018.

288. Imgard, V., An, V., Erik, V., Nils, B., Karlien, W., Mariel, Pi., Natalija, B., Joan, V., Nancy, T., Mattias, N. Responsible Use of High Risk Medical Devices. Fed. Kenniscentrum voor Gezondheidszorg. 1- 158, 2018.

289. U.S. FDA, 2017. Technical Considerations for Additive Manufactured Medical Devices - Guidance for Industry and Food and Drug Administration Staff 美國FDA 3D 列印應用醫療製品規範.

290. Draft Guidance Document - Licensing Requirements for Implantable Medical Devices Manufactured by 3D Printing - Canada.ca [WWW Document], n.d. URL https://www.canada.ca/en/health-canada/services/drugs-health-products/medical-devices/activities/announcements/notice-licensing-requirements-implantable-3d-printing/draft-guidance-document.html (accessed 6.22.20).

291. Program, S. 3D Printing and Beyond Intellectual Property and Regulation How To Order Connect With Us Find us on Facebook Read our Blog 404–405. 2019.

292. Ricles, L.M., Coburn, J.C., Di Prima, M., and Oh, S.S. Regulating 3D-printed medical products. Sci Transl Med. **10**, eaan6521, 2018.

293. Pavlovich, M.J., Hunsberger, J., and Atala, A. Biofabrication: a secret weapon to advance manufacturing, economies, and healthcare. Trends in Biotechnology. **34**, 679, 2016.

294. Gilbert, F., O'Connell, C.D., Mladenovska, T., and Dodds, S. Print Me an Organ? Ethical and Regulatory Issues Emerging from 3D Bioprinting in Medicine. Sci Eng Ethics. **24**, 73, 2018.

295. Tan, A., Rajadas, J., and Seifalian, A.M. Biochemical engineering nerve conduits using peptide amphiphiles. Journal of Controlled Release. **163**, 342, 2012.

Tables:

Table 1: Seddon-Sunderland classification of PNIs (Reproduced from 253)

	Seddon's classification	Sunderland's classification	Pathophysiologic hallmarks	Surgical intervention	Prognosis
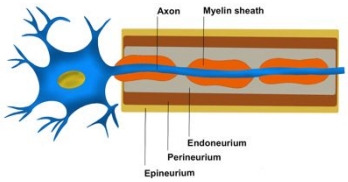	Normal	Normal			
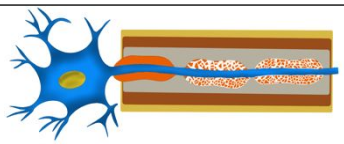	Neurapraxia	I	Focal Segmental Demyelination Conduction delay	✕	Best: potential for full recovery
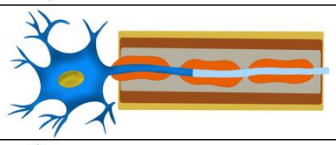	Axonotemesis	II	Axonal discontinuity	✕	Full recovery
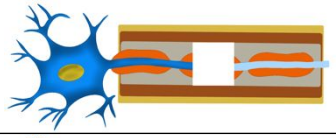	Axonotemesis	III	Interruption of neuronal axon and endoneurium	✕ Or Neurolysis	Variable
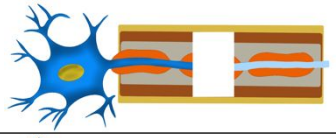	Axonotemesis	IV	Interruption of neuronal axon, endoneurium, and perineurium	✓	Poor: No recovery
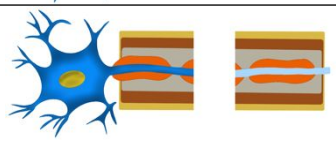	Neurotemesis	V	Complete nerve trunk discontinuity	✓	Poorest: no recovery

Table 2: FDA-approved nerve substitutes (Reproduced from 253)

Biomaterial		Trade name
POLYMERIC BIOMATERIALS		
I.	**Type I bovine collagen**	1. NeuraGen 2. NeuroMatrix 3. NeuroFlex
II.	**Poly-glycolic Acid (PGA)**	Neurotube
III.	**Poly(l-lactide-co-ε-caprolactone) (PLCL)**	Neurolac
IV.	**Polyvinyl alcohol (PVA)**	SaluTunnel
DECELLULARIZED ECM		
1)	**Acellular nerve allograft**	Avance
2)	**Acellular porcine SIS**	AxoGuard

SIS = small intestinal submucosa

Table 3: Composition and function of connective tissue layers of peripheral nerves

CT layer	*Composition*		*Function*
	Polymers	**Cells**	
1. Epineurium	1. Type I collagen (mainly) 2. Elastin	1. Fibroblasts 2. Adipocytes (more prominent in larger nerves)	1. Protects against nerve deformation 2. Facilitates gliding between fascicles 3. Carriers the vasa nervorum, the main microvascular supply of the nerve.
2. Perineurium	Type III collagen	Perineurial cells	1. Source of *main tensile strength* and *elasticity* 2. Forms the BNB 3. Protection of the endoneurial tubes
3. Endoneurium	1. Type III collagen 2. Type I collagen	1. Fibroblasts 2. Endoneurial fibroblast-like cells (EFLCs) 3. Pericytes and endothelial cells 4. Resident immune cells (lymphocytes, mast cells, and macrophages)	1. Endoneurial blood vessels participate in the BNB. 2. BNB regulates the homeostasis of the endoneurial compartment
4. Basal lamina	*Non-collagenous proteins* • Glycoproteins: 1. Laminin 2. Fibronectin • Proteoglycans 1. Chondroitin sulphate 2. Perlecan: heparan sulphate. • Nidogen/entactin *Collagens* 1. Type IV collagen (mainly) 2. Type I, III, and XVIII collagens	_	1. Important for Schwann cell development and myelination function. 2. Acts as a template for axonal regrowth following peripheral nerve injury.
References	61,62,63,64		

Table 4: Major SC phenotypes existing in peripheral nerve tissue

		Myelinating Schwann Cells	*Non-myelinating (Remak) Schwann Cells*
Surface markers	• **Common markers**	S100	
	• **Specific markers**	1. Egr2 (Krox20), 2. Myelin protein zero (MPZ, P0), 3. Myelin basic protein (MBP), 4. Myelin associated glycoprotein (MAG), 5. Periaxin, 6. Peripheral myelin protein (PMP22).	1. Neural cell adhesion molecule (NCAM), 2. p75 Neurotrophin receptor (p75NTR), 3. Glial fibrillary acidic protein (GFAP), 4. L1 (also known as L1 CAM).
Properties of axons ensheathed	• **Number**	One 1:1 ratio	> 1
	• **Types**	Mainly motor nerve fibers.	1) Sensory axons including nociceptive C fibers. 2) Autonomic nerve fibers.
	• **Diameter**	Large calibre (>1-2 µm diameter)	Small calibre (<1-2 µm diameter)
References		69, 70,71,72	73,74,75

Table 5: Most commonly used biomaterials in peripheral nerve conduit design

Polymers	FDA Approved for NGC	Advantages	Disadvantages	Ref.
Natural				
i. Collagen	✓	1. Major peripheral nerve ECM protein. 2. Bioactivity. 3. Biodegradable via enzymatic (MMPs) digestion.	1. Poor mechanical strength. 2. Risk of immunogenicity.	3 116
ii. Silk	✕	1. High tensile strength. 2. Low immunogenicity. 3. Cell adhesive due to the presence of arginine residues.	1. Slow in vivo degradation.	117 118 119
iii. Chitosan*	✕	1. Biodegradable via lysosomal digestion. 2. Free cationic amine groups promote cellular adhesion. 3. Antibacterial.	1. Brittle 2. Poor solubility in water.	120 121
iv. Hyaluronic acid	✕	1. Biocompatible. 2. Immune modulator. 3. Major ECM molecule.	1. Poor mechanical strength.	122 123
v. Gelatin	✕	1. Biodegradable via enzymatic digestion. 2. Bioactive.	1. Weak mechanical properties.	124 125
Synthetic				
i. Poly (glycolic) acid (PGA)	✓	1. Biodegradable via ester hydrolysis.	1. Extrusion. 2. Bioinert.	126
ii. Poly (l-lactide-co- ε-caprolactone) (PLCL)	✓	1. Biodegradable via ester hydrolysis 2. Excellent mechanical properties.	1. Fistula formation and FB reaction. 2. Slow in vivo degradation ~2 years.	127
iii. Poly (lactic-co-glycolic acid) (PLGA)	✕	1. Controllable degradation by adjusting the ratio of glycolide to lactide used for polymerization. 2. Biocompatibility.	1. Bioinert.	128 129
iv. Poly-3-hydroxybutyrate (PHB)	✕	1. Biodegradable via ester hydrolysis. 2. Longitudinally oriented microfibers in the inner wall.	1. Bioinert.	130 131
v. Silicone	✕	1. Impermeable to large molecules, thus helps creating an isolated microenvironment for nerve regeneration.	1. Requires second surgery for removal. 2. Chronic inflammation. 3. Risk of compression neuropathy.	132

ECM = extracellular matrix, FB = foreign body, MMPs = matrix metalloproteinases,

* Chitosan nerve conduits (Reaxon®, Medovent GmbH, Mainz, Germany) are authorized and CE-certified for sale in Europe.

Table 6: Most recently reported 3D printed nerve guides

Biomaterial	3D printing technique	3D printer	Resolution	Additional design features	Chief *in vitro* and *in vivo* findings	Ref.
Synthetic						
A) Non-degradable						
1. PEG-diacrylate	Micro-SL (μSL)	In-house μSL system	50 μm	Longitudinally aligned 20-25 μm microgrooves	• Average Young's modulus of PEG nerve conduits = 470.0 ± 24.3 MPa. • PEG channels supported the neurite extension and Schwann cell migration from the cultured DRG explant.	177
	SLA	3D Systems Model 250/50SL (Rock Hill, SC)	250 μm (beam diameter)	Multi-lumen	• The SL system enabled the fabrication of seven 400 μm lumens conduit with 2.94 mm OD and 1.72 mm ID. • PEG NGCs are suturable. • Multi-lumen design can withstand compression than a single-lumen design with an equivalent surface area. ***In vivo* studies in a 10 mm rat sciatic nerve gap model:** • Single-lumen PEG conduits supported nerve regeneration. Total number of axons in the middle section of the conduit group approached the intact group (control), 4,492.3 ± 2,810.1 fibers/mm vs. 6,080 ± 627.9 fibers/mm. • Multi-lumen conduits were not found superior to single-lumen with regard to peripheral nerve regeneration.	178,179
2. Silicone	In house microextrusion-3D printing system	Microextrusion	In house microextrusion-3D printing system	1. Bifurcated 2. Luminal microgrooves Axially oriented luminal cues: GDNF-loaded hydrogel printed along the motor pathway and NGF-loaded hydrogel printed along the sensory pathway	***In vivo* outcomes in a 10 mm rat sciatic nerve gap model:** • Path-specific biochemical gradients supported nerve regeneration and enhanced functional recovery (gait duty cycle). • 3D printing can offer personalized solutions for complex bifurcating mixed nerve injuries.	180
B) Degradable						
1. PCL-based 3D printed NGCs i. PCL	EHD 3D jetting	In-house EHD system	NA	–	• EHD jetting produced biocompatible, mechanically tunable scaffolds with controllable porosity. • EHD-jetted scaffolds with 125 ± 15 μm pore size supported the highest proliferation of PC12 cells and neural differentiation.	181

ii. PCL/rGO	EHD 3D jetting	In-house EHD system	NA	Conductive	PCL/rGO scaffolds resulted in significantly higher PC12 cell proliferation (due to the high SA to volume ratio offered by the nanostructure of rGO) and expression of neuronal differentiation markers compared to PCL only conduits.	182
iii. PCL/PPy	EHD 3D jetting	In-house EHD system	NA	Conductive	Inclusion of PPy-b-PCL into PCL-based scaffolds aids the fabrication of softer scaffolds with conductive properties, mechanical properties similar to native human peripheral nerve (~6.5 MPa)**.**	183
iv. PCL/PAA	EHD 3D jetting	In-house EHD system	NA	Conductive	• Mechanical properties can be tuned according to the concentration of PAA in the composite. • Conductivity increases with higher PAA concentrations. **PCL/PAA scaffolds supported cell proliferation and neural differentiation** better than the pure PCL scaffolds.	184
v. PLCL	Piezoelectric-based Inkjet	JetPlus® System	NA	_	• 80/20 copolymer scaffolds supported EcR-293 cell survival and attachment. Level of NGF was higher compared with control on 80/20 PLA-PCL scaffolds.	185
A) Poly (glycerol sebacate methacrylate)	SLA	In-house SL system	NA	1. Topographical cues along the internal wall (20-30 μm size) Flexible	• **Mechanical properties:** – Young's modulus = 3.2 MPa – Suture retention strength = 12.3 MPa • Longitudinal topographical grooves supported **directional alignment of neurites** extending from DRG. ***In vivo* outcomes in a 3 mm mouse common fibular nerve gap model:** • PGSm supported the regeneration of axons evidenced by sprouting index and axonal tracing. • Compared to the autograft group, PGSm showed <u>no significant increase in spinal microglial and astrocyte activation</u>, which are indicative of neuropathic pain potential.	186
A. PLGA/Graphene	Extrusion	3D BioPlotter (EnvisionTEC GmbH, Germany).	NA	1. Multi-channel 2. Conductive Flexible	• 3DG is biocompatible: does not elicit fibrous capsule formation or inflammatory response. • Mechanical properties close to that of soft tissues; elastic modulus (3.0 ± 0.4 MPa). • Graphene-based 3D-printed scaffolds promoted neurogenic differentiation of hMSCs in the absence of exogenous neurotrophic factors. • 3DG up-regulated the expression of glial and Neuron-specific markers (GFAP, TujI, Nes, and MAP2) by hMSCs.	187
Natural						
1. GelMA	Inkjet	(TD-IIA, TD ARTIST, Chengdu, China	NA	1. Single lumen 2. Bifurcated	• GelMA conduits were indirectly 3D printed using 'lock and key' molds. • Expression of neurotrophic factors (GDNF and BDNF) by ADSCs cultured on 3D NGCs was significantly higher than those seeded on tissue culture polystyrene (TCP). • Complete in vivo degradation at 2-4 months. • ***In vivo outcomes* in a 10 mm rat sciatic nerve gap model:**	171

					– No significant difference between the axon diameter, SFI, and the 16th postoperative NCV value in the autograft group and ADSCs seeded conduits.	
	Inkjet	(TD-IIA, TD ARTIST, Chengdu, China	NA	1. Single lumen EHS hydrogel filling	• Tensile modulus of the GelMA conduits = 0.489 ± 0.032 kPa. • Compressive modulus of the GelMA conduits = 0.314 ± 0.015 kPa. • ***In vivo* outcomes in a 10 mm rat sciatic nerve gap model:** – No significant difference between the NCV in the autograft and the composite conduit group (conduit + hydrogel filling) at week 14 postoperatively. – No significant difference between the CMAP in the autograft and composite conduit group at weeks 14 and 16 postoperatively. – The gastrocnemius muscle fiber was significantly larger in the composite conduit group compared to the blank conduits; however, no differences existed between the former and the autograft group. – Both blank and filled GelMA conduits showed adequate myelination (G-ratio = 0.80-0.84).	188
	DLP	In-house DLP system	NA	XMU-MP-1 loaded mPEG-PCL nanoparticles	• XMU-MP-1 is a selective Hippo signalling pathway inhibitor. Inhibition of Hippo pathway promotes peripheral nerve regeneration. • ***In vivo* outcomes in a 10 mm rat sciatic nerve gap model:** – No significant difference between 3DDCs (3D printed drug releasing conduit) and nerve autograft group as regards to NCV, mean diameter of gastrocnemius muscle fibers, CMAP peak amplitude, latency of CMAP onset, myelin sheath thickness, and axon diameter.	189
Hybrid						
A) Polyurethane-based conduits						
1. PU/collagen	Double nozzle Low-temperature deposition manufacturing (DLDM)	In-house DLDM system	NA	Double layered conduit	• The external PU layer is porous with approximately 75% porosity and 10-30 μm pore size. • Inner collagen layer had nanoscale filaments.	190
2. PU/PDA/dECM	DLP	MiiCraft DLP 3D printer-*Commercialized*	NA	-	• Addition of dECM to the PU-based conduit increased the overall hydrophilicity of the conduit evidenced by the enhanced Schwann cells adhesion and spreading on F-actin staining. • PU/PDA/dECM significantly increased the release of neural-associated ECM proteins such as type I collagen and laminin. • PU/PDA/dECM enhanced the expression of neural differentiation markers Nestin and MAP2 by human SCs compared to PU/PDA or PU only conduits.	191

B) PEGDA/GelMA	DLP	In-house DLP system	2.5 μm	1) Multichannel 2) Branched conduits	• 3D printed NGCs were mechanically tunable; increasing the light-exposure intensity from 6.7 mW/cm^2 to 16.6 mW/cm^2 resulted in more than twofold increase in the Young's modulus • ***In vivo* outcomes in a 4 mm rat sciatic nerve gap model:** – Histological examination revealed regenerating nerves branched into the microchannels and spanning the gap length connecting the proximal end of the sciatic nerve to its distal end. – Immunostaining showed multiple axons across the entire graft length. – Functional recovery of sensation was achieved 3 weeks postoperatively in the experimental limb.	192

3DG = 3D printable graphene, ADSCs = adipose derived stem cells, BDNF = brain derived neurotrophic factor, CMAP = compound muscle action potential, dECM = decellularized extracellular matrix, DLP = digital light processing, DRG = dorsal root ganglion, ECM = extracellular matrix, EHD = Electrohydrodynamic, EHS = Engelbreth-Holm-Swarm, GDNF = glial cell line-derived neurotrophic factor, GelMA = gelatin methacrylate, GFAP = glial fibrillary acidic protein, hMSCs = human mesenchymal stem cells, ID = internal diameter, MAP2 = microtubule-associated protein 2, mPEG = methoxypoly(ethylene glycol), NCV = nerve conduction velocity, NGF = nerve growth factor, OD = outer diameter, PAA = polyacrylic acid, PC12 = pheochromocytoma cell line, PCL = polycaprolactone, PDA = poly (dopamine), PEG= polyethylene glycol, PEGDA = polyethylene glycol diacrylate, PGSm = poly (glycerol sebacate) methacrylate PLGA = poly(lactic-co-glycolic acid, PPy = polypyrrole, PU = polyurethane, rGO = reduced graphene oxide, SA = surface area, SCs = Schwann cells, SFI = Sciatic Functional Index, SL = stereolithography, XMU-MP-1 = 4-((5,10-dimethyl-6-oxo-6,10-dihydro-5H-pyrimido[5,4-b]thieno[3,2-e][1,4]diazepin-2-yl)amino) benzenesulfonamide

Table 7: Peripheral nerve tissue engineering using scaffold-based bioprinting (Reproduced from 253)

Bioink formulation		*Bioprinting technique*	*Bioprinter*	Chief *in vitro*/*in vivo* findings	Ref.
Biomaterial	***Cells/ Biologic***				
Alginate Sacrificial template: gelatin	RSCs	Extrusion	3D bioplotter® (EnvisionTEC, Germany)	• Lower alginate concentrations supported multipolar, RSCs with elongated morphology. • Fabricating cell-laden constructs using indirect method of bioprinting helps achieve desired mechanical and functional properties using lower hydrogel concentrations.	227
RGD-modified Alginate/HA/Fibrin	RSCs	Microxtrusion	3D bioplotter® (EnvisionTEC, Germany)	• High cell viability: >89% on day 4 and >95% on day 10, in both 40FAH and FRAH (RGD-modified alginate, fibrinogen, and HA) scaffolds. • FRAH scaffolds depicted higher % of cells aligned parallel to the printed strand, as compared to 40FAH scaffolds (76.36□±□8.77% vs. 64.55□±□7.94% at day 10). • Both SCs-laden 40FAH and FRAH scaffolds promoted directional DRG neurite outgrowth along the printed strand.	228
		Microextrusion	3D bioplotter® (EnvisionTEC, Germany)	• Printing speed can manipulate the alignment of SCs within the 3D bioprinted scaffold. Higher printing speeds induced axial alignment of more SCs and oriented laminin expression. • 3D bioprinted SCs: (i) promoted the orientation of DRG neurons along the axial direction of the printed strands, (ii) higher oriented neurites, as compared to 2D cultured DRG neurons.	229
Gelatin/ Alginate	RSCs	Microextrusion	Tissform III, (Tsinghua University)- *Not commercialized*	• High SC viability (>85%) in 3D bioprinted scaffolds on all days tested. • 3D cultured cells release NGF which was significantly higher (days 7 and 14) than 2D cultures. • 3D bioprinting supported expression of characteristic SC marker (S100β) in encapsulated cells.	230
		Microextrusion	Medprin (China)-*Not commercialized*	• High SC viability (>90%) in 3D bioprinted scaffolds on all days tested. • 3D bioprinting did not inhibit the expression of the SC marker, S100β. • NGF secretion was higher in 3D bioprinted RSCs compared to 2D culture cells. • 3D bioprinted cells expressed higher neurotrophic genes (NGF, GDNF, BDNF, PDGF) than 2D cultures. • 3D bioprinted scaffold degraded without provoking inflammatory responses *in vivo*.	231
GelMA/GC-MS	PC12 cells RSCs NGF	Microextrusion	N/A	• Construct showed homogenous cellular distribution. • GC-MS promoted PC12 proliferation and neurite extension in 3D microniche.	224
–	Porcine SCs NG108-15 Neuronal cells	Piezoelectric inkjet	Microfab Technologies Inc. (Texas, USA)	• Inkjet printing achieved cell viabilities of 86%–96% for neuronal cells and 89%–92% for SCs using 70-270 V range of voltage. • Piezoelectric printing promoted higher number of neurites in comparison to non-printed controls during initial 3 days. • Printed neuronal NG108 cells depicted longer neurites, compared to controls. • Piezoelectric printing had no adverse effect on SC phenotype.	232

40FAH = 40% fibrinogen, alginate, and hyaluronic acid, BDNF = brain-derived neurotrophic factor, FRAH = fibrinogen, RGD-modified alginate, and hyaluronic acid, GDNF = glial cell-derived neurotrophic factor, GC-MS = gelatin methacrylate/chitosan microspheres NGF = nerve growth factor, PC12 = pheochromocytoma cell line, PDGF = platelet derived growth factor, RSCs = Rats Schwann Cells, SCs = Schwann cells,

Table 8: Scaffold-free (Cellular) bioprinting of nerve 3D bio conduits and in vivo testing (Reproduced from 253)

Cells	Bioprinter	Bioprinting technique	Nerve Gap			Chief *In vivo* findings	Reference
			Animal model	*Nerve*	*Gap (mm)*		
Human dermal fibroblasts	Regenova®, Cyfuse, Tokyo, Japan	Kenzan method	Rats	Sciatic	5	• Compared to the control silicone group, Bio 3D conduit achieved: 1. Significantly **higher mean CMAP.** 2. Significantly **higher number of myelinated axons.** 3. Significantly **less tibialis anterior muscle atrophy.** 4. Both motor and sensory recovery. Nerves bridged by the silicone conduit showed only sensory recovery. • Bio conduit promoted SC proliferation and migration.	255
			Rats	Sciatic	10	• Compared to the silicone group (control), the Bio 3D conduit had significantly higher: 1. Mean Nerve Conduction Velocity (MNCV). 2. Axons count in the distal region. 3. Myelinated axon diameter. 4. Myelin thickness.	256
GMSCs			Rats	Buccal Branch of facial	5	• 3D bio-printed graft resulted in CMAP similar to the autograft group, but **significantly higher CMAP than the silicone group**. • 3D bio-printed conduit was associated with **higher facial palsy scores** than the silicone group. • **Organized nerve fascicles** have been formed inside the 3D bioprinted conduit.	257
Canine dermal fibroblasts			Beagle dogs	Ulnar	5	• Both bio 3D conduit and control (no treatment) groups resulted in **similar sensory recovery.** • Bio 3D conduit supported the **extension of neurofilaments and migration of Schwann cells.** • Morphometric studies showed the **presence of myelinated axons in the bio conduit** in amounts comparable to the intact group.	258
BM-MSCs SCs	NovoGen MMX Bioprinter™; Organovo	Extrusion	Rats	Sciatic	10	• **Functional motor and sensory recovery similar** to nerve autograft and might be superior to collagen tube (Neuragen). • Biofabricated graft **supports axonal regrowth.**	259

BM-MSCs = bone marrow derived mesenchymal stem cells, CMAP = compound muscle action potential, GMSCs = gingival mesenchymal stem cells, MNCV = mean nerve conduction velocity, SC = Schwann cell

Figures

Figure 1: Conduit failure mechanisms in regeneration of long nerve gap

I) **Short nerve gap:**
1. Conduit depicts formation of stable fibrin cables.
2. Bands of Büngner are then formed by SC migration and alignment along preformed fibrin clots.
3. Nerve conduits bridging gaps maintain effective concentrations of neurotrophic factors.

II) **Long nerve gap:**
1. Fibrin cables fail to form, or are attenuated with a characteristic hourglass morphology as a result of contracture of the central fibrin matrix.
2. Bands of Büngner fail to form due to lack of viable ECM support to facilitate migration and axonal alignment of SCs.
3. Dilutional decrease of the effective concentration of neurotrophic factors and guidance milieu.

Figure 2: Anatomy of the peripheral nerve

Figure 3: State-of-the-art bioengineering strategies

Figure 4: 3D printing for bridging complex nerve pathways (Adapted from 180)

I) Reverse engineering of nerve pathways using 3D structure light scanning. a) The sciatic nerve is a reliable model of mixed nerve bifurcation consisting of both motor (peroneal and tibial branches; below) and sensory (sural branch; above) divisions. b) An *ex situ* approach is used to obtaining scan measurements using a transected sciatic nerve as a tissue template. c) The scans are captured from different angles to construct a CAD model that reiterates the bifurcating geometry of the sciatic nerve. d) Software-aided alignment of the separate scans into a printable 3D model of the sciatic nerve. e) Software-aided assembly of the aligned nerve scans to form a water-sealed sciatic nerve CAD model. f) The nerve CAD design is printed into a customized silicone conduit that accurately fits the original tissue geometry.

II) *In vitro* and *in vivo* testing of neural recovery within the customized 3D printed tracts. 3D printing enables modality-specific axonal regeneration by separately restoring the sensory and motor pathways using growth factor gradients. (a-b) Effects of incorporating diffusive gradients of neurotrophic factors on modality-specific nerve regeneration. a) NGF gradient effect on sensory neurite extension and elongation (inset scale bar = 1000 μm). b) Migration velocity of SCs influenced by GDNF gradient (inset scale bar = 100 μm). c) Schematic depicting the implanted 3D printed nerve

graft bridging the sensory and motor bifurcations. d) Digital image of the implanted 3D printed nerve conduit. e) Histological cross-sections depicting regenerated axons detected using anti-tubulin monoclonal antibodies, stained in green (scale bar = 50 μm). f) Gait analysis to evaluate functional nerve recovery in rats. ('*' refers to p-value < 0.05, '**' refers to p-value < 0.01).

Figure 5: 3D printing of nerve guides

I) [A-B] Demonstrating the elastic properties of poly glycerol sebacate methacrylate (PGSm) NGC when compressed; [C] Computer model of the 3D printed conduit with annotated dimensions; [D] digital image of the final 3D printed nerve conduit; [E] Suturability test of PGSm nerve conduits; [F] a NGC dissected in half. (Reproduced from 186)

II) Scanning electron microscopy (SEM) of nerve guide scaffolds fabricated using electrohydrodynamic jetting. (a-b) PCL scaffolds, and (c-d) PCL/rGO scaffolds at various magnifications. (Reproduced from 182).

III) 3D-printed PU-based conduits manufactured using DLP. PU, polyurethane; PDA, polydopamine; ECM, extracellular matrix. (Reproduced from 191)

IV) Preparation and characterization of a nanocomposite GelMA hydrogel nerve conduit using DLP 3D printing. (a) Schematic depicting the DLP apparatus for conduit fabrication. (b) TEM image of XMU-MP-1 nanoparticles (scale bar = 100 nm); XMU-MP-1 is a selective Hippo pathway inhibitor. (c) SEM micrographs of 3D printed NGCs (scale bars; lower magnification = 1 mm, higher magnification = 200 µm). (d) Conduits with varied wall thickness corresponding to 0.5 mm, 0.75 mm and 1 mm, tested for compression studies and quantitatively analysed (e). (f) Digital photograph of the microstructure and confocal microscopy of the nanoparticle distribution, (g) XMU-MP-1 nanoparticles and nanoparticle-loaded conduits evaluated for release of XMU-MP-1, *in vitro*. (h) Conduits facilitating diffusion of small molecule. (i) Enzymatic (collagenase) degradation of the nerve guides. All quantitative data are produced as the mean ± standard deviation (SD). (Reproduced from 189)

Figure 6: Engineering nerve-on-a-chip models

A) **(I)** Photolithographic approach for fabricating a 3D nerve model using SC and DRGs co-culture. In method A, exogenous rat SCs in methacrylated dextran (MeDex) were used, Step 1: creation of PEG

cast; Step 2: placement of DRG; Step 3: Combining SC with the gel solution at a predetermined cell density and transfer of the cell-laden gel precursor solution to the created cavity; Step 4: Photo-crosslinking using the negative mask and induction of gelation. In method B, endogenous SCs encapsulated in methacrylated heparin (MeHp), Step 1: creation of PEG cast; Step 2: filling up the void with gel precursor solution; Step 3: Photo-crosslinking using the negative mask and induction of gelation; Step 4: placement of DRG. **(IIA)** Field potential recording using a recording (left) and stimulating (right) electrodes inserted within DRG and axonal tracts in channel, respectively. **(IIB and IIC)** TEM of cross-sections of the DRG culture revealing myelinated nerve fibers. Compact layered myelin sheath can be identified surrounding the nerve fiber. A= Axon, M= Myelin, S= Schwann cells. (Adapted from 207)

B) **(I)** Schematic depicting the fabrication process of *in vitro* human peripheral nerve models using human SCs and iPSCs-derived motor neurons *via* photolithography **(II)** SCs stained for S100 marker (green) migrating out of the spheroidal co-culture and extending along the axons. Scale bar: 1000 µm (BII) High-magnification scan from inset BI. Scale bar: 25 µm (BIII) Confocal micrograph revealing the relationship of SCs (green) and myelinated axons (red) Egress of SCs out of the spheroidal co-culture and spreading along the axons. Slice size = 368.36 × 368.36 × 34.00 µm. (Adapted from 208)

Figure 7: 3D Bioprinting a multiscale modular bioink for peripheral nerve tissue engineering (Adapted from 224)

I) Concept of design and fabrication process of a multiscale composite 3D scaffold to reproduce the microstructure of peripheral neural tissue. (a) A 3D composite scaffold would help nerve regeneration as it reiterates the complex hierarchical organization of the native peripheral nerve. (b) Schematic outlining the sequence of steps for preparation of the neural composite scaffold based on a multiscale modular bioink. Step 1: Fabrication of gelatin/chitosan microspheres (GC-MS) using a microfluidic technique. Step 2: seeding of the nerve cells on microgels. Step 3: formulation of the modular bioink based on GelMA and microspheres. Step 4: Extrusion printing of the modular bioink into 3D multiscale scaffolds.

II) Biofabrication of gelatin/chitosan microgels-laden GelMA 3D multiscale composite scaffold. (a-c) Multi-layer bioprinting of the GC-MS/GelMA scaffold: one-layer printing (a), two-layer printing (b), and four-layer printed structure of the microspheres-laden GelMA modular bioink (c). (d-f) The composite scaffold observed under confocal microscopy, where

GC-MS (green) and GelMA (red) hydrogel could be seen. Scale = 500 μm. (g, h) Gelatin/chitosan microspheres evaluated by surface plot analysis (g) and GelMA matrix (h) obtained from the confocal micrographs. (i) 3D confocal micrographs of scaffolds: GC-MS/GelMA, GC-MS (green-yellow), and GelMA (red). Scale bar = 200 μm.

III) Biofabrication of the microgel-laden GelMA composite scaffold encapsulating cell co-culture of PC12 and RSC96 cells. (a) The illustration outlines the extrusion bioprinting process of NGF loaded microspheres. (b-d) Confocal micrographs of cross-section of bi-layered scaffold at day 1, showing the GelMA scaffold encapsulating NGF-loaded gelatin/chitosan microspheres, PC12 cells stained in green (b) and RSC96 cells stained in orange could be detected. Scale: 500 μm. Surface plot analysis of the 2D confocal images from (b) and (c) showing the spatial organization of cells: PC12 (e) and RSC96 (f). (g, h) Confocal micrographs of a single GC-MS + NGF cultured with PC12 cells (green) in the GelMA hydrogel encapsulating RSC96 cells (orange). Scale: 50 μm.

IV) Morphological study of PC12 cells seeding with gelatin/chitosan microspheres after culture for 3 days. Confocal micrographs of PC12 cells cultured on empty gelatin/chitosan microspheres (a, b) and microspheres loaded with NGF (e, f) stained for cytoskeletal (F-actin: green) and nuclear (DAPI: blue) regions. SEM micrographs of PC12 laden blank microspheres (c, d) and NGF-loaded microspheres (g, h). (i) PC12 laden GC-MS, GC-MS + NGF ($p < 0.05$) subjected to neurite length analysis. (j) PC12 cells with axonal outgrowth (%) of cultured on blank microspheres compared to NGF-loaded microspheres ($p < 0.05$).

Figure 8: Effect of bioprinting speed on regulating the alignment of SCs and laminin. (Reproduced from 229).

I) SC morphologies in 40RAHF (RGD-modified alginate, hyaluronic acid, and 40 $mg.ml^{-1}$ fibrinogen) scaffolds using different printing speeds. 9 mm/s extrusion speed resulted in notably higher SC alignment with > 75% of cells oriented within ±20° relative to strand direction compared to lower speeds. Cell circularity is assessed on a 0.0–1.0 scale, with 1.0 being an ideal circle. Low circularity values denote a more spread, attached, or differentiated state of bioprinted cells. Although a higher bioprinting speed was associated with lower circularity values, no statistically significant difference existed. Scale bar = 50 µm, '**' and '&&' refer to $p < 0.01$, '###' refers to $p < 0.001$, and '****' refers to $p < 0.0001$.

II) Extrusion speed impacts the orientation of expressed laminin protein. It is noted that a higher printing speed induces more oriented laminin expression.

Figure 9: Scaffold-free bioprinting of nerve 3D bio conduits

I) Fabrication of a cellular nerve graft using sacrificial extrusion bioprinting (A-F). The printed graft was composed of an outer ring of bioink consisting of BM-MSCs (red) only. Interiorly, alternating cylinders of 90% BM-MSCs and 10% SCs (grey) were printed along with agarose rods (C-E). The latter resulted in multiple lumens within the graft substance upon removal. The entire structure was bolstered by supporting agarose rods (E) that allow the bioink cylinders to self-aggregate into the biofabricated nerve graft (F). Agarose rods were removed after 7 days. Panel (G) demonstrates the cross-section of the cellular nerve graft with fluorescently labelled SCs (green). Elimination of the inner agarose rods resulted in three hollow channels that mimic the native fascicles of the peripheral nerve. (Reproduced from 259)

II) Schematic depicting nerve graft biofabrication using the Kenzan-based approach for spheroidal bioprinting. (Adapted from 213, 256).

Figure 10: Using Micro-MRI scans 3D reconstruction as a proof-of-concept to develop 3D-printed customized nerve graft (Adapted from 276)

I) Biofabrication model replicating the ultrastructure of the peripheral nerve fascicle based on 3D scans database. (a) Proximal and distal parts of the nerve gap. (b) Variations in the fascicular morphology of the distal and proximal ends of the neural gap model. (c) Customized 3D nerve graft model created based on the micro-MRI library scans of nerve fasciculi. (d and e) Simulation test of the homology between the 3D printed nerve graft and gap model.

II) 3D printed nerve model revealing the morphological features of the customized nerve graft that imitates the ultrastructure of peripheral nerve fascicles. (a and c) Noticeable variations in the amount and spatial organization of the nerve fascicles in the proximal and distal ends of the nerve gap. (b and d) The position of the two nerve tracts matches that of the original micro-MRI scans. (e) 3D printed PLA nerve model depicting the congruency of the artificial 3D printed graft with the created nerve gap model. (a, b, c, and d) Scale bar = 1 mm. (e) Scale bar = 1 mm.

Figure 11: 3D reconstruction of the lower limb nerve fascicles using micro-MRI imaging (Reproduced from 276)

I) A1) Micro-MRI scan of the human sciatic nerve, A2) 2D image segmentation, A3) 3D reconstruction of nerve fascicles.

II) A1) Micro-MRI scan of the human tibial nerve, A2) 2D image segmentation, A3) 3D reconstruction of nerve fascicles.

III) A1) Micro-MRI scan of the human common peroneal nerve, A2) 2D image segmentation, A3) 3D reconstruction of nerve fascicles. Scale bar = 1 mm in A2, B2, C2; Scale bar = 2 mm in A3, B3, and C3.

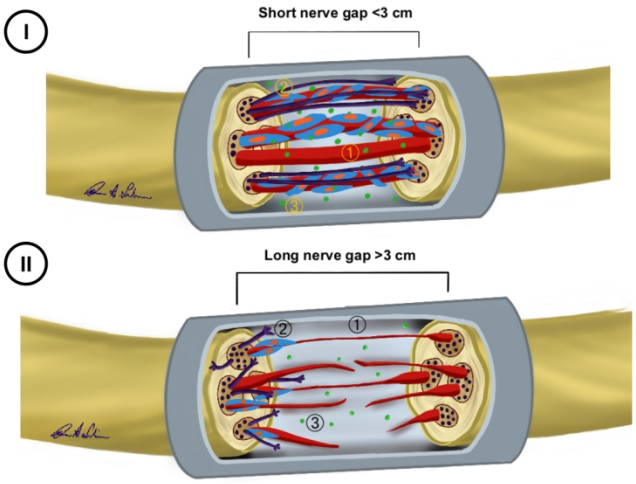

Figure 1.

599x776mm (72 x 72 DPI)

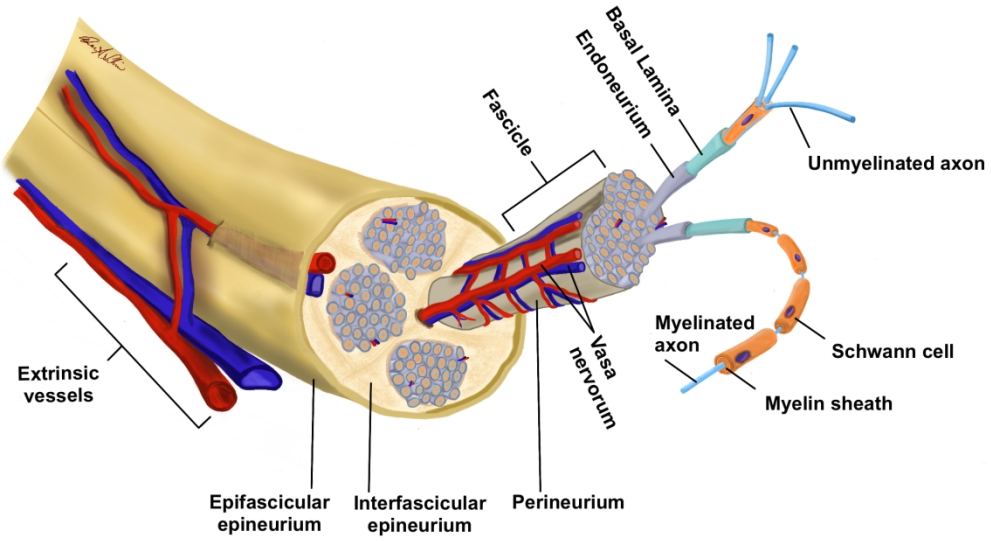

Figure 2

418x232mm (132 x 132 DPI)

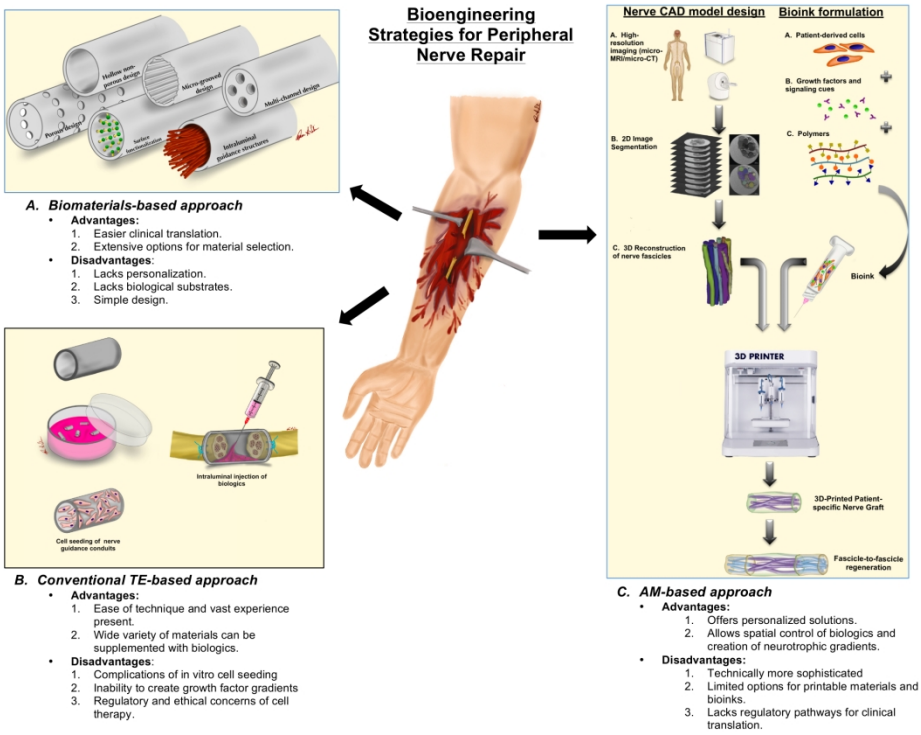

Figure 3

776x599mm (72 x 72 DPI)

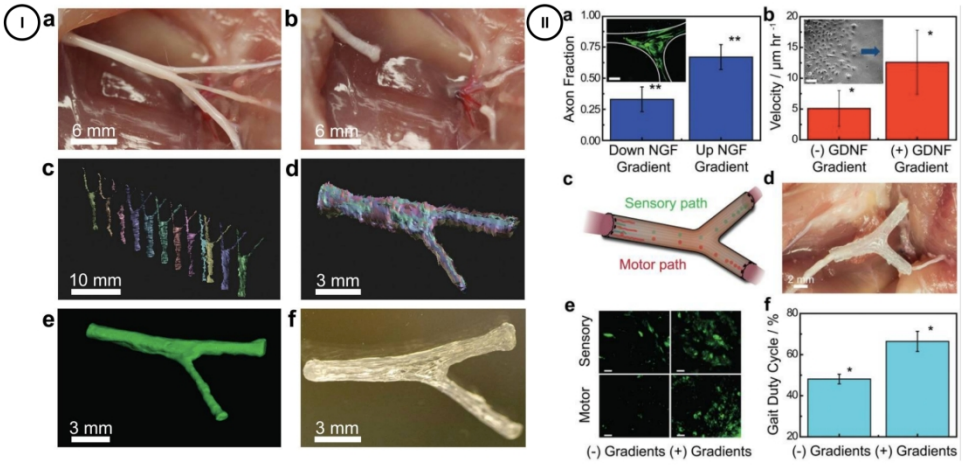

Figure 4

776x599mm (72 x 72 DPI)

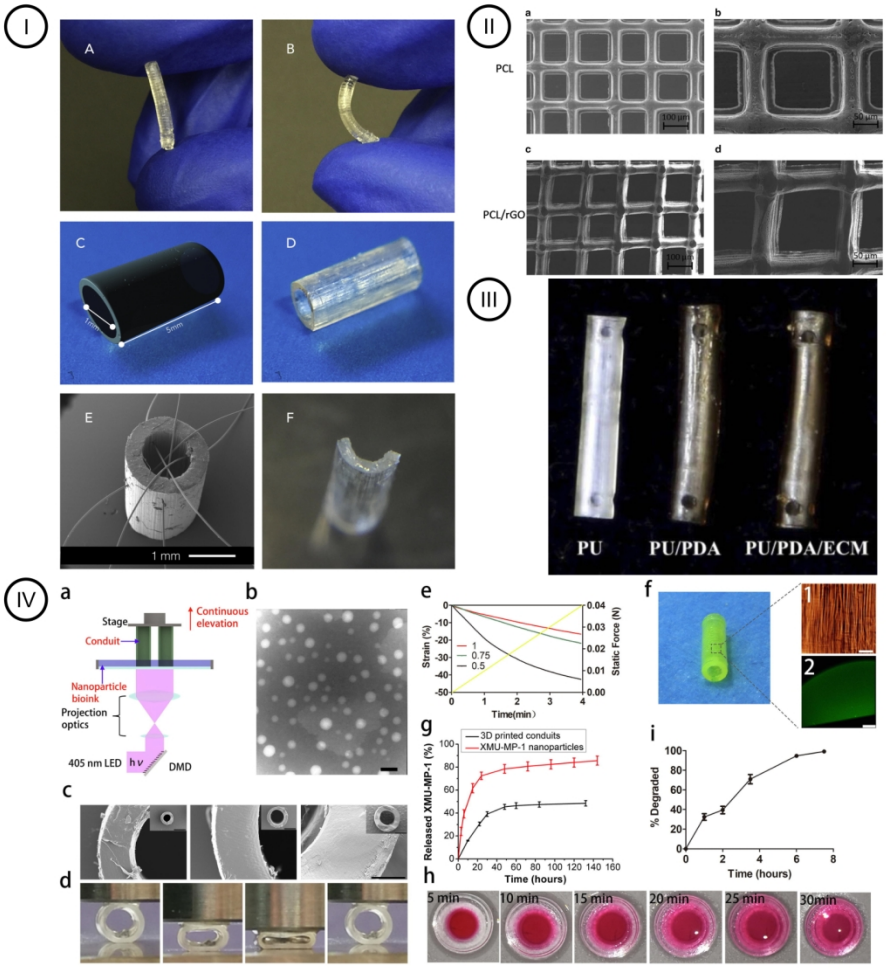

Figure 5

599x776mm (72 x 72 DPI)

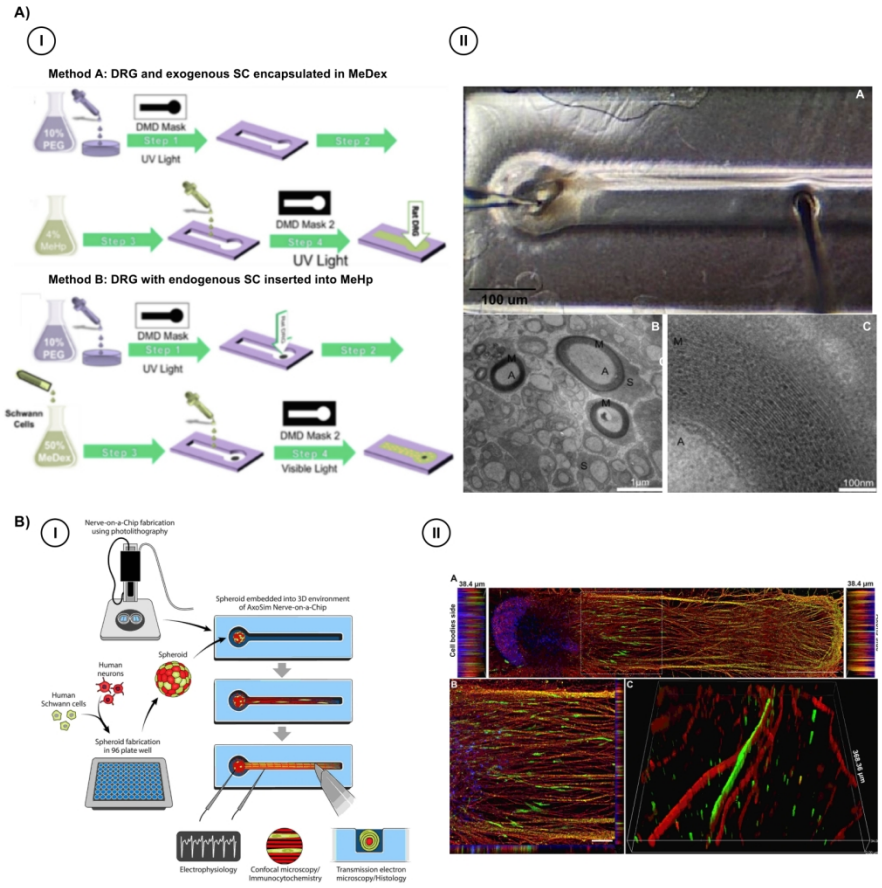

Figure 6

599x776mm (72 x 72 DPI)

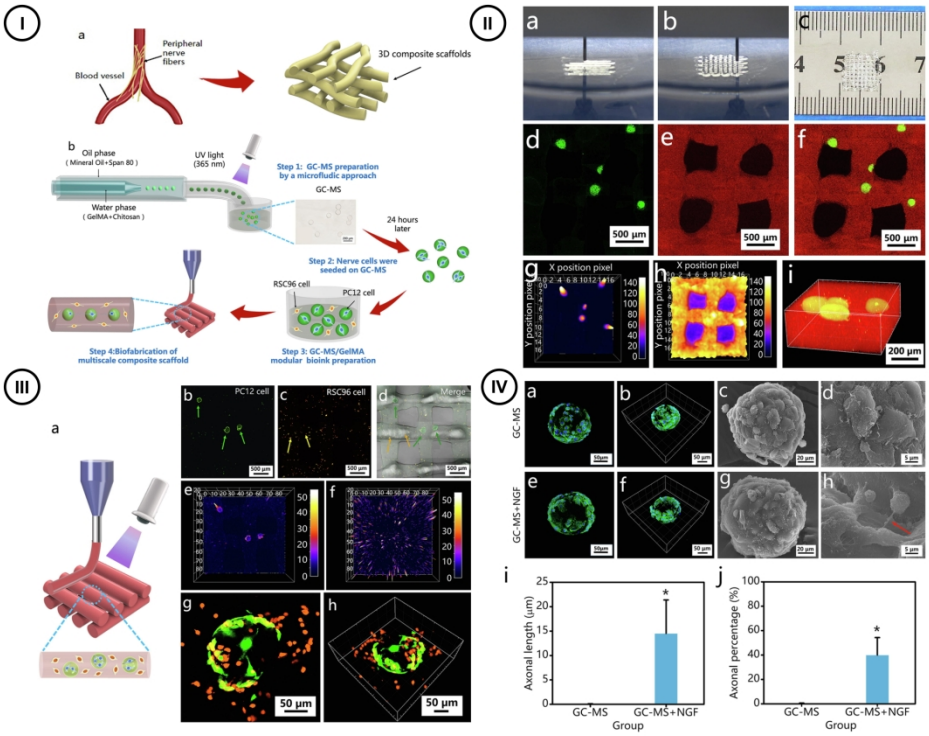

Figure 7

776x599mm (72 x 72 DPI)

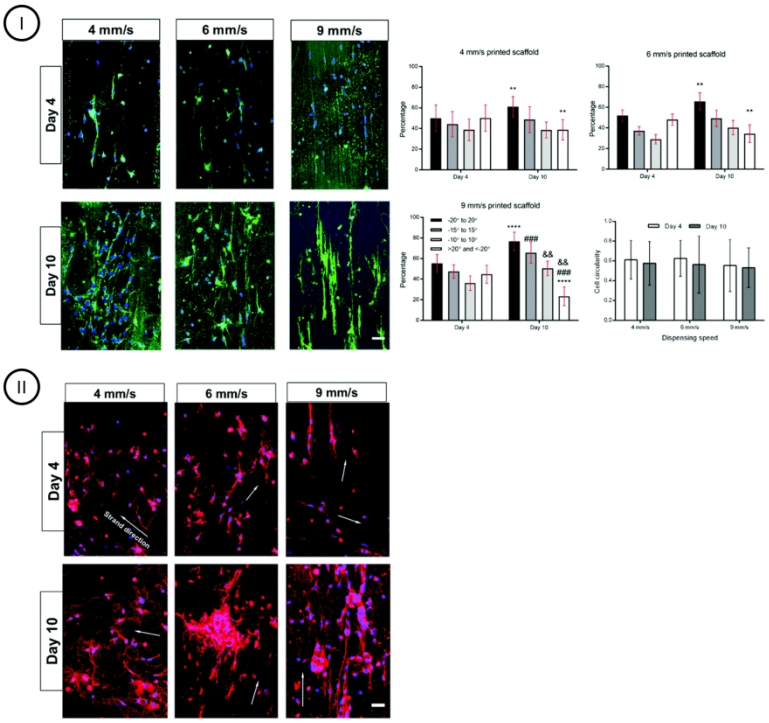

Figure 8

776x599mm (72 x 72 DPI)

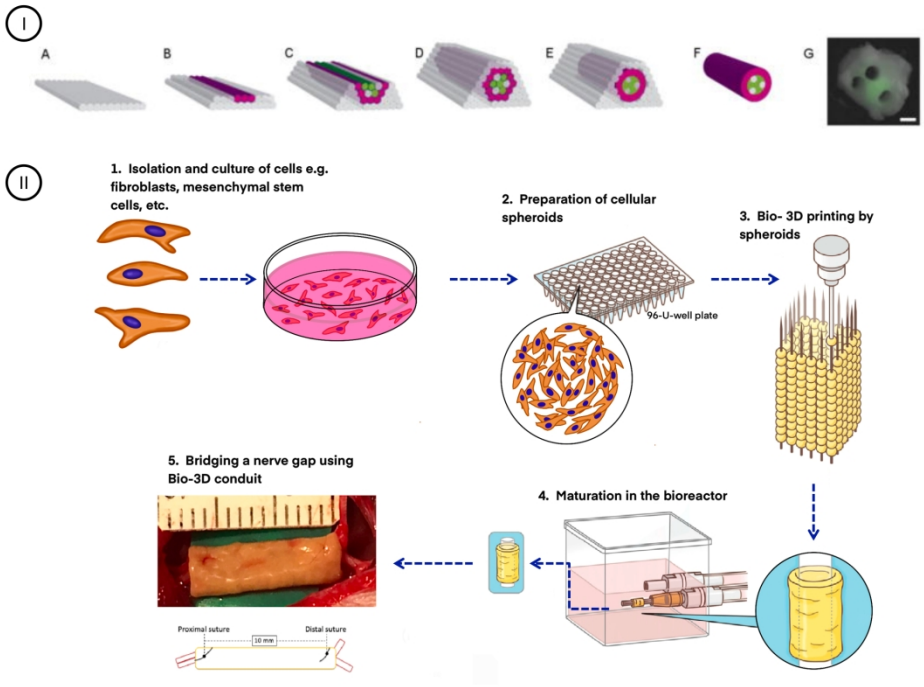

Figure 9

776x599mm (72 x 72 DPI)

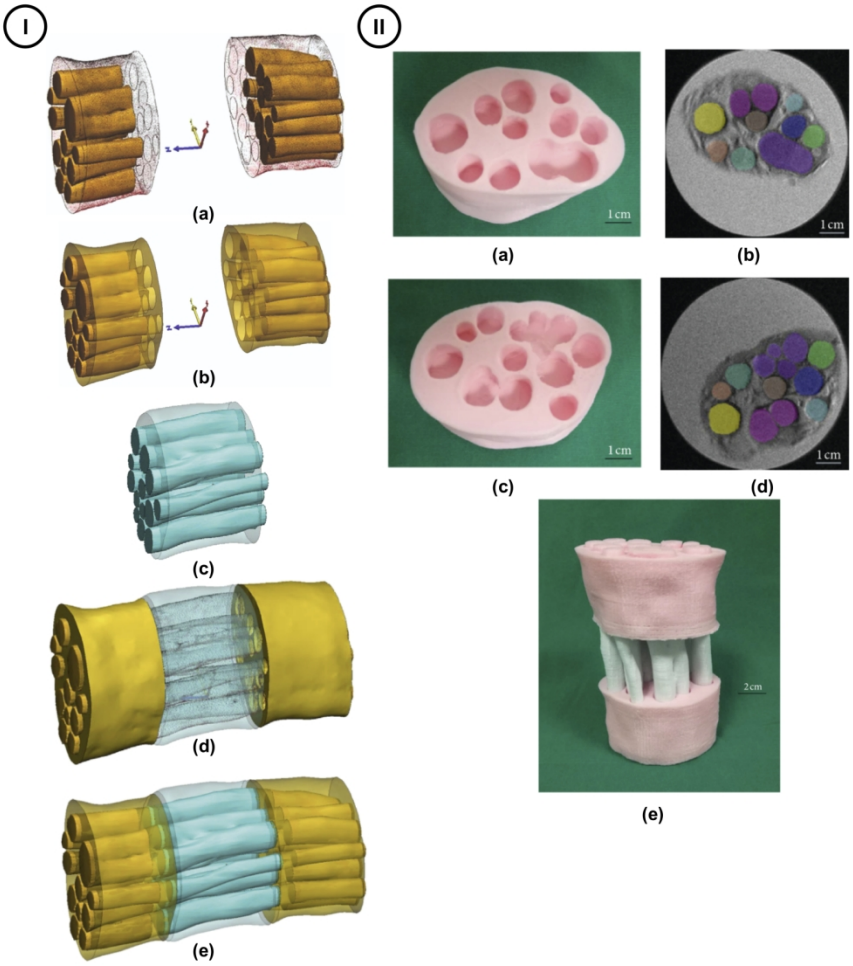

Figure 10

599x776mm (72 x 72 DPI)

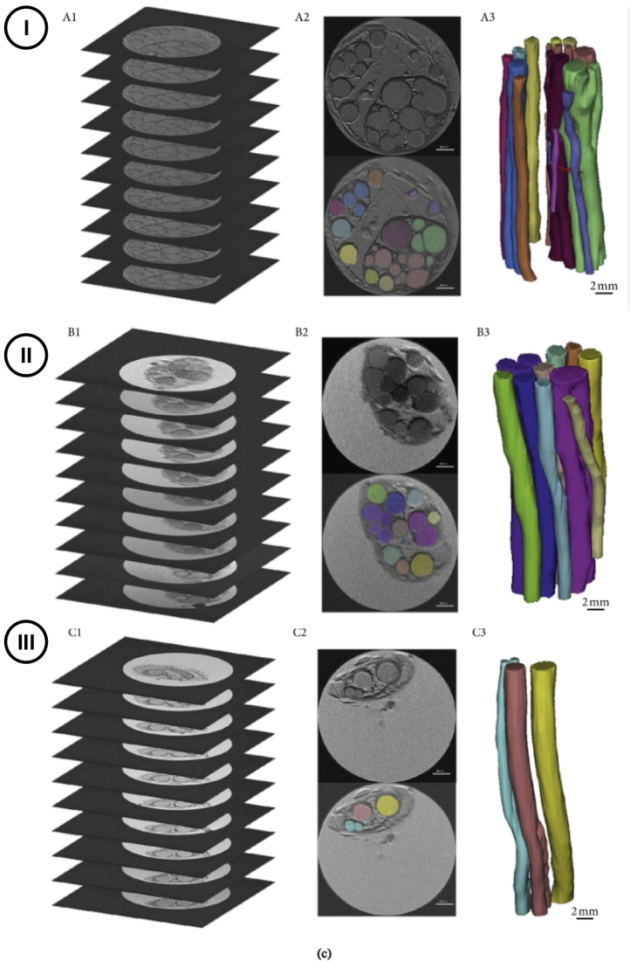

Figure 11

599x776mm (72 x 72 DPI)